

https://dspace.org/

# The properties and performance of selected thin spray on liners for rock support

**Mpunzi, Philani**

**2012-02-14**
http://hdl.handle.net/10539/11316

Downloaded from a DSpace repository. https://dspace.org/

# Declaration

I declare that this dissertation is my own unaided work. It is being submitted to the Degree of Master of Science to the University of the Witwatersrand, Johannesburg. It has not been submitted before for any degree or examination to any other University.

……

(Signature of candidate)

…….. day of ……..... (year) …...

at ……

# Abstract

Thin spray-on liners (TSLs) are a type of surface rock support used in underground excavations, for maintaining stability at the excavation boundary. Different products are emerging in the market, while little is known about the mechanisms by which the liners support the excavation. There are no generally accepted tests which determine the performance of TSLs for rock support. In the research described in this dissertation, an attempt has been made to investigate the mechanisms of behavior of TSLs for rock support through laboratory tests. Brazilian indirect tensile strength tests, material compression tests, 3-point bending tests and physical model tests were carried out to investigate the performance and the characteristics of the liners for rock support. The Brazilian and the 3-point bending tests are new tests as far as TSL evaluation is concerned. The reviews of literature indicate that no similar testing appears to have been done previously.

The laboratory test results of samples coated with TSL material showed that the sprayed liners enhance the strength of the rock. The load at which failure occurred increased for coated hard rock samples and the mechanism of behavior depends on the type of liner and curing time. The test methods showed that the performance of the TSLs depend on the type of the rock and the quality of the liner. The results for the 3-point bend test revealed that the application of a weak liner to weak porous rocks such as sandstone does not enhance the strength, but further weakens the rock. An explanation is that the moisture contained in the TSL is deleterious to the already delicate sandstone rocks. Such behavior in practice could compromise the safety of the workers in the period shortly after application.

The laboratory test methods showed different mechanisms of behavior of the liners, but all reflected the similar qualities of the liners. The physical model was used to validate the mechanisms that were shown by the specific test methods which are responsible for rock support. The model revealed all the mechanisms of behavior of the TSLs that were displayed by Brazilian, compression and the bending tests. Results of the model tests showed that stability of the excavation and performance of the liner depends on the

orientation of the jointing. The test methods provided invaluable information for comparing the properties and support mechanisms provided by the TSLs.

The research carried out has contributed new knowledge in the “new” field of TSLs.

# Acknowledgements

I would like to express my sincere gratitude on the assistance and support rendered by the following persons and institutions:

- Professor T. R. Stacey for his supervision, guidance, encouragement and motivation throughout this research
- University of the Witwatersrand for granting me the opportunity to embark on this research
- GENMIN Laboratories for affording me the opportunity to carry out laboratory tests
- My family, friends and colleagues for their motivation and support

…….To the three most important people in my life; my wife Sinqobizitha, my sons Mqhelewenkosi Ntandwehle and Kwandokuhle Nkosana……

## TABLE OF CONTENTS

**DECLARATION** ..... **I**

**ABSTRACT** ..... **II**

**ACKNOWLEDGEMENTS** ..... **IV**

**LIST OF FIGURES** ..... **XI**

**LIST OF TABLES** ..... **XIV**

**LIST OF SYMBOLS AND TERMS USED** ..... **XVI**

**CHAPTER 1** ..... **1**

**INTRODUCTION** ..... **1**

1.1 BACKGROUND ..... 1

1.2 DEFINITION OF THE PROBLEM ..... 3

1.3 OBJECTIVES ..... 4

1.4 RESEARCH METHODOLOGY ..... 4

1.5 CONTENT OF THE DISSERTATION ..... 5

**CHAPTER 2** ..... **6**

**MECHANISMS OF ROCK SUPPORT AND ROCK FAILURE** ..... **6**

2.1 TYPES OF SUPPORT ..... 6

2.2 ROCK FAILURE MECHANISMS ..... 7

2.3 MECHANISMS OF ROCK SUPPORT ..... 10

2.3.1 Promotion of Block interlock ..... 11

2.3.2 Basket Mechanism ..... 12

2.3.3 Air Tightness ..... 13

2.3.4 Extended Face Plate ..... 13

2.3.5 Durability Enhancement ..... 13

2.4. SURFACE SUPPORT PRESSURE ..... 14

2.5 SURFACE SUPPORT LOADING MECHANISMS ..... 16

2.5.1 Gravity Loading by Wedge and Key Block ..... 16

2.5.2 Distributed Surface Loading ..... 17

2.5.3 Bending Surface Loading ..... 17

2.5.4 Stress Induced Loading ..... 18

2.5.5 Water Pressure Loading ..... 19

2.6 PROPERTIES OF TSL'S ..... 20

2.6.1 Chemical Properties of TSL's ..... 21

2.6.2 Physical Properties of TSL's ..... 21

2.7 CONCLUSIONS ..... 23

**CHAPTER 3 ..... 24**

**LABORATORY TESTS AND RESULTS ..... 24**

3.1 TSL FAILURE MECHANISMS ..... 24

3.1.1 Tensile Strength Tests ..... 25

3.1.2 Adhesion Tests ..... 27

3.1.3 Compression Failure Tests on Coated Core ..... 29
3.1.4 Punch Type of Testing ..... 29
3.1.5 Shear Bond Strength Tests ..... 30
3.2 LABORATORY TESTING ..... 31
3.3 TEST GUIDELINES ..... 32
3.4 LABORATORY CONDITIONS ..... 32
3.5 LABORATORY TESTING EQUIPMENT ..... 33
3.6 SELECTED TSLS ..... 33
3.7 TESTING METHODS ..... 34
3.7.1 Brazilian Tensile Strength Testing ..... 34
3.7.1.1 Brazilian Strength Test Description ..... 35
3.7.1.2 Determination of Brazilian Tensile Strength Results ..... 36
3.7.1.3 Brazilian Tensile Strength Test Results ..... 37
3.7.2 Compressive Strength Test ..... 41
3.7.2.1 Compressive Strength Test Description ..... 41
3.7.2.2 Determination of Compressive Strength Results ..... 41
3.7.2.3 Compression Strength Results ..... 42
3.7.3 Three-point Bending Strength Test ..... 45
3. 7.3.1 Three-point Bending Test Description ..... 46
3. 7.3.2 Three-point Bending Strength Results ..... 47

3.8 PHYSICAL MODEL ..... 50

3.8.1 Physical Model Test Description ..... 52

3.8.2 Physical Model Results ..... 55

3.9 CONCLUSIONS ..... 57

**CHAPTER 4 ..... 59**

**DISCUSSION OF RESULTS ..... 59**

4.1 COMPARISON OF THE LINER PERFORMANCE FOR BRAZILIAN TESTS ..... 59

4.2 COMPARISON OF LINER PERFORMANCE FOR THE COMPRESSION TESTS ..... 60

4.3 COMPARISON OF LINER PERFORMANCE FOR THE 3-POINT BENDING TESTS ..... 61

4.4 PHYSICAL MODEL TESTS ..... 62

4.4.1 Modes of TSL failure ..... 63

4.4.1.1 Adhesion failure ..... 63

4.4.1.2 Shear Failure ..... 64

4.4.1.3 Compression failure ..... 66

4.4.1.4 Flexural Failure ..... 67

4.4.1.5 Tensile Failure ..... 69

4.4.2 Liner Support Performance and Practical Implications ..... 71

4.4.2.1 Performance of TSL A at $45^0$ Orientation ..... 71

4.4.2.2 Performance of TSL A at $60^0$ Orientation ..... 72

4.4.2.3 Performance of TSL A at $80^0$ Orientation ..... 73

4.4.2.4 Performance of TSL B at $45^0$ Orientation.....74

4.4.2.5 Performance of TSL B at $60^0$ Orientation.....75

4.4.2.6 Performance of TSL B at $80^0$ Orientation.....76

4.4.2.7 Performance of TSL C at $45^0$ Orientation.....77

4.4.2.8 Performance of TSL C at $60^0$ Orientation.....79

4.4.2.8 Performance of TSL C at $80^0$ Orientation.....79

4.5 COMPARISON OF TEST PROCEDURES ..... 81

4.6 CONCLUSIONS ..... 82

**CHAPTER 5 ..... 84**

**CONCLUSIONS AND RECOMMENDATIONS ..... 84**

**REFERENCES ..... 89**

APPENDIX A BRAZILIAN TESTS ..... 103

APPENDIX B COMPRESSION TESTS ..... 115

APPENDIX C 3-POINT BENDING TESTS ..... 118

APPENDIX D PHYSICAL MODEL TESTS ..... 121

# List of Figures

Caption Page

FIGURE 2. 1 MODES OF FAILURE IN HARD ROCK MINES (AFTER HOEK ET AL, 1995) ..... 8

FIGURE 2. 2 A) SHEAR AND ROTATIONAL RESISTANCE, B) CRACK INFILLING AND C) TENSIONAL RESISTANCE (AFTER STACEY 2001) ... 12

FIGURE 2. 3 SUPPORT REACTION CURVE AFTER (BRADY AND BROWN, 1985) ..... 15

FIGURE 2. 4 KEY BLOCK THEORY; SHADED BLOCKS ARE UNSTABLE (AFTER BARRETT AND MCCREATH 1995) ..... 17

FIGURE 2. 5 SQUEEZING GROUND (AFTER STACEY 2001) ..... 18

FIGURE 2. 6 A) STRESS INDUCED SPALLING B) SEISMIC SPALLING OF BRITTLE MEMBRANE (AFTER STACEY 2001) ..... 19

FIGURE 2. 7 PLASTIC FITTED DRAIN HOLES AFTER (HOEK, 2011) ..... 20

FIGURE 3. 1 TENSILE TEST AFTER, TANNANT *ET AL* (1999), SPEARING AND GELSON (2002) ..... 26

FIGURE 3. 2 A) ADHESION TEST (TANNANT *ET AL*, 1999) B) CORE TO CORE ADHESION TEST (SPEARING, 2001) .... 28

FIGURE 3. 3 CORE SAMPLE AND CONTROLLED LINED ROCK CORE FAILURE (TARR *ET AL* 2006) ..... 29

FIGURE 3. 4 PUNCH THROUGH TEST (SPEARING *ET AL* 2001) ..... 30

FIGURE 3. 5 SHEAR BOND STRENGTH TESTING (YILMAZ 2007) ..... 31

FIGURE 3. 6 TEST SETUP FOR BRAZILIAN TEST ..... 35

FIGURE 3. 7 FAILED BRAZILIAN SPECIMEN ..... 36

FIGURE 3. 8 BRAZILIAN STRENGTH TEST RESULTS FOR TSL A, B AND C ..... 40

FIGURE 3. 9 COMPRESSION STRENGTH DEVELOPMENT OVER CURING TIME ..... 43

FIGURE 3. 10 STIFFNESS RESULTS ..... 45

FIGURE 3. 11 BENDING TEST SET UP AFTER (VESEL Ý, 2007) ..... 46

FIGURE 3. 12 FAILED SANDSTONE SAMPLE ..... 48

FIGURE 3. 13 BENDING TEST GRAPHS ..... 49

FIGURE 3. 14 POSITIONS OF APPLIED LOAD AND DEFORMATION MEASUREMENTS ..... 54

FIGURE 3. 15 TUNNEL MODEL SET UP ..... 54

FIGURE 3. 16 PARAMETERS THAT WERE MEASURED INSIDE A TSL SUPPORTED TUNNEL ..... 55

FIGURE 3. 17 CRACK LOCATION A), B), C) AND D) ..... 56

FIGURE 4. 1 TSL A SHEAR FAILURE ..... 61

FIGURE 4. 2 EXAGGERATED ECCENTRIC LOADING ..... 62

FIGURE 4. 3 ADHESION LOSS AT THE CORNER OF THE TUNNEL ..... 63

FIGURE 4. 4 ADHESION FAILURE OF THE LINER A)ON THE SIDEWALL B) AT THE CORNER OF THE TUNNEL ..... 64

FIGURE 4. 5 A) SHEAR FAILURE AT THE TOP RIGHT HAND CORNER OF THE TUNNEL B) SHEAR BOND FAILURE ..... 65

FIGURE 4. 6 SHEARING OF THE LINER AT THE RIGHT HAND CORNER A) AND B) ..... 66

FIGURE 4. 7 A)SHEARING AND FLEXURE AT THE RIGHT CORNER B) BLOCK CRUSHING AT THE LEFT CORNER ..... 66

FIGURE 4. 8 COMPRESSION FAILURE OF THE LINER AT THE CORNER ..... 67

FIGURE 4. 9 FLEXURAL FAILURE A) ON THE LEFT SIDEWALL FOR $60^0$ B) ON THE SIDEWALL FOR $80^0$ ORIENTATION 68

FIGURE 4.10 FLEXURAL FAILURE AT THE ROOF OF THE TUNNEL A) FOR $60^0$ ORIENTATION B) FOR $80^0$ ORIENTATION ..... 69

FIGURE 4.11 TUNNEL SQUEEZING BEFORE SIDEWALL COLLAPSE ..... 69

FIGURE 4.12 A) TENSILE FAILURE ON THE SIDEWALL B) TENSILE FAILURE ON THE SIDEWALL NEAR THE FOOTWALL ..... 70

FIGURE 4. 13 LINER A SUPPORTING LOOSE BLOCK IN THE ROOF OF THE TUNNEL AT THE END OF TEST ..... 71

FIGURE 4.14 LOADING STAGES OF THE TUNNEL MODEL FOR TSL A AT $45^0$ ORIENTATION A), B) AND C) ..... 72

FIGURE 4.15 LOADING STAGES OF THE TUNNEL MODEL FOR TSL A AT $60^0$ ORIENTATION A), B) AND C) ..... 73

FIGURE 4.16 LOADING STAGES OF THE TUNNEL MODEL FOR TSL A AT $80^0$ ORIENTATION A), B) C), D) AND E).... 74

FIGURE 4.17 LOADING STAGES OF THE TUNNEL MODEL FOR TSL B AT $45^0$ ORIENTATION..... 75

FIGURE 4.18 LOADING STAGES OF THE TUNNEL MODEL FOR TSL B AT $60^0$ ORIENTATION A), B) AND C)..... 76

FIGURE 4.19 LOADING STAGES OF THE TUNNEL MODEL FOR TSL B AT $80^0$ ORIENTATION A), B) AND C)..... 77

FIGURE 4.20 LOADING STAGES OF THE TUNNEL MODEL FOR TSL C AT $45^0$ ORIENTATION A), B1), B2) AND C) .... 78

FIGURE 4.21 LOADING STAGES OF THE TUNNEL MODEL FOR TSL C AT $60^0$ ORIENTATION A), B) AND C)..... 79

FIGURE 4.22 LOADING STAGES OF THE TUNNEL MODEL FOR TSL C AT $80^0$ ORIENTATION A), B), C) AND D) ..... 80

FIGURE 4.23 A) BASKET AND PROMOTION OF BLOCK INTERLOCK B) SECTION LINE ON A BRAZILIAN DISC..... 81

FIGURE A.1 TSL A BRAZILIAN TEST GRAPHS A), B), C) ..... 112

FIGURE A.2 BRAZILIAN TEST GRAPHS A), B), C)..... 113

FIGURE A.3 BRAZILIAN TEST GRAPHS A), B) AND C) ..... 114

# List of Tables

TABLE 2.1 IDEAL TSL PROPERTIES (ESPLEY-BOUDREAU, 1999) ..... 22

TABLE 3.1 PREVIOUS TSL TESTING (POTVIN *ET AL*, 2004) ..... 25

TABLE 3.2 BRAZILIAN STRENGTH RANKING ..... 37

TABLE 3.3 BRAZILIAN INDIRECT TENSILE STRENGTH TSL A ..... 38

TABLE 3.4 BRAZILIAN INDIRECT TENSILE STRENGTH TSL B ..... 38

TABLE 3.5 BRAZILIAN INDIRECT TENSILE STRENGTH TSL C ..... 39

TABLE 3.6 STRENGTH EQUATIONS AND CORRELATION COEFFICIENTS ..... 40

TABLE 3.7 COMPRESSION STRENGTH RESULTS ..... 43

TABLE 3.8 COMPRESSION STRENGTH EQUATIONS AND CORRELATION COEFFICIENTS ..... 44

TABLE 3.9 THREE-POINT BENDING RESULTS ..... 49

TABLE 3.10 BENDING STRENGTH EQUATIONS AND CORRELATION COEFFICIENTS ..... 50

TABLE 3.11 TOTAL DEFORMATION MEASURED AT COLLAPSE OF THE TUNNEL, IN MILLIMETRES. ..... 57

TABLE A.1 BRAZILIAN INDIRECT TENSILE STRENGTH USED ON 1MM THICKNESS FOR TSL A ..... 103

TABLE A.2 BRAZILIAN INDIRECT TENSILE STRENGTH USED ON 3MM THICKNESS FOR TSL A ..... 104

TABLE A.3 BRAZILIAN INDIRECT TENSILE STRENGTH USED ON 5MM THICKNESS FOR TSL A ..... 105

TABLE A.4 BRAZILIAN INDIRECT TENSILE STRENGTH USED ON 1MM THICKNESS FOR TSL B ..... 106

TABLE A.5 BRAZILIAN INDIRECT TENSILE STRENGTH USED ON 3MM THICKNESS FOR TSL B ..... 107

TABLE A.6 BRAZILIAN INDIRECT TENSILE STRENGTH USED ON 5MM THICKNESS FOR TSL B ..... 108

TABLE A.7 BRAZILIAN INDIRECT TENSILE STRENGTH USED ON 1MM THICKNESS FOR TSL C ..... 109

TABLE A.8 BRAZILIAN INDIRECT TENSILE STRENGTH USED ON 3MM THICKNESS FOR TSL C ..... 110

TABLE A.9 BRAZILIAN INDIRECT TENSILE STRENGTH USED ON 5MM THICKNESS FOR TSL C ..... 111

TABLE B.1 COMPRESSION RESULTS FOR TSL A ..... 115

TABLE B.2 COMPRESSION RESULTS FOR TSL B ..... 116

TABLE B.3 COMPRESSION RESULTS FOR TSL C ..... 117

TABLE C.1 BENDING TEST RESULTS TSL A ..... 118

TABLE C.2 BENDING TEST RESULTS TSL B ..... 119

TABLE C.3 BENDING TEST RESULT FOR TSL C AND D ..... 120

TABLE D.1 CUMULATIVE DEFORMATION APPLIED TO THE SIDE PLATES IN MILLIMETRES ..... 121

# List of Symbols and Terms Used

| | |
|---|---|
| A | cross sectional area ($m^2$) |
| $a_0$ | crack depth (mm) |
| b | sample width (m) |
| Cov | coefficient of variance |
| D | diameter of the disc (m) |
| $d_{1, 2}$ | diagonals of the tunnel model (m) |
| $E_f$ | flexural Modulus of elasticity, (MPa) |
| h | sample height (m) |
| $h_{r, c, l}$ | tunnel model heights measured from right, centre and left (m) |
| L | support span (m) |
| LHS | left hand side |
| *m* | Slope of the tangent to the initial straight-line portion of the load deflection curve, (N/mm) |
| P | maximum applied load, Newton's |
| RHS | right hand side |
| $R^2$ | correlation coefficient |
| Stdev | standard deviation |
| t | thickness of the disc (m) |
| TSL | thin spray-on liner |

| | |
|---|---|
| $w_{t, c, b}$ | tunnel model width measured at the top, centre and bottom (m) |
| $\Delta d_{1, 2}$ | deformation of the diagonals of the tunnel model (m) |
| $\Delta h_{r, c, l}$ | deformation of the tunnel model heights measured from right, centre and left (m) |
| $\Delta u_{lt, lc, lb}$ | applied displacement on the left hand side of the frame at the top, centre and bottom (m) |
| $\Delta u_{rt, rc, rb}$ | applied displacement on the right hand side of the frame at the top, centre and bottom (m) |
| $\Delta w_{t, c, b}$ | deformation of the tunnel model width measured at the top, centre and bottom (m) |
| $\sigma_f$ | Stress in outer fibres at midpoint, (MPa) |
| $\sigma_t$ | indirect tensile strength of rock, (MPa) |

# CHAPTER 1

# Introduction

## 1.1 Background

The mining industry in South Africa has been a main driving force of the country's economy, fostering growth, development and providing the foundation for the strongest economy on the African continent for decades (Chamber of Mines of South Africa, 2008). South Africa has the deepest mines in the world and the gold mining companies are looking to mining even deeper, as long as the metal prices allow profitable operation. The prize for going deeper than ever before is driven by vast reserve of mineral resources at least equal to what has been mined already (Internet, 2000). This mining would extend the life of South Africa's mines into the next century, but mining deeper presents challenges that include heat, flooding, explosive gases, rockfalls and seismic events. The incidences of stress induced rockfalls and rock bursts are projected to increase with depth (Archibald *et al*, 2004 B), potentially influencing safety negatively.

The largest cause of injuries and fatalities in South African platinum and gold mines is rockmass instability (Daehnke *et al*, 2000, 2000B). In 2008 Henning and Ferreira (2010) reported that 57 lives were lost due to falls of ground and 748 people were seriously injured by falls of ground. Kuijpers *et al* (2004), suggest that the most common location of rock-related accidents is near active faces such as production excavations and development ends, where workers spend most of their time. Instability is caused by the lack of support coverage between support units, and in unsupported area between the face and permanent support. As a result rock blocks tend to be destabilized by the effects of gravity, bursting ground or rock deteroriation and the instability is influenced by their shape and volume. Application of surface support near the mining face would reduce the risk of rock-fall injuries before significant tunnel or stope deformation occurs.

In the 1930s shotcrete was introduced to the mining industry as surface support (Hoek *et al,* 1995) and it has been in use in combination with wire mesh and fibre reinforcement and has been widely accepted as a surface support system to mitigate falls of ground. Shotcrete however, once applied to the surface of the rock, takes time to reach optimum strength. The required thickness of the shotcrete results in large volumes of raw materials being transported to the face. Shotcrete is brittle and weak in tension and shear (Spearing *et al,* 2004). Tannant (2001) reported that a number of Canadian mines underwent substantial deformations, these lead to displacement capacity of shotcrete to be exceeded rendering it a hazard. Venter and Gardner (1998) explained the falls of shotcrete as resulting from poor adhesion of shotcrete with the rock. If shotcrete is used in combination with wire mesh, an additional cost is incurred through the installation of additional bolts to pin the mesh tightly against the excavation valleys without the benefits on safety and where mesh overlaps extra shotcrete thickness is required.

Thin sprayed liners (TSL) have been used in civil engineering as sealants before being tried in the mining industry (Kuijpers *et al,* 2004) however, in the early 1990s trials were initiated in Canada mines (Archibald, 2004). This was to substantiate the concept that TSLs enhance the structural performance of the excavation. Common TSLs, also referred to as membranes, are reactive or non-reactive polymer or water-based materials formed from a combination of cement and sand, or cement only, that are sprayed onto the rock surface at a thickness between 3mm and 5mm, and form part of surface support system. They are more flexible compared to shotcrete (which has a typical thickness of 25mm to 100mm depending on the need) and their structural capacity is negligible, but their performance is almost always reported as being better than expected (Spearing *et al,* 2001 and Stacey, 2004). Despite growing support for the concept, their use in the mining industry is still limited.

The advantages offered by TSLs are fast application rates, rapid curing times ranging from seconds to hours, reduced materials handling compared to shotcrete, high tensile strength with high areal coverage, high adhesion which enables early reaction against

ground movement, and ability to penetrate into joints (Tarr *et al*, 2006, Kuijpers *et al*, 2004, Finn, 2004, Pappas *et al*, 2004). Stacey (2001) suggests that these advantages lead to improved cycle times, increased mechanisation and improved safety.

The use of flexible support membranes prevents rock degradation and structural failure of excavations by mobilizing and conserving the inherent strength of the rock mass immediately about the excavation surface. Thus the opening of fractures is restricted and key blocks are maintained in place from an early stage, and the rockmass strength and excavation stability can be enhanced. Kuijpers *et al* (2004), Güler *et al* (2001) state that it is in practice difficult to quantify the parameters that accurately reflect the combined effects of fracturing and induced stresses on rockmass stability. As a result, the mechanisms by which the liners support the rock need to be understood and incorporated into an engineering support design. Kuijpers *et al* (2004) and Daehnke *et al* (2001) suggest that design of surface support systems has to be based on experience, assumptions and cost considerations. The mechanisms of behaviour need to be reviewed to enhance the understanding by which the TSL supports an excavation.

## 1.2 Definition of the problem

A number of different TSLs have been developed in the market. The problem identified is that there is a need to differentiate between conditions where the liner would be appropriate or inappropriate for ground stabilisation techniques, and to be able to compare liner products. There is very little knowledge and understanding with regard to the properties and support mechanisms offered by TSLs. The manner in which the liners react to imposed forces and their failure mechanisms are also still largely unknown. This is because of the absence of generally agreed testing methods, and a resulting lack of acceptable parameters, which are important in evaluating the quality and performance capabilities of TSL materials.

A number of testing procedures have been identified in the literature, and tensile and bond strength tests have met with acceptance from researchers (Yilmaz 2007, 2010, Kuijpers *et*

*al,* 2004, Saydam *et al,* 2003). These tests tend to isolate the product characteristics as opposed to generating design data. Hence the need to evaluate specific physical properties of the liner materials so as to provide valuable information regarding the characteristics of the liners for design purposes in rock engineering. The research described in this dissertation is aimed at investigating the mechanisms by which different TSL materials support an excavation. This is done by carrying out laboratory tests on coated rock samples and moulded samples as well as on demonstrational physical models.

## 1.3 Objectives

The objective of the research is to improve understanding of the mechanisms of behaviour provided by TSL materials for rock support. The primary objective is to compare the physical properties and the mechanisms of behaviour of the liners, by carrying out laboratory tests and physical model tests. The absence of generally agreed testing methods has resulted in a lack of defined "evaluation" parameters, which are important for determining the quality and performance capabilities of TSL materials. The testing procedures are meant to facilitate comparison of the TSL products, so that an informed unbiased selection process of the appropriate liner may be made.

## 1.4 Research Methodology

A review of the current knowledge on the mechanisms by which TSLs support excavations was carried out. This made use of the University of the Witwatersrand library facilities and past research carried out in the School of Mining Engineering. Further, to build a better understanding on the suitability of different liners, laboratory tests were carried out to determine physical properties and the support mechanisms of the liners.

The following is a summary of the tasks that were carried out:

- Past research on the physical properties of TSLs was reviewed;
- Past research on the mechanisms by which the TSLs support the rock and mechanisms of liner loading was reviewed;
- Laboratory testing of coated rock samples to determine the performance of different liner products;
- Physical model testing to determine the performance of the liner under multiple loading conditions.

## 1.5 Content of the Dissertation

The next chapter details background information on TSLs as surface support. Covered in this Chapter are the mechanism by which the liners support the rock, and rockmass loading conditions in relation to surface-support capacity and previous tests done on TSLs. Chapter 3 deals with the testing of TSLs, which was integral to the quantification of the physical properties and support potential. The results of the tests are also presented in this chapter. The tests allow comparisons to be made between the various products and between test procedures, so that an unbiased selection process of an appropriated surface support may be made. Discussion of the results is presented in Chapter 4, and Chapter 5 concludes this dissertation. Detailed laboratory test results are summarized in the Appendices.

# CHAPTER 2

# Mechanisms of Rock Support and Rock Failure

Chapter 1 provided the definition of a TSL, the objectives of the research and the research methodology. It was shown in Chapter 1 that the mechanisms of rock support and loading conditions of the liners cannot be ignored. This prompted a review of the literature dealing with the mechanisms by which the rock fails around excavations, the properties of liners and the mechanisms of rock support provided by TSLs. This review is included in the following sections, as well as a brief description of the mechanisms by which liners are loaded.

## 2.1 Types of Support

There are two types of support in off reef underground hard rock excavations. These are rock reinforcement and retainment elements such as rock bolts and cable bolts, which are installed in boreholes, and rock containment components such as wire mesh, shotcrete, TSLs, lacing and straps which are applied on the surface of the excavation. Surface support provides areal coverage, while faceplates and straps or lacing provide point load and strip restraint respectively (Thompson, 2004).

Rock containment support (surface support) is classified into active or passive. Mesh and lacing fall into the passive category, where the rock mass is required to move or deform in some manner before the support system becomes active. As a result, passive support does not fulfil the function of maintaining rockmass integrity, since deformation has to occur first for support to take effect. In extreme cases, contained rock fragments have to be bled out, causing further disintegration of the rockmass surrounding excavation. Shotcrete and TSLs fall into the active category, where the liner material maintains the initial rockmass integrity. It is essential that rock containment support be installed timeously after the excavating process, to ensure any movement that takes place in the rockmass is arrested

while generating load on the support elements. Such installation has to be coupled with the liner curing time and the material properties, as well as rockmass mechanisms of failure, so that an effective support action can be archieved.

## 2.2 Rock Failure Mechanisms

The behaviour of an excavation in rock depends on the structure of the rockmass in which it is constructed. Amin *et al* (2004) defined instability in a rockmass as the incapability of the rockmass to support its own weight. According to Diederichs (1999), rockmass instability in underground excavations was classified into two categories, which are: structurally controlled or gravity driven fallout, and strength controlled or stress driven rockmass failure respectively. The two categories of instability and failure can occur either individually or in combination. Structurally controlled failure is driven by the presence of discontinuities such as faults, shear zones, bedding planes and joints. Figure 2.1 by Hoek *et al* (1995) provides a simplified representation of rock mass failure around an underground opening as a result of in-situ stress levels, and degree of jointing and fracturing in the rockmass structure.

In massive rock, the structure of the rockmass has an insignificant effect on the excavation behaviour in low stress conditions. Massive rocks under low stress are free of instability, while under high stress the rock responds to stresses by spalling (Figure 2.1). However, features such as faults and dykes provide surfaces on which deformation and failure occurs. Hoek (2006) points out that failure of the intact rock is not often a problem in cases where deformation and failure are caused by sliding along individual discontinuity surfaces. Hoek *et al* (1995) suggested that, depending on the number and orientations of the discontinuities, the intact rock pieces will translate, rotate and crush in response to stresses imposed on the rockmass. Failure occurs in low and high stress environments, and in moderately jointed to highly jointed rockmasses.

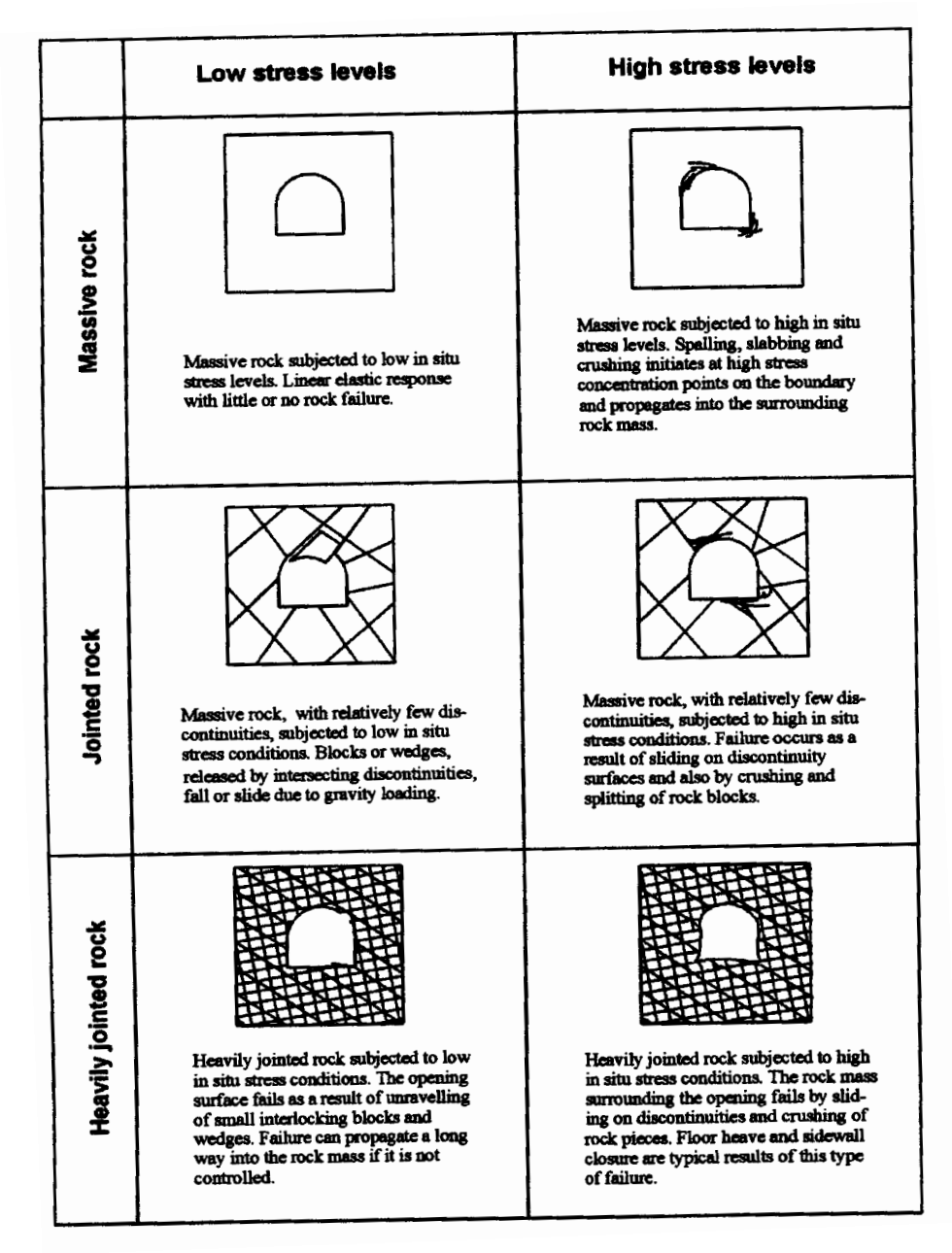


**Figure 2. 1 Modes of Failure in Hard rock Mines (after Hoek et al, 1995)**

Jointed rockmasses, besides being affected by stresses surrounding the excavation are also affected by weathering. Vorster and Franklin (2008) pointed out that exposure to water and air can accelerate deterioration of the immediate rock excavation surface, leading to roof and sidewall failure and possible collapse. Laubscher (1990) emphasized that

weathering affects rock parameters such as intact rock strength (IRS) and rock quality designation (RQD) often with devastating effects as shown by Kimberlitic rocks.

Heavily jointed rock masses respond by unravelling in low stress conditions and by convergence under high stress in the presence of clay gouge or slickensides. Vandewalle (1998) added that failure of heavily jointed rockmasses is ductile. Hoek and Brown (1980) further explained that, for a block of rock to fall, it should be separated from the surrounding rockmass by at least three intersecting discontinuities, and in low stress environments, failure is due to gravity loading. Malan and Basson (1998) point out that the extent of the failure zone depends on the geotechnical conditions and the magnitude of stress relative to rock mass strength. Under high stress conditions failure may occur gradually as spalling or slabbing or may occur suddenly in the form of a rock burst. Archibald *et al* (2004A) mentioned that spalling and crushing of the excavation walls leads to continuous failure if the excavation was not supported.

Failure in weak rock is progressive and occurs in the rock surrounding an underground excavation (Figure 2.1). Hoek (2006) points out that this is a difficult analytical problem and there are neither simple numerical models nor calculations that can be used to define acceptable limits to this failure process. He suggests that judgment on the adequacy of a support design has to be based upon an evaluation of the magnitude and distribution of deformations in the rock and the stresses induced in support elements.

Control of displacements of a fractured rockmass requires the installation of support elements, or the implementation of a mining sequence which limits the adverse consequence of extensive fracturing. Diederichs (1999) emphasized that it is important to understand both structurally controlled and stress driven failure, the effects of tensile strength and confinement for predictions of ground fall potential or rock failure. He states that stable excavation conditions occur when the field stresses are 1/5 of the UCS of the rock in an unweathered massive rock.

Analysis of the stability of excavations depends on the correct interpretation of the structural geological conditions in the rock mass. These include the identification of the blocks and wedges that can be released by the creation of the excavation. Hoek (2006) places emphasis on the analysis of the stability of the blocks and wedges. Kuijpers (2004) argues that in practice, it is difficult to quantify parameters which accurately reflect the combined effects of fracturing and induced stresses on rock mass stability and that the design process of support systems can therefore not be accurate, but must be based on assumptions and experience. However, Hoek et al (1995) and Brady and Brown (1985) suggested that the objective of the ground control system was not to prevent the failure from occurring, but to control and manage the deformations that result from the failure. Therefore, ground control systems need to cater for the behaviour of the rockmass based on assumptions and experience. Brady and Brown (1985) pointed out that the key step in the design process was the determination of stress distribution around the excavations. Napier *et al* (1995) suggest that the identification of the mechanisms of rock failure presents a basic step in the understanding of the rockmass behaviour and provides a foundation for the design of appropriate surface support.

## 2.3 Mechanisms of Rock Support

The stability of the rockmass skin in an excavation is initially controlled by the competence of the rockmass and the load bearing resistance of the intact rock pieces. Sliding and opening of the fractures, relaxation of confinement, and weathering all reduce the competence, and load bearing capacity, of the skin of the rockmass with time. Sliding and opening of fractures starts on the surface of the excavation, and preventing this type of surface failure and further unravelling is important for maintaining a stable excavation. The effectiveness of any stabilising method, according to Amin *et al* (2004), depends on the rockmass characteristics and the stabilising mechanisms of the selected support method. There are various methods for stabilising rock such as rock reinforcement support systems and rock containment support systems. Different rock containment systems display different mechanisms of behaviour and different mechanisms by which they

support the excavation. Stacey (2001) described the most common mechanisms of loading and mechanisms of behaviour of TSL support. These mechanisms occur either individually or in combination, and they are particularly relevant in determining the characteristics of the liner support mechanisms with regard to their containment function. The following sub sections provide a brief description of the relevant liner support mechanisms.

### 2.3.1 Promotion of Block interlock

According to Daehnke *et al*, (2000) the fragments on the boundaries of excavations are created by natural discontinuities such as bedding planes, joints and faults, as well as mining induced fractures due to blasting and excessive static stress. These fragments, if not supported, may rotate and move obliquely, resulting in block failure. Thus, by retaining the fragments together, surface support prevents the rock mass from dilating, loosening and unravelling, reducing the likelihood of formation of further cracks. Stacey (2001) identified the mechanism of promotion of interlock of small key blocks in the preservation of stability. Promotion of block inter lock involves other sub mechanisms such as penetration of the liner into the joints and restricting rotational shear, due to the tensile and bond strengths of the material (Figure 2.2). Archibald *et al* (2000) estimated that a 2mm liner is capable of supporting a wedge that imposes gravity loading of as much as 7 tonnes per square metre, as long as liner adhesion and crack filling exist. Hoek and Brown (1980) pointed out that this mechanism is particularly important in assisting the rockmass to support itself.

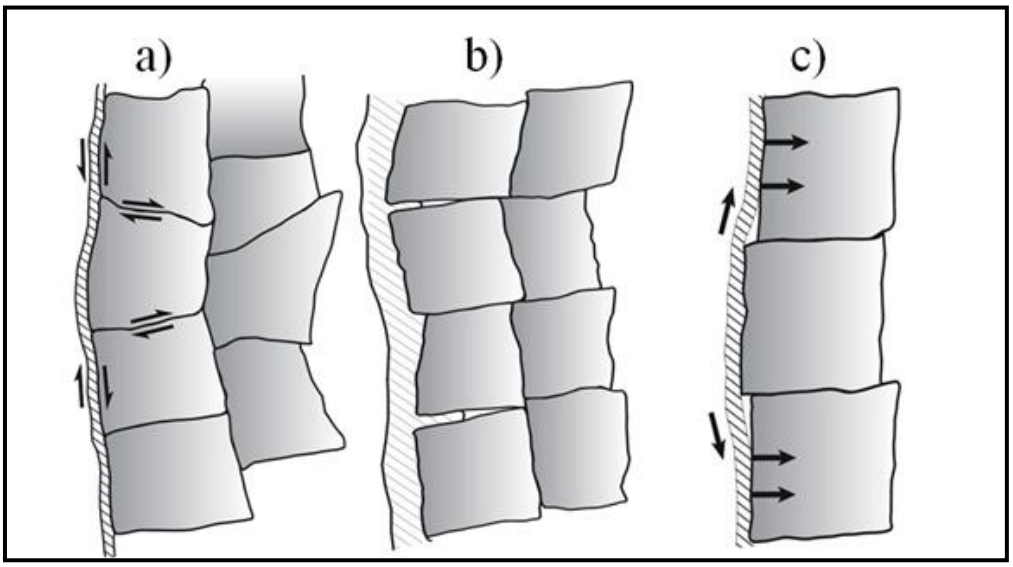


**Figure 2. 2 a) Shear and rotational resistance, b) crack infilling and c) tensional resistance (After Stacey 2001)**

### 2.3.2 Basket Mechanism

This mechanism occurs in two situations. The first situation involves a combination of rock reinforcement elements and rock containment elements where the liners provide support to failed rock by containing it forming a basket while using the rock reinforcement as the stable medium. Stacey (2001) identified the main support functions as the flexural rigidity or ductility, which resist deflection of the liner to form a basket between tendons, and the tensile strength of the liner. However, stress concentration in between the tendons may lead to premature failure of the liner and then to overall instability (Güler *et al,* 2001). Joughin *et al* (2010) added that the liner acts as load distributing conduit during secondary failure between tendons.

The second situation involves the rock containment element only where partial adhesion and tensile strength of the liner material is considered. A basket is developed between stable relatively large blocks and unstable small blocks. Kuijpers and Toper (2002) indicated that, if partial loss of adhesion between the liner and unstable rock blocks occurs, while adhesion is maintained with stable rock blocks, then the liner tensile

strength is responsible of containing failed rock. Kuijpers *et al* (2002) added that, in fragmented rockmasses, large loads are transmitted to the liner and hence surface support elements are designed in terms of their tensile strength, stiffness and yielding capacity. A relatively stiffer liner will fail before a basket is formed. They go on to say that, it is equally important to avoid high stress concentrations as these locations lead to premature failure of surface support.

### 2.3.3 Air Tightness

Coates (1970) identified this mechanism, namely that if the applied surface support is air tight, entry of air is prevented. Hence, dilation is restricted and as a result, failure would be prevented or inhibited. However, Stacey (2001) argues that this mechanism could be applicable to dynamic loading situations where rapid entry of air into the rock mass is restricted, and an airtight membrane would promote stability, but the mechanism is unlikely to occur under static loading.

### 2.3.4 Extended Face Plate

Stiff support will extend the area of influence of the rock bolt or cable bolt faceplate (Stacey, 2001) if the faceplate is placed on top of the liner. The choice of the type of faceplate is important. Ortlepp and Stacey (1997) identified that faceplates formed by conventional punching increase the likelihood of point loading and guillotining of containment support in dynamic loading conditions.

### 2.3.5 Durability Enhancement

This mechanism is applicable for those rock types that deteriorate rapidly when exposed to wetting and drying such as Kimberlite. The fractured rock continues to unravel or weather through the micro fracturing process, resulting in block failure leading to bed separation. With the application of the liner, the rock is supported, by sealing it from weathering elements, thereby preserving the inherent strength of the rockmass (Finn *et al*, 1999, Bartlett and Nesbitt, 2000 and Stacey, 2001). Non-water based liners will provide

better support capabilities to those rocks that deteriorate when exposed to moisture. The use of surface support also protects other support elements such as wire mesh and bolts from corroding (Dube, 2009).

## 2.4. Surface Support Pressure

Brady and Brown (1985), Cristescu and Duda (1989), Vandewalle (1998) and Kuijpers *et al* (2004) report that the stiffness and time of installation of the support element has an influence on displacement control. The effectiveness of surface support for an underground excavation, can be assessed in terms of support pressure. According to Cristescu and Duda (1989) the main aspects are the stress evolution in the support, the pressure and the displacement at the interface of the surface support, taking into consideration the thickness of the unstable ground. Furthermore, the condition under which stabilization was reached was dependent on the characteristics of the surface support and the post failure residual strength of the rockmass. Brady and Brown (1985) presented a conceptual surface support reaction curve shown in Figure 2.3. The following discussions concern the development of displacement at a point on the periphery of the excavation as the heading advances, and the behaviour of different surface support systems represented by line 1, line 2, line 3 and line 4 as seen in Figure 2.3. In the discussion the term surface support refers to a TSL and will be used in the section to describe the effectiveness of support that was encountered in the support reaction curve.

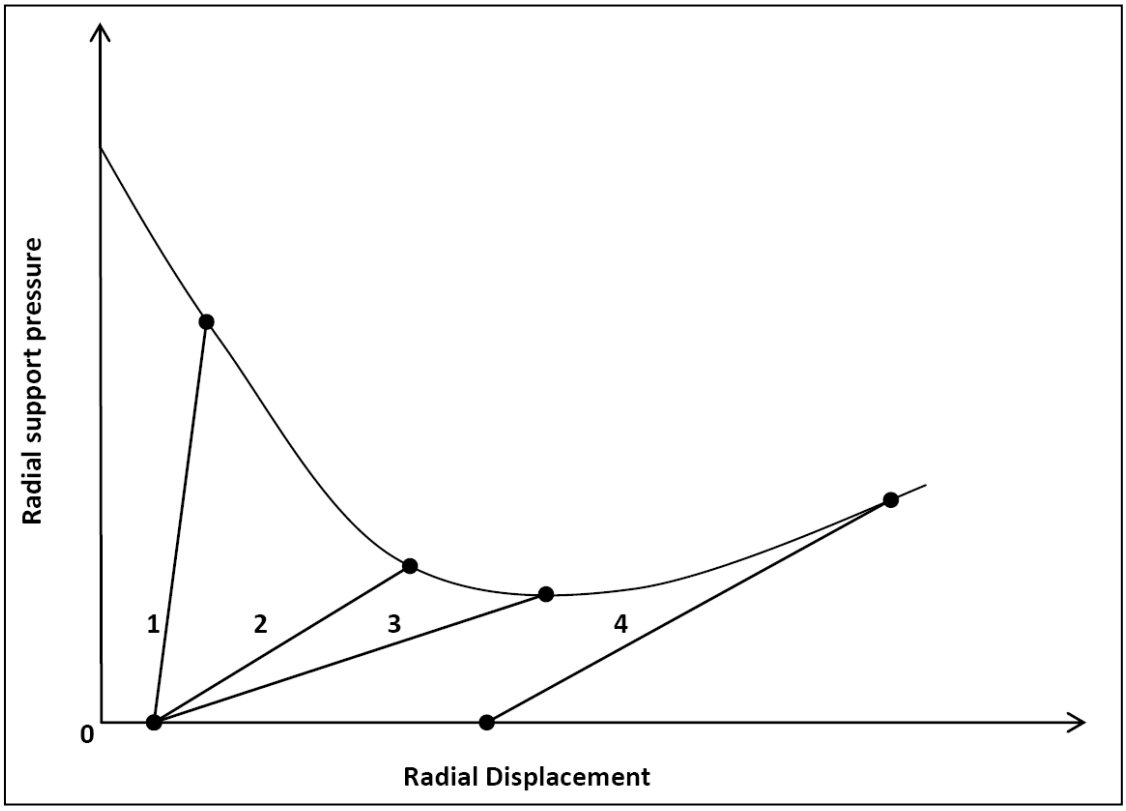


**Figure 2. 3 Support Reaction Curve after (Brady and Brown, 1985)**

- Figure 2.3 line 1 shows that a stiff surface support system was installed after a small displacement has occurred, but fails following further loading when the excavation advances. The surface support was applied early before significant deformation had occurred resulting in support failure before equilibrium is reached. The system shows poor support design and support installation time.

- Figure 2.3 line 2 shows a surface support system that was less stiff than the Line 1 support and that was installed at the same time as line 1 support, but reaches equilibrium with the rockmass. This surface support system was ideal for effective ground support where ground deforms as the tunnel advances and surface support is installed on time to absorb deformation, thereby increasing the residual strength of the rockmass. This system preserves the initial excavation conditions using the

rockmass and surface support to reach equilibrium as suggested by Hoek *et al* (1995) and Brady and Brown (1985).

- Figure 2.3 line 3 shows a surface support system that was soft compared to line 2 support, installed at the same time as line 1 and line 2 support, but that reaches equilibrium when failure of the skin of the excavation has occurred. Stacey (2001) described this mechanism as the basket mechanism. This mechanism utilises the material's tensile strength to contain the failed rock pieces. Kirsten (1998) adds that such surface support was used to hold rock fragments in ground that is subjected to steady state convergence.

- Figure 2.3 line 4 shows a surface support system with similar properties to line 2 support which is installed at a time when considerable radial deformation has occurred. Hence, support will fail without fulfilling its purpose as it is carrying the dead weight of the rockmass. This was due to initial rock movement and the on-going unravelling process, such that the surface support will be loaded beyond its support capacity. If the surface support is not stiff enough, the support reaction curve and ground reaction curve never intersect and equilibrium is not achieved, resulting in support collapse and excavation failure.

## 2.5 Surface Support Loading Mechanisms

Stacey (2001) and Tannant (2001) determined the common loading mechanisms for liner support. These mechanisms can occur under static or dynamic loading conditions. The next sections discuss the mechanisms by which the liners are loaded.

### 2.5.1 Gravity Loading by Wedge and Key Block

This type of liner loading occurs in excavations where the major rock failure mechanism is gravitational loading. As previously mentioned, the movement of a key block subjects the liner to punch loading across the joints giving rise to tensile or shear loading depending on the relative block movement (Figure 2.4).

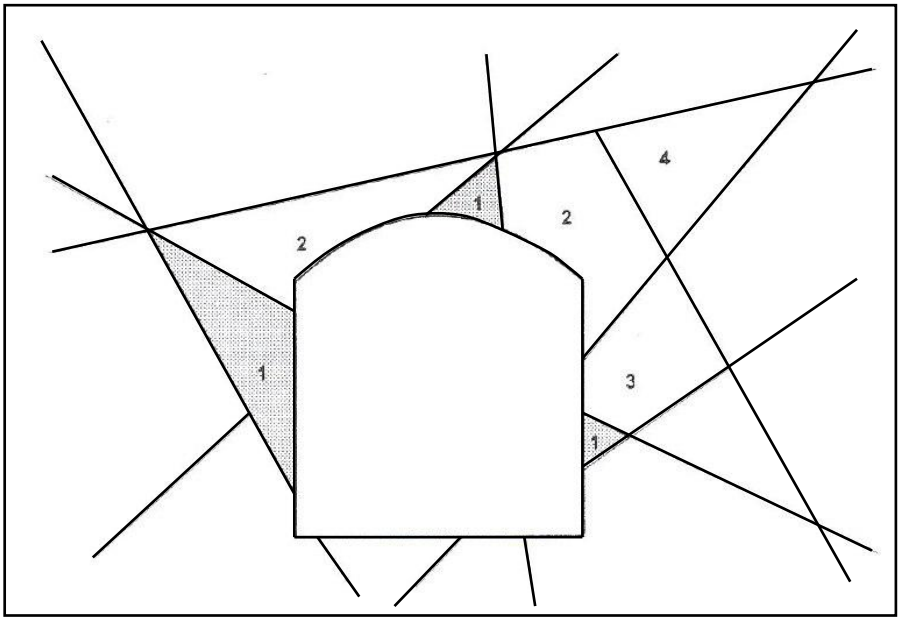


**Figure 2. 4 Key block theory; shaded blocks are unstable (After Barrett and McCreath 1995)**

### 2.5.2 Distributed Surface Loading

Espley *et al* (1999) and Swan and Henderson (2001) investigated distributed loading using loose blocks and, as discussed in the previous section they found that a significant portion of the supporting function comes from block-to-block interaction. The distributed loading is due to failed rock under the action of gravity, squeezing ground (because of elevated field stresses) and dynamic loading. Stacey (2001) highlighted that, if a membrane bonds well with the rock, concentrated loading occurs at the locations of joints resulting in localized failure of the liner.

### 2.5.3 Bending Surface Loading

The bending loading mechanism is found in highly stressed ground such as deep level gold mines. Stacey (2001), Stacey and Yu (2004) reported that, if support is installed on the sidewall and the roof leaving the floor to deform freely Figure 2.5 then, squeezing ground present localized loading of surface support resulting in bending or rotational moments on the sidewall and the roof, while the haunch areas are subjected to compression loading.

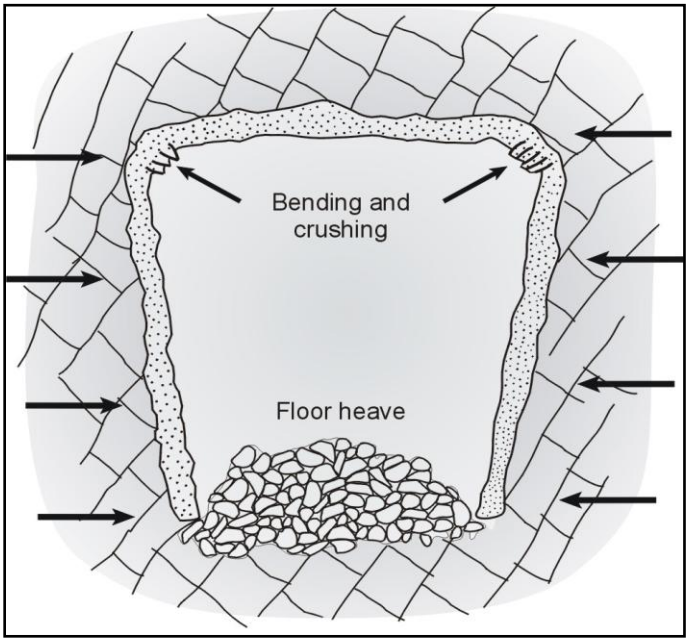


**Figure 2. 5 Squeezing ground (After Stacey 2001)**

### 2.5.4 Stress Induced Loading

When an excavation is created underground stresses are redistributed on the boundary of the excavation. In high-stress static conditions surface support is loaded due to fracturing or dog-earing (Figure 2.6 a). If the liner support is applied early before the development of fracturing as described by Brady and Brown (1985) stability could be maintained. A number other mechanisms of loading are involved such as shear and buckling (Stacey, 2001).

If induced stresses increase in the rockmass such that, they exceed the rock strength, violent failure of the rock surrounding excavations occurs. The dynamic load is transferred to the surface support and regardless of the mechanical properties of the surface support, the load imposed on the liner is greater than the mechanical properties of the liner (Figure 2.6 b). However, a flexible liner reduces the impact even though ultimate failure occurs.

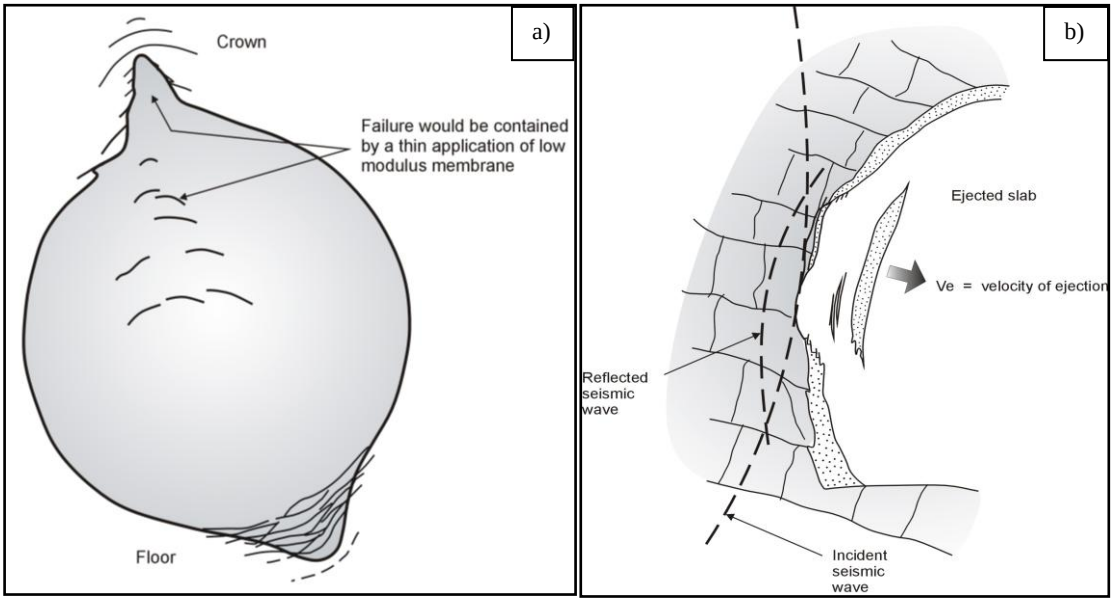


**Figure 2. 6 a) Stress induced Spalling b) Seismic spalling of brittle membrane (After Stacey 2001)**

### 2.5.5 Water Pressure Loading

Water pressure loading reduces the effective adhesive strength of the liner. Stacey (2001) pointed out that the accumulation of ground water in the rockmass induces water pressure loading to the liner, which may be sufficient to cause failure if undrained. Drain holes fitted with plastic pipes (Figure 2.7) or a porous fibre mat attached to the surface of the rock are used for this purpose (Hoek, 2011).



**Figure 2. 7 Plastic fitted drain holes After (Hoek, 2011)**

## 2.6 Properties of TSL's

The mechanism by which the rock fails around excavations presents the basis for review of the properties of the liners. Different situations encountered underground require specific TSL material properties. Rock engineering design of surface support relies on the properties of the liner products, which dictate the requirements of the membranes in terms of rock support.

TSLs are manufactured with a variety of components, which are mixed at the nozzle of the spray gun or prior to spraying. A single component consists of powder, which can be mixed with water during application. Double components consist of powder and polymer liquid, while the triple components consist of powder, sand and polymer. On mixing the components of the liner material, monomer chemicals are polymerized to form the polymer (Finn, 2004). The physical and chemical properties of the resulting polymers depend on the ratio of the initial components.

According to Finn (2004), the change in physical properties caused by altering the ratio or chemistry of the starting components is not well understood. He emphasizes that an understanding of the chemistry of the liner products is the key to understanding the support potential and limitations, as well as the environmental impact. Furthermore, advantage should be taken in manipulating the properties of the liners to suit local rockmass conditions.

### 2.6.1 Chemical Properties of TSL's

Despite the economic advantages offered by the membrane materials in terms of support, there is still concern over the environmental, occupational health and safety risks associated with the use of some TSL materials containing diphenylmethane diisocyanate (MDI). Archibald (2004), Finn (2004) and Pappas *et al* (2004) found out that 5 to 20% of exposed workers can become sensitized, and may develop life-threatening asthmatic symptoms following repeated exposures either by inhalation or skin contact. Potvin *et al* (2004) suggest that if proper procedures are used, it is possible for TSLs to be used without adverse effects on humans. It is suggested that, for a TSL to be considered a safe and efficient ground support system, it should be manufactured such that all issues affecting the health of people working it, and the environments containing TSLs, are understood and addressed.

### 2.6.2 Physical Properties of TSL's

Polymeric materials display a wide range of mechanical behaviour: brittle solid, rubbery, leathery plastic and strong fibre, and the characteristics change with temperature. A binder is used so that a variety of qualities such as strength, hardness and abrasion resistance, weathering performance and resistance to chemical attack can be used to control polymeric properties (Hall, 1981). Reinforcing fillers such as fine carbon powder serve to improve mechanical end use properties such as modulus, hardness, abrasion and tear resistance (Hall, 1981). However, Dyson (1990) suggests that it is difficult to produce a polymer that will have all the required attributes since factors that enhance some

properties diminish others. Grain boundaries of the polymers also play an important role in the properties of the materials since they are lines of weaknesses and discontinuities.

Espley-Boudreau (1999) provided some guidelines that could be used as the TSL attributes as seen in Table 2.1. The physical properties of the liner materials depend on the ambient conditions in which the liners work, such as the temperature, humidity and the condition of the surface of the substrate. Polymer materials such as polyethylene are unaffected by prolonged contact with acids or alkalis. Espley *et al* (2001) suggest that a relationship between relative humidity, air temperature and rock temperature should be considered for TSL materials, to attain appropriate site conditions for optimal liner performance.

**Table 2.1 Ideal TSL properties (Espley-Boudreau, 1999)**

| **Characteristics** | **Recommended Range** |
|---|---|
| Non-combustible | Flame spread rating < 200 |
| High tensile strength | > 5MPa |
| High adhesive strength | > 1 MPa on rock substrates |
| Tough (Hardness) | Shore A, hardness 80 |
| Elasticity | 100% to 150% elongation |
| High shear strength | > 1 MPa |
| Rapid cure time | < 1 hour |
| Water Resistant | Able to be sprayed onto humid/ wet surfaces |
| Temperature tolerant | 0°C to 40°C |
| Rapid application rates | > 1m² / minute |
| Long pot life | > than 2 hours |
| Environmentally friendly | Only mild solvents |
| Low cost | < $15/m² (Canadian Dollar) |
| Simple application | Minimal surface preparation |

## 2.7 Conclusions

The literature survey revealed that TSLs are used as surface support in jointed rockmasses in order to stabilise the excavation. The mechanisms by which the excavation fails provides important information on how the liners are loaded. It was noted that there is need to match the mechanical properties of the liners with the failure mechanisms of the rockmass so that an effective support design can be carried out. A number of mechanisms of support provided by the TSLs for rock support were covered in the literature survey. The survey shows that combinations of the mechanisms of support provided by the liners achieve stability of an excavation. An understanding of the ambient conditions in which membranes work, as well as the component mix ratio play important role in the long-term performance of the membranes and should be considered in the design of sprayed liners. The survey provided invaluable information leading to the design of test procedures in the next chapter.

# CHAPTER 3

# Laboratory Tests and Results

A review of the mechanisms of support provided by the liners and mechanisms of loading of surface support was covered in Chapter 2. Also covered was a review of the mechanisms by which rock fails around underground excavations. The reviews provide invaluable information for identifying objectives for appropriate test procedures. Based to a large extent on this type of information, various "existing" laboratory tests on TSL materials have been described in the literature. In the following sub-sections, some of these tests are described briefly, before dealing with the tests carried out as part of the research described in this dissertation.

## 3.1 TSL Failure Mechanisms

Standard material properties tests provide valuable information regarding the characteristics of the liners (Table 3.1). A number of tests have been performed in determining mechanical properties of TSLs on both a small scale and a large scale using modified standard testing procedures. The failure modes of the TSLs indicate the properties of the liners and, depending on specific considerations, some of these properties may be more critical than others. That is, the desired type of structural action to be provided by the TSL for the ground conditions and the corresponding mechanical performance.

**Table 3.1 Previous TSL testing (Potvin *et al*, 2004)**

| Test description | Reference |
|---|---|
| Tensile strength and elongation testing | Tannant et al, 1999; Archibald, 2001; Spearing and Gelson, 2002 |
| Bond (adhesive) strength testing | Tannant and Ozturk, 2003; Lewis, 2001 |
| Core to core bond strength testing | Spearing, 2001 |
| Torque testing method | Yilmaz et al, 2003 |
| Double sided shear strength testing | Saydam et al, 2003 |
| Asymmetric core punch testing | Stacey and Kasangula, 2003 |
| Punch (TSL displacement) testing | Spearing et al, 2001; Kuijpers, 2001 |
| Large scale Plate pull testing | Tannant, 1997; Espley et al, 1999 |
| Coated panel testing | Kuijpers, 2001; Naismith and Steward,2002 |
| Coated core compressive testing | Espley et al, 1999; Archibald and DeGagne, 2000; Kuijpers, 2001 |
| Box of rocks (baggage load) testing | Swan and Henderson, 1999 |
| Perforated plate pull testing | Tannant et al., 1999; Archibald, 2001 |
| Material plate pull testing | Tannant et al., 1999; Archibald, 2001 |

### 3.1.1 Tensile Strength Tests

The tensile strength and elongation tests that have been carried out were usually done according to ASTM D 638, the standard test method for testing plastics (Figure 3.1). A number of researchers (Tannant *et al*, 1999, Archibald, 2001; Spearing and Gelson, 2002, Kuijpers *et al*, 2004) have used the testing procedure for primary liner characterisation.

The test utilizes standard dog-bone shaped specimens prepared by machining, stamping, or moulding the liner material using prepared plastic moulds. The test provides an easy comparison between liner products. However, Nielsen (1962) argues that the results obtained at a single temperature and single loading rate are inadequate, as the variation in properties is a function of time and temperature. He found that at lower temperatures the material the strength and the modulus are higher. This is relevant to the properties of the TSL in mine situations where ambient conditions are subject to considerable variations.

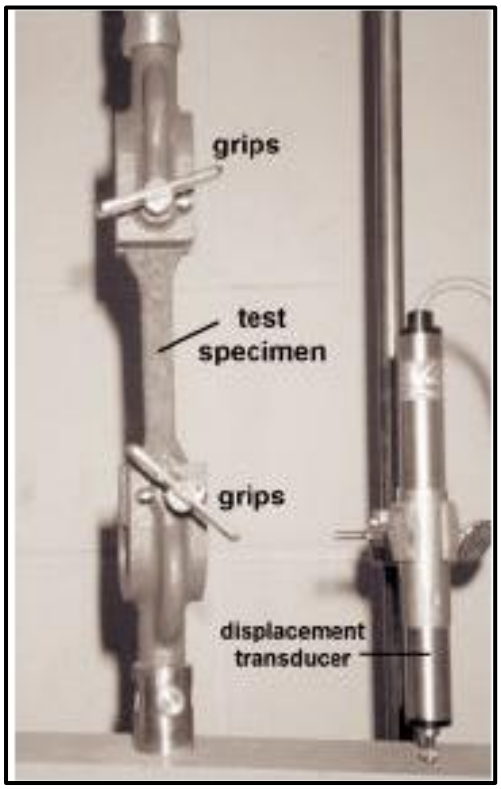


**Figure 3. 1 Tensile test after, Tannant *et al* (1999), Spearing and Gelson (2002)**

The test is sensitive to material composition and the thickness of the specimen. Potvin *et al* (2004) and Archibald (2001, 2004) found that the load deformation results vary between different liner materials evaluated and that the thickness of the TSL has an effect on load-deformation behaviour. Jansson and Thuvander (2004) studied the influence of the thickness on polymer films on their mechanical properties. They performed tensile strength tests on 7x70mm bars with thickness varying from 0.28mm to 2.6mm, at a temperature of $23.8^0$C and humidity of 50%, and loading rate of 5mm/minute. They concluded that thin films gave lower tensile strength values than the thicker films. They suggested that the reason for this was that, the short drying time of thin films "stretched" the molecules while thick films had enough time for the molecules to relax and orient themselves. Therefore the difference in tensile strength is due to crystallinity of the starch film. This calls for the minimum liner thickness to be determined for effective support design.

Nielsen (1962) quoted the study done by Carswell and Nason (1944) on the stress strain curve of polymers and they deduced the following classes, which may be useful for TSL characterisation: soft weak, hard brittle, soft tough, hard strong, and hard tough.

### 3.1.2 Adhesion Tests

The adhesion test characterises the ability of membranes to "stick" to the substrate. The significance of this test is that it indicates the ability of the liner to prevent block rotation, which is responsible for instability. Liners transfer the load created by gravity loading of loose blocks of rock onto nearby stable rock surfaces, to which the liner adheres. Seymour *et al* (2010) pointed out that the primary failure of surface support in underground mines was adhesion loss, which led to a number of different failure mechanisms. Ozturk and Tannant (2010) added that liners serve to prevent unravelling or loosening of discrete rock blocks, which may be free to dislodge from the excavation surface if there was no adhesion restraint. Kuijpers *et al* (2002, 2004B) concluded that maintaining the initial integrity and competence of the fragmented rockmass are the important functions of the surface support. Joughin *et al* (2010) highlights that relying on adhesion is not a solution for excavation support except in low stress fields for key block support. Stacey and Yu (2004) added that the rock liner bond is not a significant contributor to the capacity of the liner and high rock liner bonds causes tearing along the fracture.

Different tests have been carried out by a numbers of researchers (Tannant *et al*, 1999, Espley *et al*, 2001, Kuijpers *et al*, 2004, Kuijpers *et al*, 2004B) which include; de-bonding (shear and tension), core adhesion test, embedded dolly, glued dolly and perforated steel disc (Figure 3.2 a). These were performed under laboratory conditions and in underground situations. The results for the perforated steel disc Tannant *et al* (1999) displayed some dependence on the size of the holes and some variation with irregular surfaces of the substrate, porosity of the substrate and mineralization. However, the results of the tests by Espley *et al* (2001) have shown that the liner failed in tension and shear, which was similar to a punch through test, and therefore the influence of the bond strength was not

quantified. The tests carried out by Ozturk and Tannant (2010) established that the liner thickness has an influence on the adhesion strength.

Spearing (2001) describes the core adhesion tests consisting of two pieces of core bonded together by TSL and then pulled apart until de-bonding at the liner-rock interface occurs (Figure 3.2 b). The challenges associated with this test are the core alignment during preparation so as to prevent eccentric loading, and that curing starts at the edges of the core, affecting the curing rate at the centre of the core, and hence affecting the credibility of the results. Kuijpers (2004) carried out embedded dolly test using wet cubes of concrete that were submerged in water for 24 hours. The results showed that under humidity or with wet surfaces the adhesive bond between the liner and the rock degrades. The results of core adhesion tests carried out by Espley *et al* (2001) showed that bond strength increases with clean, dry hard surfaces and curing time. Potvin *et al* (2004) concluded that no standard methods currently exist for determining adhesion bond strength, though researchers have considered many adhesion test protocols.

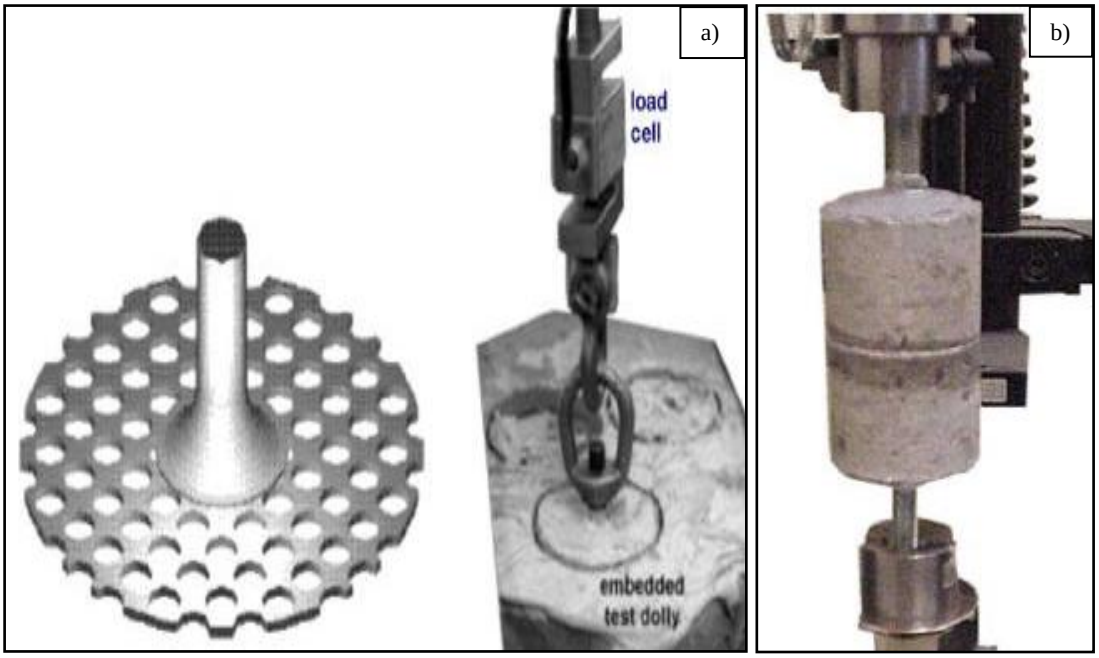


**Figure 3. 2 a) Adhesion test (Tannant *et al*, 1999) b) Core to core adhesion test (Spearing, 2001)**

### 3.1.3 Compression Failure Tests on Coated Core

The test method demonstrates the ability of surface support to provide structural reinforcement to pillars by reducing damage and by absorbing stored strain energy. Best results are achieved when de-bonding of the liner occurs. A number of researchers (Lau *et al,* 2008, Tarr *et al,* 2006, Kuijpers, 2004, Archibald and DeGagne, 2000) carried out tests on coated cylinders of core to verify support offered by TSLs. They found that flexible TSL has the ability to absorb stored strain energy following non-violent post peak failure, that is, basket mechanism. However, Kuijpers (2004) notes that while results of coated core samples are difficult to interpret in terms of TSL design, they demonstrate how the limited support could have a relatively large effect in terms of stability and load carrying capacity of the supported rock (Figure 3.3). The results also show the change from violent and brittle failure to smooth ductile failure, and the extent is directly related to the thickness of the liner. The challenge associated with this test is to achieve a uniform thickness of the liner on a curved surface.



**Figure 3. 3 Core sample and controlled lined rock core failure (Tarr *et al* 2006)**

### 3.1.4 Punch Type of Testing

This type of test demonstrates two mechanisms of support through the tensile strength and bond strength of the liner, (Figure 3.4) and demonstrates the ability of the liner to hold

loose blocks, a property that is important in the basket mechanism. Both adhesion and tensile strength are involved in supporting loose rocks and keeping them in place, and therefore in assisting the rockmass to support itself. Joughin *et al* (2010) emphasized that in hard rock excavations, the purpose of TSLs is to prevent small blocks from falling.

Spearing *et al* (2001) performed the punch through test to provide performance data for evaluating TSL materials and established that the combined effects of tensile, tear, shear and bond strength occurred in this test. Kuijpers *et al* (2004) added that tear strength cannot be ignored in punch through tests.

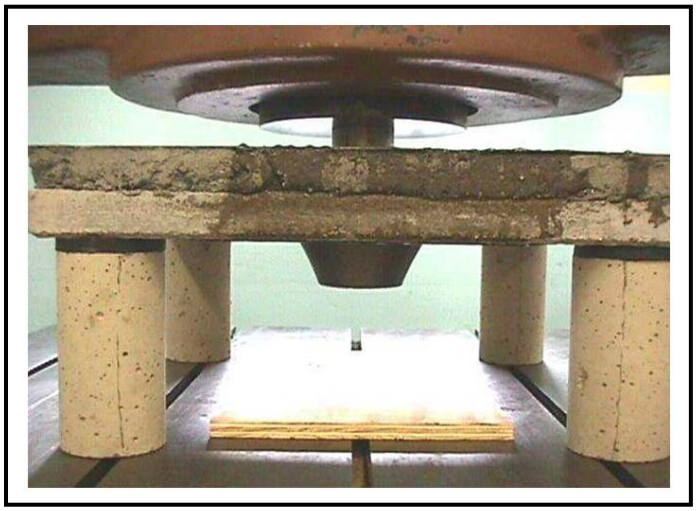

**Figure 3. 4 Punch through test (Spearing *et al* 2001)**

### 3.1.5 Shear Bond Strength Tests

The shear bond strength test was developed by Yilmaz (2007) (Figure 3.5), aimed at quantifying bond resistance against shear in particular cases where the TSL penetrates into the cracks of fractured rocks. Liner material penetrates into joints of fractured rocks promoting block interlock thereby improving the integrity of the rockmass. The results showed an increase in shear bond strength with increasing curing time. In addition, the comparison of shear-bond strength for various TSLs in the market was possible.

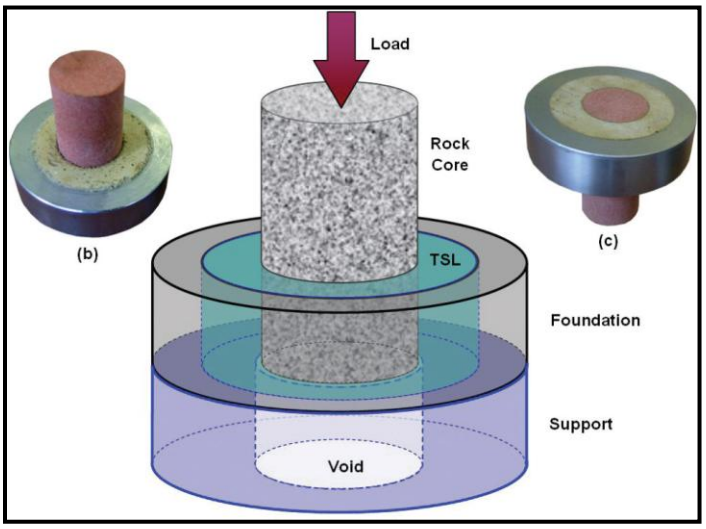


**Figure 3. 5 Shear bond strength testing (Yilmaz 2007)**

## 3.2 Laboratory Testing

The review of the literature provided invaluable information about the mechanisms by which the liners are loaded and the modes of failure. The mechanisms of support provided by the liners provided means of identifying attributes that were critical for the design of the testing procedures. To build a better understanding on the use of different liner materials that match the jointed rock conditions, new laboratory tests have been developed and carried out. The tests concentrate on determining the physical characteristics of the liner materials and comparing the performance of different TSLs materials associated with rock support. The material strength tests represent the structural competence that has to be considered for surface support (Kirsten and Labrum, 1990).

Laboratory tests that were carried out are as follows:

- Brazilian indirect tensile (TSL coated rock sample),
- Compressive strength (TSL material) and
- 3-point bending (TSL coated rock sample).

In addition, a physical model was developed to demonstrate the performance of the TSL under multiple loading conditions.

Results are presented in the form of tables showing peak strength, and graphically showing strength development for different curing times. Also presented are the results for the model tunnel, showing the mechanisms involved in surface support.

The laboratory testing was carried out to achieve the following objectives:

- To identify the failure mechanisms of the TSLs,
- To validate the mechanisms of support provided by the TSLs and,
- To compare the performance characteristics of the liners.

## 3.3 Test Guidelines

Based on the work of Spearing *et al* (2001), Naismith and Steward (2002), Saydam *et al* (2003), Yilmaz *et al* (2003) and Yilmaz (2007), the following requirements were used as guidelines for design and development of testing procedures for TSLs:

- Simple and uncomplicated,
- Test to be easily prepared at low cost,
- Practical,
- Representative of relevant properties,
- Test should have relationship to in-situ performance, and
- Statistically valid data should be generated

## 3.4 Laboratory Conditions

The environmental conditions at the University of the Witwatersrand, Rock Mechanics Laboratory at the time of testing were observed to be within the range of $15^0$ to $25^0$C, with humidity ranging from 55% to nearly 100% for winter and summer respectively. The compressive, Brazilian and three point bending tests were performed under laboratory conditions while the model testing was done outside the workshop in winter.

## 3.5 Laboratory Testing Equipment

The Material Testing System (MTS) machine was used for the Brazilian strength, compression and 3-point bending tests. The testing system consists of three major components. These include the personal computer workstation, the digital controller and the load frame. The personal computer workstation system software provides the link between the control system and the operator. The graphical user interface assists in finding and displaying the information needed to run the specific tests.

The machine loading frame assembly consists of the following items;

- Load frame – integrated construction that provides high stiffness, reducing deflection energy stored in the frame, making it ideal for testing brittle materials.
- Actuator – single ended, double acting design suitable for testing in compression and in tension and provides high loading capacity.
- Differential Pressure Transducer – provides force readout without affecting load frame stiffness. Records the pressure difference on each side of the actuator piston and this represents the force output of the actuator
- Internal Linear Variable Differential Transducer (LVDT), which is calibrated to provide the positioning control, preloading and measuring actuator displacement during testing.

## 3.6 Selected TSLs

The liner materials selected for testing were:

- TSL A, which is  a cement based liner with a mixing ratio of 4.5litres of water to 25kg cement,
- TSL B, with a mixing ratio of 1 part polymer, 2.89 parts sand and 1.78 parts cement,
- TSL C with a mixing ratio of 1part polymer to 5 parts cement.

- TSL D with a mixing ratio of 1 part polymer, 1.71 parts cement and 3.75 parts sand.

## 3.7 Testing Methods

### 3.7.1 Brazilian Tensile Strength Testing

The Brazilian test measures the tensile strength of rock indirectly. The test specimen is a disc of rock, which is subjected to diametrical compression between two opposing steel platens until failure occurs. According to linear elasticity theory, the maximum tensile stress acts in a direction perpendicular to the loaded diameter and its magnitude is proportional to the load (Fairhurst, 1964, Hudson *et al,* 1972). The literature survey did not reveal that, such testing of coated rock specimen has been done before.

The test is important since excavation boundaries often fail in tension or extension, and tensile cracking occurs as a result of elevated stress, stress relaxation, blasting and seismic activity. Napier *et al* (1995), Ryder and Jager (2002) and Ndlovu (2007) suggest that rocks in biaxial stress fields fail in tension at their uniaxial tensile strength when one principal stress is tensile and the other is compressive with a magnitude not exceeding three times that of the tensile stress. Evaluation of tensile strength is important for the analysis of rock response on the boundaries of underground excavations in biaxial stress fields. The indirect tensile strength of the rock was used to characterise different liner material properties and the results are compared for the liners used.

The Brazilian strength test was chosen as the appropriate test to assess the liner support mechanisms of rocks failing in tension under uniaxial stress field. The ultimate aim was to assess the behaviour of the sprayed liner when fractures develop in hard rock mines in unconfined areas such as stope face, tunnels and pillars. Tensile cracking is common in underground stopes, because of sagging of the roof and in structures such as pillars and bull nose areas in platinum and gold mines in South Africa due to elevated stresses. Anorthosite rock, which occurs in the bushveld complex in South Africa, was chosen as

the rock to be tested. This is a hard brittle rock common in the platinum mines, which usually fails by spalling around underground excavations.

### 3.7.1.1 Brazilian Strength Test Description

Brazilian strength testing was carried out using the MTS testing machine. A loading rate of 0.001mm/s was used with specimen dimensions of 36mm in diameter and 18mm in thickness as shown in (Figure 3.6). The liner was applied to both sides of the circular specimen on the flat faces and perspex with thicknesses of 1mm, 3mm and 5mm was used to guide the thickness of the applied liner material. The diameter of the applied liner was 34mm, slightly smaller than the diameter of the rock specimen. The reasons for smaller liner diameter as compared to the rock specimen are ease of application of the liner using the perspex as the guide to control the thickness and hold the liner in place during drying. The other reason is to isolate the liner from being loaded directly by the platens so that an unbiased assessment of the liner performance can be made. It is also possible that the liner could detach from the rock sample if loaded directly. The liner was then allowed to cure for 1day, 7days, 14days and 28days before testing.

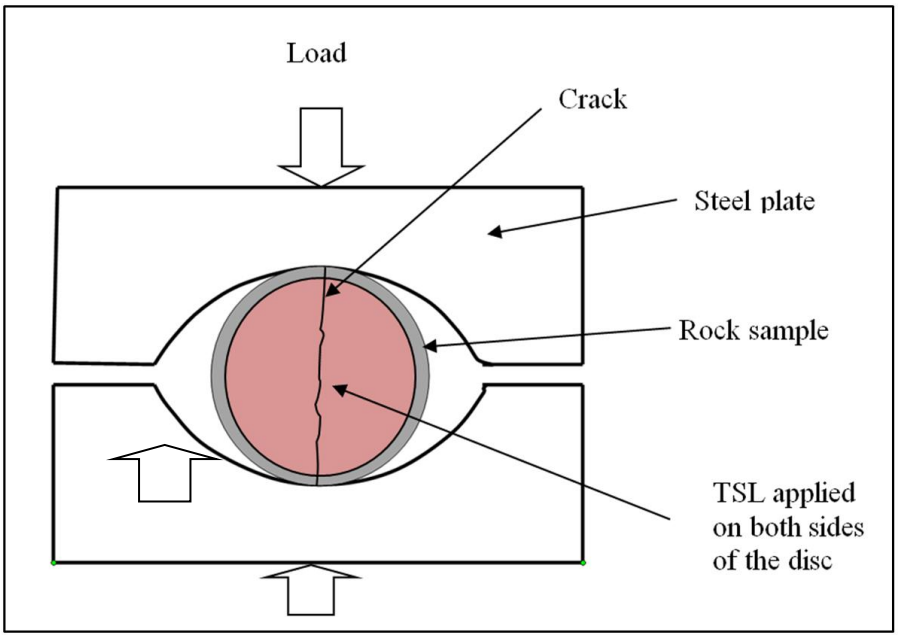


**Figure 3. 6 Test setup for Brazilian test**

### 3.7.1.2 Determination of Brazilian Tensile Strength Results

The indirect tensile strength $\sigma_t$ was determined from the following relationship:

$$\sigma_t = \frac{2P}{\pi D t}$$

Where, $P$ = load in Newtons

D = diameter of the disc in metres and

t = the thickness of the disc in metres.

The above equation assumes isotropic material properties. The formula gives the indirect tensile strength perpendicular to the loaded diameter at the centre of the disc at the time of failure when the applied load is *P*. Failure initiates at the centre of the core and propagates outwards along the loading line in the loading direction, splitting the specimen into two halves (Figure 3. 7). The strength characteristic of the liner is thought to be responsible for inhibiting the tensile failure of the rock specimen.



**Figure 3. 7 Failed Brazilian specimen**

### 3.7.1.3 Brazilian Tensile Strength Test Results

The percentage strength gain due to the liner was calculated from the mean strength of the uncoated samples and the coated samples. The liner ranking was based on the scale of strength gain (Table 3.2). Ranking of liners based on the strength gain was similar to the ranking done by (Yilmaz 2010) for his tensile strength testing. The strength gain was determined from the following relationship;

% Strength gain = (Coated mean – Uncoated mean) * 100 / Uncoated mean

**Table 3.2 Brazilian Strength Ranking**

| TSL Strength Ranking | | Percentage Strength Gain |
|---|---|---|
| Weak Liners | I | 0 - 20% |
| Medium Liners | II | 21 - 40 % |
| Strong Liners | III | >40% |

The Brazilian strength test results for the liners are presented below in Tables 3.3 to 3.5. The results shown for 191 tests carried out are the averages of the peak strengths for different curing times and different liner thicknesses of 1mm, 3mm and 5mm. Also presented are the standard deviation, coefficient of variability, percentage strength gain and liner ranking. Detailed Brazilian strength tests results are summarized in Appendix A.

The results in terms of the percentage strength gain show that TSL A lies in the weak zone for all thicknesses and curing times except 28-days for 1mm thickness where it lies in the lower medium zone with 23% strength gain. TSL B also falls largely in the weak zone except for a few values that fall in the lower medium zone. For TSL C 1mm and 5mm thicknesses fell in the medium zone, while the 3mm thickness displays a weak ranking. The results for TSL C confidently display strength improvement for the 28 day curing time. The ranking was similar to the one that was established by (Yilmaz 2010) in his tensile strength tests.

The coefficient of variability is higher for the lower rank and lower for the medium rank zone with about 10% and higher for TSL C where it ranges from 13% to 20%. The

standard deviations for all the liners are comparable, and the trend displayed is a general decrease with increase in liner thickness. There is no general trend with regard to the curing time. A large coefficient of variability displays a wide dispersion of the test results.

**Table 3.3 Brazilian indirect tensile strength TSL A**

| TSL A | Curing Time | | | | Strength |
|---|---|---|---|---|---|
| | 1 | 7 | 14 | 28 | |
| No liner | **6.4** | | | | **Mean MPa** |
| | 0.6 | | | | **Stdev MPa** |
| | 8.8 | | | | **Cov (%)** |
| 1mm | **6.5** | **7.5** | **7.6** | **7.9** | **Mean MPa** |
| | 0.9 | 0.8 | 1.1 | 0.4 | **Stdev MPa** |
| | 13.3 | 10.7 | 13.9 | 5.0 | **Cov (%)** |
| | 1 | 18 | 18 | 23 | **% Strength** |
| | I | I | I | II | **Rank** |
| 3mm | **6.8** | **7.3** | **6.8** | **6.5** | **Mean MPa** |
| | 0.3 | 0.8 | 1.1 | 0.5 | **Stdev MPa** |
| | 4.2 | 10.6 | 16.3 | 7.7 | **Cov (%)** |
| | 6 | 13 | 6 | 1 | **% Strength** |
| | I | I | I | I | **Rank** |
| 5mm | **7.3** | **7.4** | **6.9** | **7.6** | **Mean MPa** |
| | **0.8** | **0.6** | **1.0** | **0.6** | **Stdev MPa** |
| | 10.5 | 8.3 | 14.4 | 8.4 | **Cov (%)** |
| | 14 | 16 | 8 | 19 | **% Strength** |
| | I | I | I | I | **Rank** |

Total number of samples tested for TSL A = 69

**Table 3.4 Brazilian indirect tensile strength TSL B**

| TSL B | Curing Time | | | | Strength |
|---|---|---|---|---|---|
| | 1 | 7 | 14 | 28 | |
| 1mm | **7.4** | **7.5** | **7.4** | **8.3** | **Mean MPa** |
| | 0.6 | 0.8 | 1.3 | 0.2 | **Stdev MPa** |
| | 8.3 | 10.2 | 17.4 | 2.7 | **Cov (%)** |
| | 16 | 17 | 16 | 30 | **% Strength** |
| | I | I | I | II | **Rank** |
| 3mm | **7.0** | **7.1** | **7.4** | **7.6** | **Mean MPa** |
| | 0.5 | 1.1 | 0.5 | 1.0 | **Stdev MPa** |
| | 7.7 | 15.0 | 7.2 | 13.4 | **Cov (%)** |
| | 9 | 10 | 15 | 19 | **% Strength** |
| | I | I | I | I | **Rank** |
| 5mm | **7.0** | **7.9** | **7.2** | **7.7** | **Mean MPa** |
| | 0.4 | 0.3 | 0.4 | 0.4 | **Stdev MPa** |
| | 5.6 | 4.2 | 4.9 | 5.7 | **Cov (%)** |
| | 9 | 23 | 12 | 21 | **% Strength** |
| | I | II | I | II | **Rank** |

Total number of samples tested = 58

**Table 3.5 Brazilian indirect tensile strength TSL C**

| TSL C | Curing Time | | | | |
|---|---|---|---|---|---|
| | 1 | 7 | 14 | 28 | Strength |
| 1mm | **7.2** | **8.0** | **7.8** | **8.5** | **Mean MPa** |
| | 0.9 | 1.0 | 1.3 | 1.7 | **Stdev MPa** |
| | 12.7 | 13.0 | 16.4 | 20.5 | **Cov (%)** |
| | 12 | 25 | 22 | 33 | **% Strength** |
| | I | II | II | II | **Rank** |
| 3mm | **6.7** | **7.8** | **7.2** | **7.5** | **Mean MPa** |
| | 0.7 | 0.8 | 1.3 | 0.6 | **Stdev MPa** |
| | 10.1 | 10.0 | 17.6 | 8.4 | **Cov (%)** |
| | 5 | 22 | 13 | 17 | **% Strength** |
| | I | II | I | I | **Rank** |
| 5mm | **7.0** | **9.2** | **8.8** | **8.3** | **Mean MPa** |
| | 0.8 | 0.5 | 0.9 | 0.7 | **Stdev MPa** |
| | 10.9 | 5.2 | 9.7 | 8.9 | **Cov (%)** |
| | 10 | 45 | 38 | 29 | **% Strength** |
| | I | II | II | II | **Rank** |

Total number of samples tested = 64

The strength development over the curing time is best represented by a logarithmic function. The strength function and correlation coefficient ($R^2$) were determined by setting the trend line to the best fit, giving the highest ($R^2$) for all liners. The correlation coefficient for TSL A 3mm gave the lowest value, which displays loss of strength with curing time. A similar situation is experienced with the 5mm coating where a loss of strength curve is obtained as well, although the correlation coefficient is reasonably high 0.89. TSL A 1mm displayed strength gain over the curing time. The correlation coefficients for TSL B are high and display strength improvement for all the liner thicknesses as shown in Table 3.6 and Figure 3.8.

**Table 3.6 Strength equations and correlation coefficients**

| TSL | Tensile Strength Equation | $R^2$ |
|---|---|---|
| TSL A 1mm | y = 0.311In(x) + 6.411 | 0.88 |
| TSL A 3mm | y = 0.171In(x) + 6.891 | 0.36 |
| TSL A 5mm | y = 0.943In(x) + 8.473 | 0.89 |
| TSL B 1mm | y = 0.253In(x) + 7.575 | 0.84 |
| TSL B 3mm | y = 0.560In(x) + 6.348 | 0.99 |
| TSL B 5mm | y = 0.236In(x) + 7.094 | 0.53 |
| TSL C 1mm | y = 0.876In(x) + 6.289 | 0.92 |
| TSL C 3mm | y = 0.722In(x) + 6.485 | 0.68 |
| TSL C 5mm | y = 0.218In(x) + 8.056 | 0.54 |

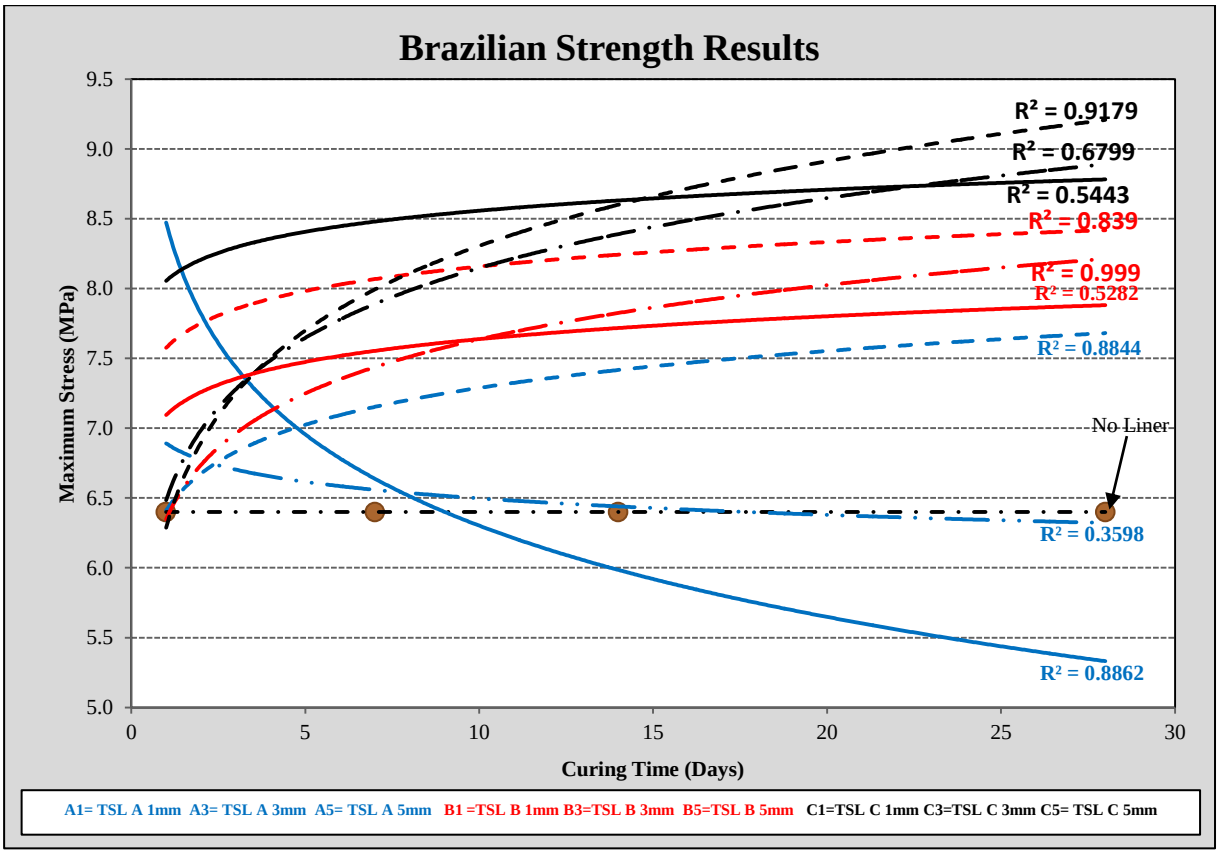


**Figure 3. 8 Brazilian Strength Test Results for TSL A, B and C**

### 3.7.2 Compressive Strength Test

Various techniques exist for the compression test and in this research, a uniaxial compression test was done on moulded samples of TSL material for different TSLs. The compression test is one of the prime test methods by which strength can be judged. When the specimen is compressed, deformation occurs and this is a function of the material properties which determines the behaviour of materials under crushing loads. Kuijpers *et al* (2004) point out that when an excavation is curved, the rock mass skin has the shape of a shell in which compressive stresses are generated, as well as in the surface support. This test seeks to assess the strength and to characterize the compressive properties of the TSL materials.

#### 3.7.2.1 Compressive Strength Test Description

The rectangular TSL material specimens were prepared by pouring the material into a rectangular plastic mould, which was 500 mm long, and allowing it to cure. The final specimen dimensions used were 70mm x 35mm x 30mm. A curing time of 7 days was used and the rectangular length was then cut into 70mm lengths which were kept for the appropriate curing times, namely 7 days, 14 days and 28 days. The 1 day curing time specimens were cut and tested 24 hours after casting. All uniaxial compression tests were carried out using the MTS machine with a loading rate of 0.01mm/sec.

#### 3.7.2.2 Determination of Compressive Strength Results

The test results were plotted in stress-strain curves, which were used to determine the yield strength. Stiffness was calculated from the load-deformation curve. The following relationships show the parameters used to determine the results:

$$\text{Compessive Stress} = \frac{p}{A}$$

$$\text{Stiffness} = \frac{\Delta P}{\Delta Deformation}$$

Where:

$P$ = peak load at failure

$A$ = cross sectional area

### 3.7.2.3 Compression Strength Results

The results of 62 tests carried out are presented in the form of tables displaying the averages strength and stiffness of the liner material. Stress and deformation values were determined at failure while stiffness was determined from the slope of the load deformation curve in the elastic region for all curing times. The deformation presented here is the one obtained from the machine readings and hence the stiffness results were used to highlight the differences of the materials.

Table 3.7 shows the mean strength values, standard deviation and percentage coefficient of variability. Detailed test results are presented in Appendix B, Tables B.1 to B.3. TSL A shows a higher percentage coefficient of variability for all curing times compared to TSL B and TSL C. This trend is similar to the one revealed by the Brazilian strength tests where weak liners display higher percentage coefficient of variability. No trend was established over the curing time for the coefficient of variability.

**Table 3.7 Compression strength results**

| Curing Time | Curing Time (Days) 1 | 7 | 14 | 28 | Strength |
|---|---|---|---|---|---|
| **Liner** | **0.1** | **4.6** | **7.0** | **8.9** | **Mean MPa** |
| **TSL A** | 0.0 | 0.4 | 1.4 | 1.9 | **Stdev MPa** |
| | 22 | 9 | 20 | 22 | **% Cov** |
| | **0.9** | **9.1** | **14.4** | **15.9** | **Mean MPa** |
| **TSL B** | 0.0 | 0.8 | 0.7 | 0.9 | **Stdev MPa** |
| | 3 | 9 | 5 | 6 | **% Cov** |
| | **1.2** | **19.1** | **22.8** | **23.1** | **Mean MPa** |
| **TSL C** | 0.1 | 1.9 | 1.3 | 0.5 | **Stdev MPa** |
| | 6 | 10 | 6 | 2 | **% Cov** |

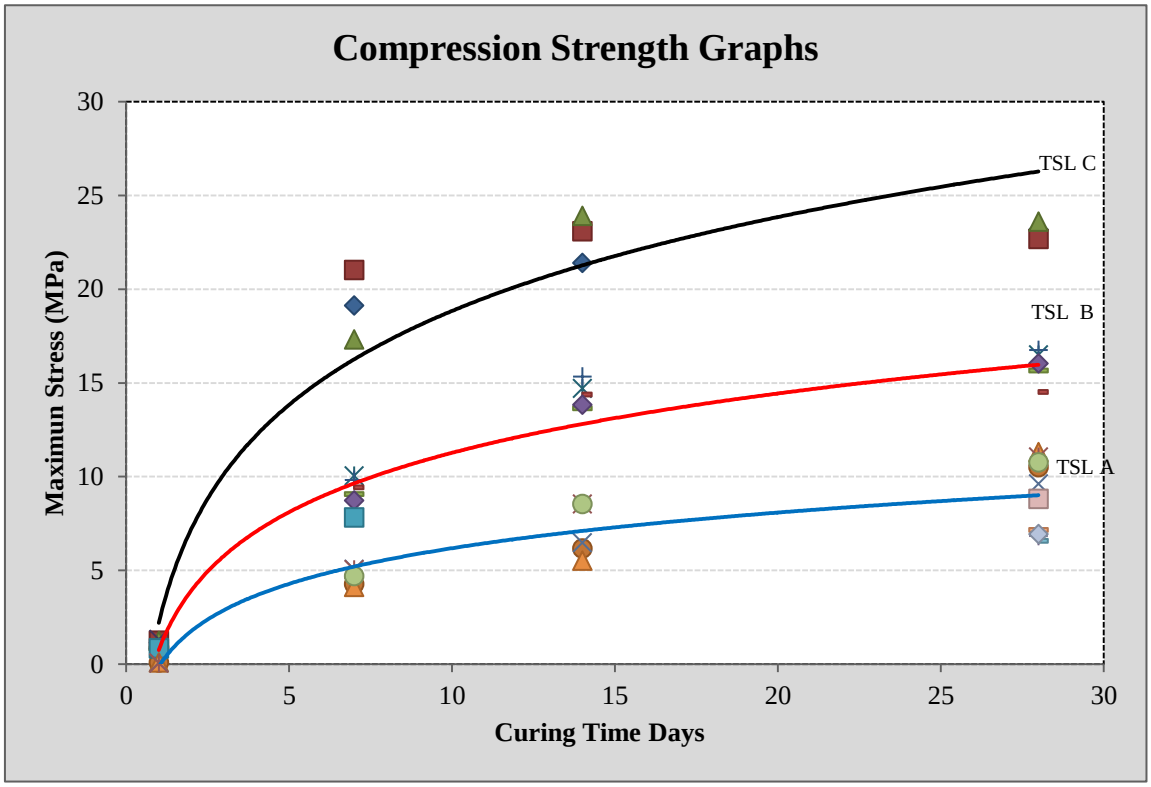


**Figure 3. 9 Compression strength development over curing time**

A logarithmic function was most suitable to represent compression strength development over the curing time and the best fit equation giving the highest ($R^2$) was used. Relative

capabilities of the sprayed liners in terms of compression strength are best compared with reference to graphs in Figure 3.9 and Table 3.8. In these, strength development over the curing time is displayed as well as compression strength equations and correlation coefficients ($R^2$). Strength development increases rapidly from 1 day to 7days and thereafter increases steadily for all the liners, but with different magnitudes. The correlations coefficient ($R^2$) decrease with increase in compression strength which compares well with the findings by Yilmaz (2010) for his tensile strength testing. The trends provide an understanding of the TSL mechanical behaviour under compression loading conditions and sensitivity towards curing time.

**Table 3.8 Compression Strength Equations and Correlation Coefficients**

| TSL | Equation | $R^2$ |
|---|---|---|
| A | y = 2.742In(x) - 0.127 | 0.98 |
| B | y = 4.564In(x) + 0.763 | 0.99 |
| C | y = 7.222In(x) + 2.209 | 0.95 |

The results of the modulus of compressibility of the liner materials are not presented since strain gauges were not used to measure the deformation of the materials. However, material stiffness was determined using the deformation measurements from the MTS machine and assuming that the platens and components deformation is constant. Figure 3.10 show that TSL C displays the highest values followed by TSL B in terms of the material stiffness, however TSL A displayed very low values and this could be attributed to the moisture content in this cement based liner. Stacey (2001) highlighted that the stiffer the liner the more effective it is in inhibiting the initial rock movement, but once rock movement has started, the liner can no longer offer any support.

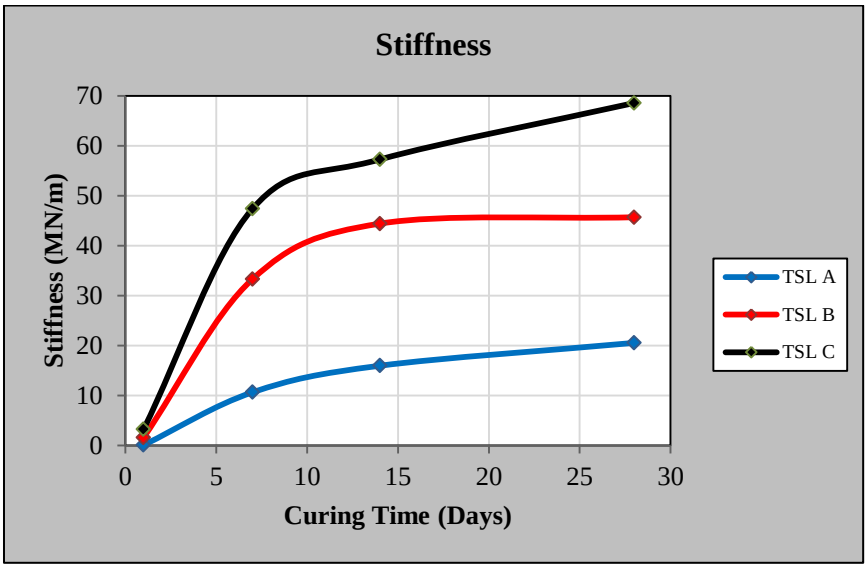


**Figure 3. 10** **Stiffness results**

Strain results are not presented because strain measurements were not taken on all TSL materials.

### 3.7.3 Three-point Bending Strength Test

The three- point bending test is a revised version of the 4-point bending tests carried out by Tarr *et al* (2006) and 3-point bending tests carried out by Lau *et al* (2008). The test configuration is similar to the tests performed by Veselý, (2007) for cracked beams to determine fracture energy of shotcrete.

South African underground coal mines use bord and pillar mining methods for extracting coal underground. The roof is composed of relatively soft sedimentary rocks supported by tendons. The formation of beams in between tendon support is common and failure of the beams can lead to tendon failure. Straight underground excavation walls, when subjected to external load tend to bend and induce compressive and tensile stresses. Therefore, it is relevant to determine the flexural strength and an appropriate procedure for this is the three point loading of small beams. A beam is used to demonstrate the reinforcing mechanism of a surface support. The test is based on the slab enhancement support mechanism.

The flexural strength is an important characteristic that has to be included in the TSL design method. This means that the design assumptions and loading conditions taking into consideration the material characteristics in terms of curing has to be included at the design stage. Thus, the surfaces of the beams were coated with a layer of TSL to absorb the tensile stresses caused by the bending. Sandstone was used as the rock beam to assess the liners in this regard, as it is uniform in composition, giving more consistent test results. It is also a soft rock and therefore the influence of the liners in terms of rock support can easily be recognized.

### 3. 7.3.1 Three-point Bending Test Description

The three-point bending flexural test was carried out in two sets of experiments. Firstly it was performed on rock specimens with 10mm "cracks" $a_0$ as shown in (Figure 3.11), and secondly it was done on rock specimens without a crack. The tests were performed using the MTS machine at a loading rate of 0.01mm/sec. The liner was applied on one side of the rock specimen with a 10mm crack depth. A perspex glass 3mm thick was used to guide the thickness of the applied liner. TSL A, B, C and D were used for the bending tests. Exadaktylos *et al* (2001) suggests that in three point bending both the bending moment and the tensile stress reach maximum value immediately beneath the point of load application and consequently the crack starts at specimen mid span. The test was also used to investigate the effect of penetration of the liner into the cracks for rock support.

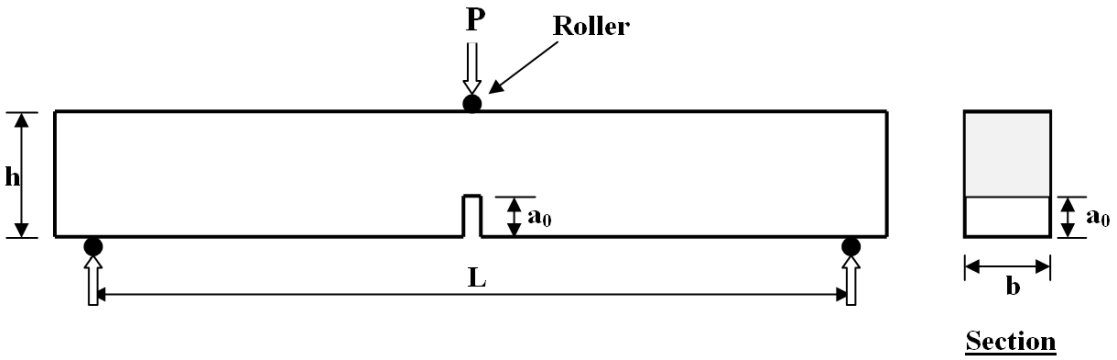


**Figure 3. 11 Bending Test set up after (Vesel ý, 2007)**

Where, L= 160mm, h = 40mm, b = 25mm, and $a_0$= 10mm.

### 3. 7.3.2 Three-point Bending Strength Results

The results were determined from the following relationship, after Exadaktylos *et al* (2001) and Cooper (1977);

$$\sigma_f = \frac{3PL}{2bh^2}$$

Where, $\sigma_f$ = Stress in outer fibres at midpoint, (MPa)

*P* = load at a given point on the load deflection curve, (N)

L = support span

b = sample width

h = sample height

*m* = Slope of the tangent to the initial straight-line portion of the load deflection curve, (N/mm)

Flexural strength is measured in terms of stress, and the value represents the highest stress experienced on the outer surface of the material at its moment of rupture (Figure 3.12). Hence, the test is designed to investigate the effect of the liner on the outer surface of the rock beams.

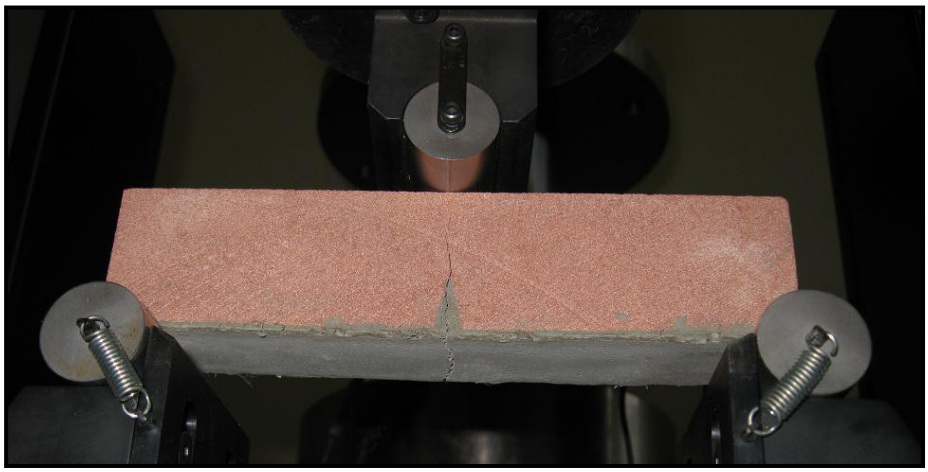

**Figure 3. 12 Failed Sandstone Sample**

The mean values for 68 samples tested are presented in Table 3.9 and in Figure 3.13. Detailed test results are presented in Appendix C, Tables C.1 to C.3. The results show great variability for one day and seven days curing time. The flexural strength of the coated sandstone for one day was reduced as compared to the uncoated rock samples. TSL B gave the lowest value of 2.8MPa for 7days curing time. TSL A and C show a general increase in beam strength with curing time, though it was not significant in terms of rock support. The results for the no-crack red sandstone were 14.4MPa whilst the cracked for seven days curing time were 12.3MPa for TSL C. Only seven days curing was done because the results showed a similar trend as the cracked red sandstone samples. Also presented in Table 3.9 are the results for white sandstone coated with a stronger TSL D, and the results show increased beam strength as compared to the uncoated samples.

The statistics of the test results in terms of the standard deviation and the percentage coefficient of variability show high values for 24 hours curing time. TSL B displays predominantly high coefficient of variability followed by TSL C and the least being TSL A.

**Table 3.9 Three-point Bending Results**

| | Uncoated | 1 | 7 | 14 | 28 | Strength |
|---|---|---|---|---|---|---|
| TSL A | **5.3** | **4.0** | **5.4** | **6.0** | **5.4** | **Mean MPa** |
| | 0.1 | 1.6 | **0.1** | **0.2** | 0.1 | **Stdev MPa** |
| | 2 | 41 | 1 | 3 | 2 | **% Cov** |
| **TSL B** | | **3.4** | **2.8** | **4.5** | **4.4** | **Mean MPa** |
| | | 2.1 | 0.5 | 2.0 | 1.6 | **Stdev MPa** |
| | | 61 | 17 | 44 | 36 | **% Cov** |
| TSL C | | **4.3** | **4.5** | **5.5** | **6.8** | **Mean MPa** |
| | | 2.9 | 1.7 | 1.7 | 0.2 | **Stdev MPa** |
| | | 68 | 38 | 31 | 2 | **% Cov** |
| **TSL D** | **1.6** | | **6.7** | | | **Mean MPa** |
| | 0.1 | | 0.5 | | | **Stdev MPa** |
| | 5 | | 8 | | | **% Cov** |
| **No-Crack** | **14.4** | | **12.3** | | | **Mean MPa** |
| TSL C | 0.6 | | 1.0 | | | **Stdev MPa** |
| | 4 | | 8 | | | **% Cov** |

Total number of tests done = 68

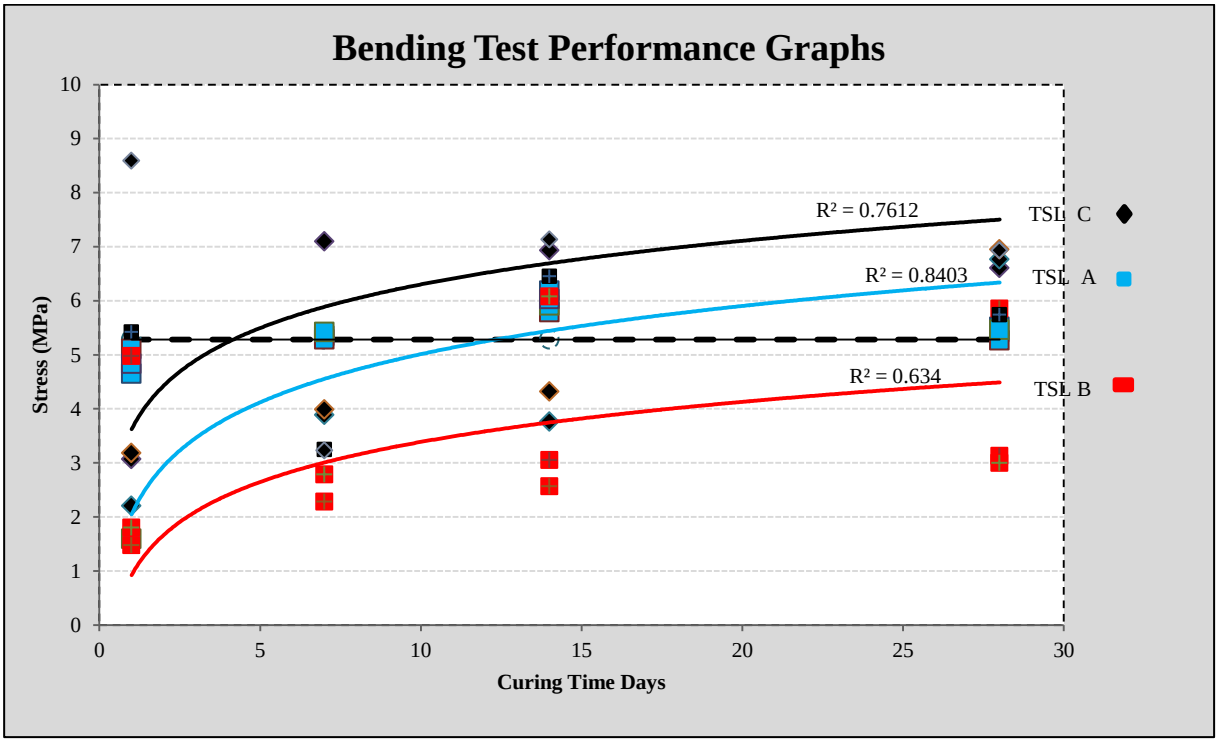


**Figure 3. 13 Bending Test Graphs**

The strength equations and the correlation coefficients for all the liners are shown in Table 3.10. The correlation coefficients show low values indicating that the test method was not clearly displayed over the 28 days curing time and decrease from TSL A to TSL C and the least is TSL B.

**Table 3.10 Bending Strength Equations and Correlation Coefficients**

| TSL | Equation | $R^2$ |
|---|---|---|
| A | y = 1.287In(x) + 2.050 | 0.84 |
| B | y = 1.070In(x) + 0.925 | 0.63 |
| C | y = 1.164In(x) + 3.622 | 0.76 |

## 3.8 Physical Model

Modelling is one of the most important engineering tools used in design and the commonly used methods are physical modelling and numerical modelling. Usually these methods are combined to solve actual problems (Park and Kicker, 1985). In design the aim is to optimise an engineering system based on predefined criteria while in mechanics the idea is to build up and improve understanding of an engineering system (Lightfoot and Maccelari, 2000). Part of this research described in this dissertation aims to improve understanding of the mechanisms of behaviour of a surface support system (TSL) and the mechanisms of support provided by sprayed liners.

Physical modelling refers to the design and implementation of systems that are based on or derived from physically recordable observations and measurements made in the field or in the laboratory. The observations and measurements are then expressed as numbers that are then, in different ways, combined into a final product (Palmstrom and Broch, 2006) and the product is transformed into a description, that expresses the objectives of the model. There are two types of physical models, qualitative and quantitative. Walliman (2004) suggests that qualitative models emphasize the relationship between entries without trying to quantify them while quantitative models not only describe the

relationship, but also accurately measure the magnitude. The two-dimensional physical model described in this dissertation, is aimed at defining, collecting and comparing qualitatively the behaviour of liners under multiple loading conditions.

Rock engineering investigational methods have a problem of limited data and with some time delays in the availability (Ivanicova, 2004, Ndlovu, 2007). As a result in rock engineering numerical modelling is used to solve complicated situations, while satisfying the laws of equilibrium and the constitutive laws in considerable detail. However, König (2002) and De Souza (2002) pointed out that while modern numerical modelling can fulfil the modelling requirements, they still need to be verified by physical modelling under a well known boundary condition. As such, in geotechnical engineering a more practical approach is to perform a simple analysis using physical models, which focus on identifying key mechanisms such as modes of deformation and failure. The analyses can form the basis for rock engineering design.

The best design parameters are often obtained through large size field tests. However, this is extremely difficult to achieve because of cost implications and delays before results are available, as well as due to difficulties in interpreting data. Physical models provide an alternative solution (Singh and Rao, 2005). Physical models are portable and can demonstrate simply the characteristics features of rock mass behaviour that are not always evident in other models (Singh and Farmer, 1985). According to Viswanathan and Linsey (2009) and Green and Smrcek (2006) the simplicity of physical models assist the designer in reasoning and linking theory and knowledge with practical implementation. Prediction of conditions is of great significance in rock engineering for designing stable support systems.

However, models are not perfect because of the many difficulties faced by the researcher (Walliman, 2004), including problems originating from boundary conditions and scale effect. According to Singh *et al* (2007) rockmass samples of a scale suitable for testing in

the laboratory that satisfy geometrical and similitude conditions are difficult to retrieve from the field in an undisturbed state.

To overcome shortcomings associated with physical models, the objective of this project was not to generate similitude conditions, but rather to produce models that could illustrate practical behaviour of the actual situations so that comparison of the mechanisms of behaviour of surface support under multiple loading conditions can be made.

### 3.8.1 Physical Model Test Description

Physical model tests were conducted to understand the mechanical response of surface support to jointed rock mass deformation. These tests were aimed at improving the knowledge of liner support action in a rock mass. The previous tests described address specific mechanisms, which do not fully describe the mechanisms of support provided by sprayed liners in jointed rockmasses. Therefore, a demonstrational tunnel model (1.5m x 1.5m in size) was built to evaluate the behaviour and performance of different liner materials under multiple loading conditions, as well as the liner failure patterns and the support mechanisms that could typically be encountered in an underground situation.

The material used for this experiment was concrete paving bricks. The following are the reasons for using bricks:

- Cheap, recyclable and readily available
- Provide surface conditions that can be related to a rock surface for this purpose and
- Bricks are weak enough to crumble under reasonable applied loads so that desired squeezing conditions could be obtained.

Bricks were cut into 100mm x 100mm x 50mm blocks so that the ratio of joint spacing to bedding plane spacing is 2. A ratio of 2 would enable failure direction to be predetermined. Stacey (1974) and Kulatilake *et al* (1997) pointed out that failure modes of

jointed rockmasses are dependent on the joint configuration. According to Singh *et al* (2007), the following failure modes are expected:

- splitting of intact material,
- shearing of intact material,
- rotation of blocks and
- sliding along the critical joints.

The liners used were TSL A, B and C. They were applied by hand using a trough to a thickness of 5mm and the 5mm thick internal steel frame as the guide. Effectively the liner covered (60mm) of the block face (Figure 3.18d). The total number of tests carried out was 9 for all liners and orientations. Three additional control tests were done, one for each orientation so that the mode of failure of the tunnel would be determined.

All tunnel model tests were carried out with horizontal loading (uniaxial loading) so that tunnel squeezing conditions would be realized. Loading in the horizontal direction was to allow for sliding along the simulated bedding planes to take place. Loading was done by displacing steel pressure plates using bolts, and the magnitude of the load was not measured. There were three pressure plates on each side of the frame where load was applied, that is the top, centre and the bottom (Figure 3.15). Each plate was loaded by turning two bolts $360^0$ starting with the right hand side centre plate followed by the top plate and the bottom plate was last. The same sequence of loading was used starting from the right hand side to the left for all liners and bedding orientations. The applied deformations on the pressure plates were measured at six fixed positions for all tests ($u_{rt}$, $u_{rc}$, $u_{rb}$, $u_{lt}$, $u_{lc}$ and $u_{lb}$) between the pressure plates and the model steel frame using the vernier callipers on each successive loading (Figure 3.14 and 3.15). The reference measurements were taken before removing the internal steel frame that supported the tunnel during the curing period.

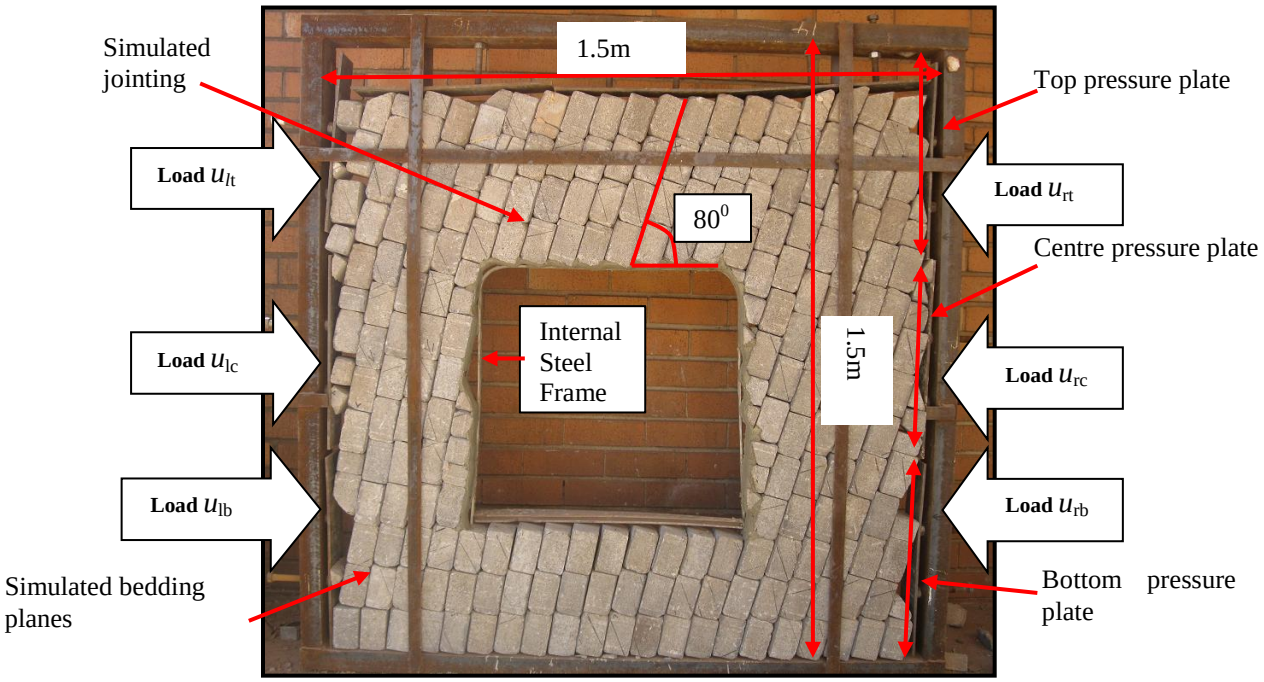


**Figure 3. 14 Positions of applied load and deformation measurements**

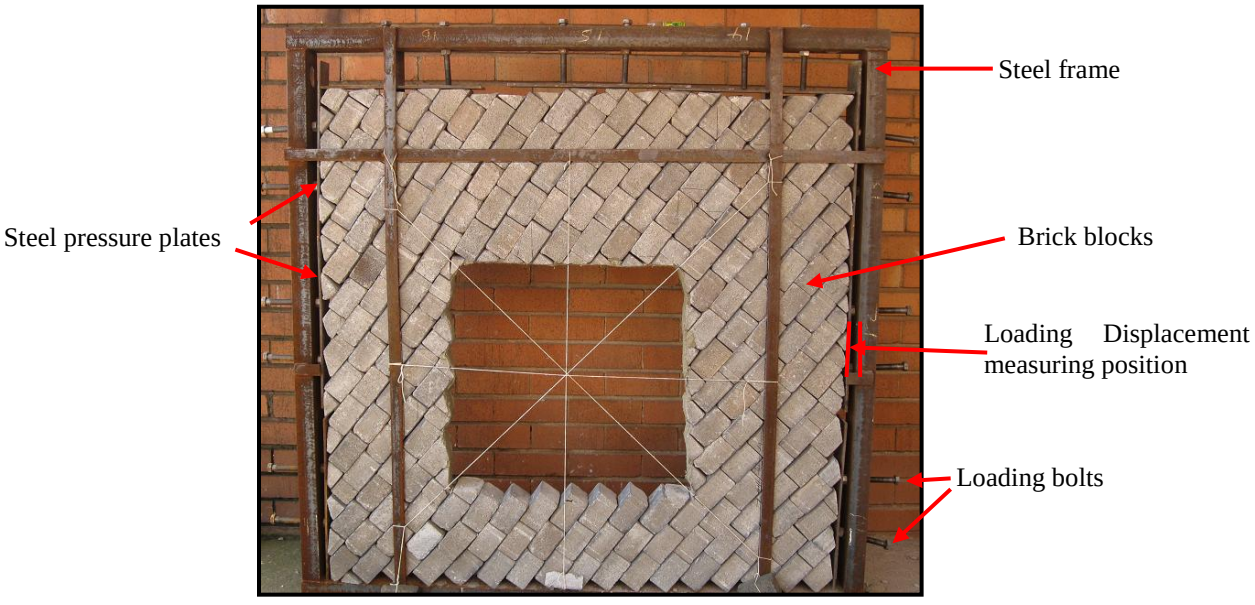


**Figure 3. 15 Tunnel model set up**

Internal measurements were taken at eight different marked positions for each successive loading (Figure 3.16). Results of deformation due to gravity loading were measured after removal of the internal steel support frame. The parameters that were measured inside the model tunnel excavation are as follows where;

$d_1$, $d_2$ = tunnel diagonals

$w_t$, $w_c$, $w_b$ = width of the tunnel measured at the top, centre and bottom

$h_r$, $h_c$, $h_l$ = height measured at the right hand side, centre and left hand side

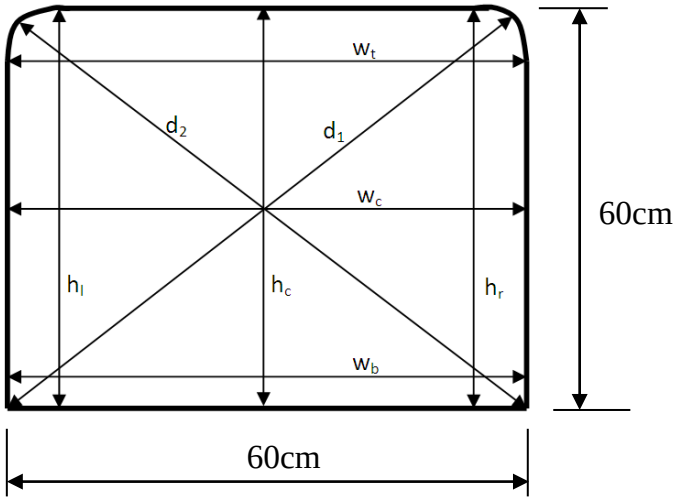


**Figure 3. 16 Parameters that were measured inside a TSL supported tunnel**

### 3.8.2 Physical Model Results

The results of the tunnel model are best shown pictorially, illustrating typical areas of interest from start to end of the test, describing the mechanisms observed. The most easily quantifiable damage to the surface support was cracking of the liner. Cracks were observed to be parallel to the long axes of the tunnel and were located within 1cm proximity of the jointing (Figure 3.17 a, b, c and d). For weak liners such as TSL B, cracking started on the roof and the right hand side of the tunnel for $60^0$ bedding inclination. However, the tunnel remained stable and no collapse was recorded for this

orientation. The importance of this assessment was to show how liner failure influences the stability of the model tunnel as a whole and this will be covered in the discussion of the physical model.

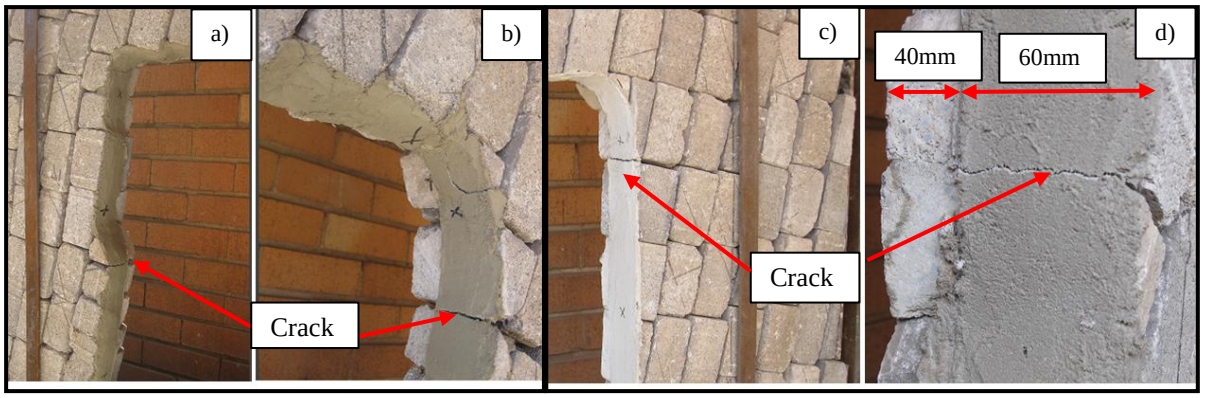


**Figure 3. 17 Crack location a), b), c) and d)**

Table 3.11 shows the measured deformation inside the tunnel model and load applied on to the blocks up to total collapse. The negative values reflect the opening up of excavation when load was applied and was observed for TSL B and C $80^0$ orientation and TSL C $60^0$ orientation.

**Table 3.11 Total deformation measured at collapse of the tunnel, in millimetres.**

| | 45° | | | 60° | | | 80° | | |
|---|---|---|---|---|---|---|---|---|---|
| | **TSL A** | **TSL B** | **TSL C** | **TSL A** | **TSL B** | **TSL C** | **TSL A** | **TSL B** | **TSL C** |
| **$\Delta d_1$** | **6** | **19** | **7** | **4** | **2** | **8** | **9** | **18** | **0** |
| **$\Delta d_2$** | **13** | **18** | **7** | **15** | **8** | **7** | **17** | **1** | **-5** |
| $\Delta h_r$ | 1 | 2 | 1 | 1 | 1 | -1 | 17 | -3 | -3 |
| $\Delta h_c$ | 1 | 1 | 16 | 1 | 2 | 2 | -2 | -1 | -3 |
| $\Delta h_l$ | 0 | -1 | 1 | 1 | 3 | -1 | -3 | 5 | -3 |
| **$\Delta w_t$** | **2** | **24** | **13** | **16** | **8** | **16** | **15** | **26** | **19** |
| **$\Delta w_c$** | **2** | **38** | **66** | **24** | **18** | **19** | **53** | **25** | **31** |
| **$\Delta w_b$** | **10** | **21** | **32** | **8** | **9** | **10** | **43** | **8** | **8** |
| $\Delta u_{rt}$ | 7 | 15 | 10 | 5 | 5 | 7 | 3 | 4 | 3 |
| $\Delta u_{rc}$ | 4 | 12 | 17 | 3 | 6 | 8 | 23 | 11 | 29 |
| $\Delta u_{rb}$ | 4 | 13 | 23 | 5 | 10 | 10 | 37 | 8 | 12 |
| **$\Delta u_{lt}$** | **5** | **15** | **13** | **10** | **7** | **6** | **3** | **2** | **1** |
| **$\Delta u_{lc}$** | **5** | **15** | **25** | **5** | **6** | **3** | **27** | **9** | **18** |
| **$\Delta u_{lb}$** | **5** | **12** | **15** | **3** | **5** | **5** | **16** | **4** | **5** |

Number of models tested = 9

## 3.9 Conclusions

Mechanisms of failure of TSLs were reviewed in the literature. The mechanisms of failure reflect the properties of the TSLs. The design of the laboratory tests was based on the mechanisms of behavior of the TSLs. It was concluded that, there was no single laboratory test that accurately describes the performance of TSLs.

The laboratory tests carried out were Brazilian strength tests and bending strength test on coated rock samples, and compression strength tests on TSL materials. The results for the Brazilian strength tests displayed strength gain for the coated samples compared with the uncoated rock samples. The values obtained were ranked so that the liners could be compared. The compression strength tests, displayed strength improvement with curing time and clearly revealed the differences in terms of material strength and stiffness. The results for the 3-point bending tests showed that weak sprayed liners are not effective as surface support for sandstone rocks and that the liners further weaken the rock in the early

stages of curing. The mean values for the bending tests for day one curing time were less that of uncoated beams for TSL A, B and C.

The demonstrational tunnel model displayed differences in TSL performances.

The next chapter discusses the results obtained from the laboratory tests.

# CHAPTER 4

# Discussion of Results

The previous chapter discussed laboratory tests carried out to improve understanding of surface support behavior for rock support. Chapter 3 provides invaluable information regarding the test procedures used and suitability of the tests. Chapter 4 involves the discussion of different test results for all the selected TSL materials mentioned earlier. This includes a comparison of the mechanisms of behaviour of TSLs and comparison of the results obtained by different test methodologies. The results are discussed in sections in the following order: Brazilian strength, Compressive strength, 3-point bending and the tunnel model.

## 4.1 Comparison of the Liner Performance for Brazilian Tests

The results described in section 3.7.3 assist in understanding the benefit provided by sprayed liners on rocks that are subject to tensile loading conditions. Laboratory tests have established that TSLs offer reinforcement potential in controlling pre and post yield rock failures. This was confirmed by the Brazilian test results performed on anorthosite rock samples. Coated samples have shown an increase in strength compared to uncoated rock samples. All coated samples exhibited less severe post failure behaviour. The strength increase was ranked for TSL A, B and C so that the liners can be compared.

As mentioned in Section 3.7.3, TSL A and B fell in the weak zone category. The reason for lower strength values could be the moisture contained in TSL A since the liner was composed of a mixture of cement and water. TSL B was a mixture of cement, river sand and polymer, but remained wet for longer compared to TSL C, and showed cracking as drying occurred, and this could account for lower strength values. TSL C fell in the transition zone between weak and medium strength. The general trend of the average peak strength of all the TSLs show that the strength increases with an increase in curing time.

However, the results display high values for TSL thicknesses 1mm and 5mm, while for the 3mm, lower strengths were measured. The reason for the change in strength from 1mm to 5mm could be the influence of the faster drying rate for thinner liners, as pointed out by Hall (1981).

The implications are that a weak liner such as TSL A does not offer significant support for thickness of 1mm and 3mm. Liners that crack during drying provide areas of weakness which then compromise support potential.

## 4.2 Comparison of Liner Performance for the Compression Tests

The results confidently display strength increase with curing time for all the liner materials. The ultimate strength in compression is greater than the tensile strength of the material. Stiffness of all the TSLs increased with increasing in curing time as pointed out by Nielsen (1962). The strength of the liners shown by this test method is comparable with the strength ranking revealed by the Brazilian test. The type of failure observed was shear failure (Figure 4.1) and it compared with that displayed in the physical model tests, which will be discussed in Sections 4.4.1.2 and 4.4.1.3.

Parameters such as modulus and stiffness capacity of the material are important for the analysis of the support system. The modulus is important since it indicates the response of surface support to the deformation of the rockmass. The earlier the support system is mobilized, the greater the likelihood of preventing further stress-induced fracturing of the rock mass.

Although the liners selected fell in the weak and medium strength category according to the Brazilian strength ranking, the physical model for $80^0$ bedding orientation displayed the importance of stiffness in maintaining initial rockmass integrity. Stability was maintained without failure of the TSLs compared with the $45^0$ and the $60^0$ bedding orientations. Such a factor is key in underground workings where the support is intended

to withstand various amounts of energy such as that from blasting, bursts or seismic events.

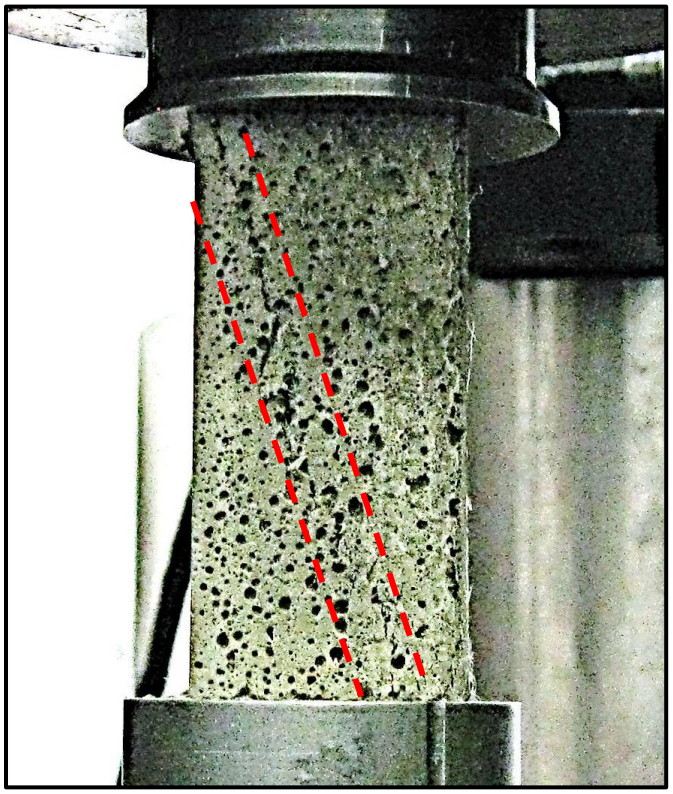

**Figure 4. 1 TSL A Shear failure**

## 4.3 Comparison of Liner Performance for the 3-Point Bending Tests

All liner types registered a decrease in bending strength 24 hours after application of the liner compared to uncoated samples. The strengthening effect was not realized, which could be the result of moisture being absorbed into the porous sandstone rock. Another reason could be surface irregularities after the application of the liner resulting in eccentric loading of the sample (Figure 4.2), thereby reducing the flexural strength of the specimen. Also the flexural strength was estimated from the peak loads which occurred at very low deflections, and hence the rock failed before the liner could take full effect. The same effect was not displayed using the same liners for the Brazilian strength tests, although the predominant mode of failure in both situations was tensile failure.

Anorthosite rocks were used in the Brazilian tests and this rock type is hard and non porous. For longer curing times TSL A and C indicated a general increase in strength compared to the uncoated samples. TSL B indicated no strength gain, with values lower than the uncoated samples throughout the 28 days curing time.

The crack bending test, using stronger TSL D on white sandstone, revealed that the liner offered significant support potential compared to the uncoated samples.

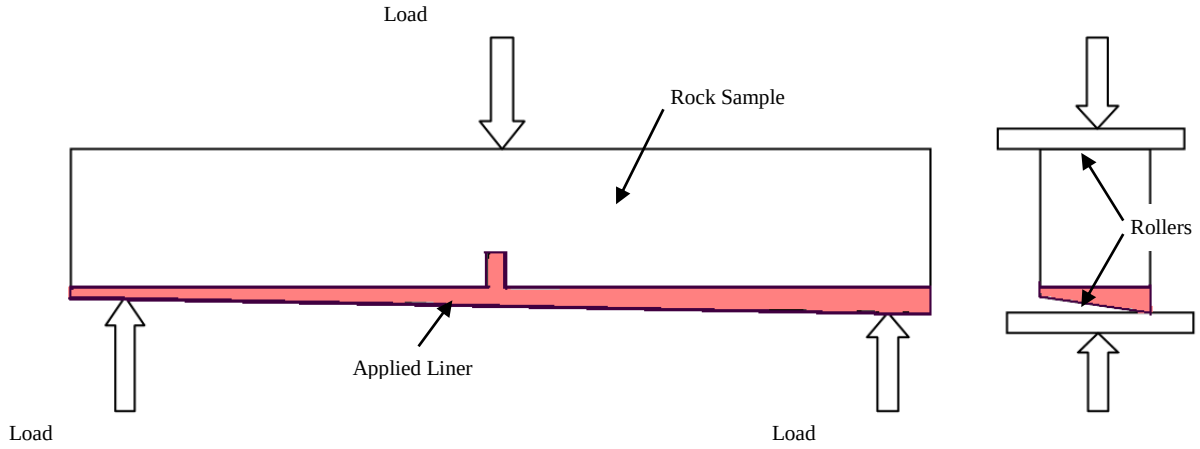


**Figure 4. 2 Exaggerated Eccentric Loading**

The practical implications of using weak liners to support underground excavations in weak rock such as sandstone are that the initial strength of the rock could be reduced and safety compromised. Also compromised is the capacity of other support systems such as bolts, by weakening the beam between them. This suggests that, for weak porous rocks, strong liners should be considered. Hence, the choice of the liner for soft rock is of prime importance.

## 4.4 Physical Model Tests

This section discusses the results obtained from the physical model tests and the mechanisms of behaviour of different liners observed. The results from the tests, with reference to measured deformation, visual and photographic observation of the

performance of the liner materials, made it possible to compare and characterise different liners in terms of support mechanisms. Comparison of the physical test procedure with the other test methodologies will be discussed in section 4.5.

### 4.4.1 Modes of TSL failure

The mechanisms of liner support and loading conditions are presented below in the form of photographs. Goodman (1980) pointed out that there are varieties of loading configurations and that no single mode of failure predominates. The modes of failure that were observed are adhesion failure, shear failure, compression failure, bending failure and tensile failure.

#### 4.4.1.1 Adhesion failure

Figure 4.3 illustrates the adhesion loss where the liner is very thin, in conjunction with the apex of the block which is supportive of the failure mapping done by Malmgren *et al* (2005) on shotcrete linings.

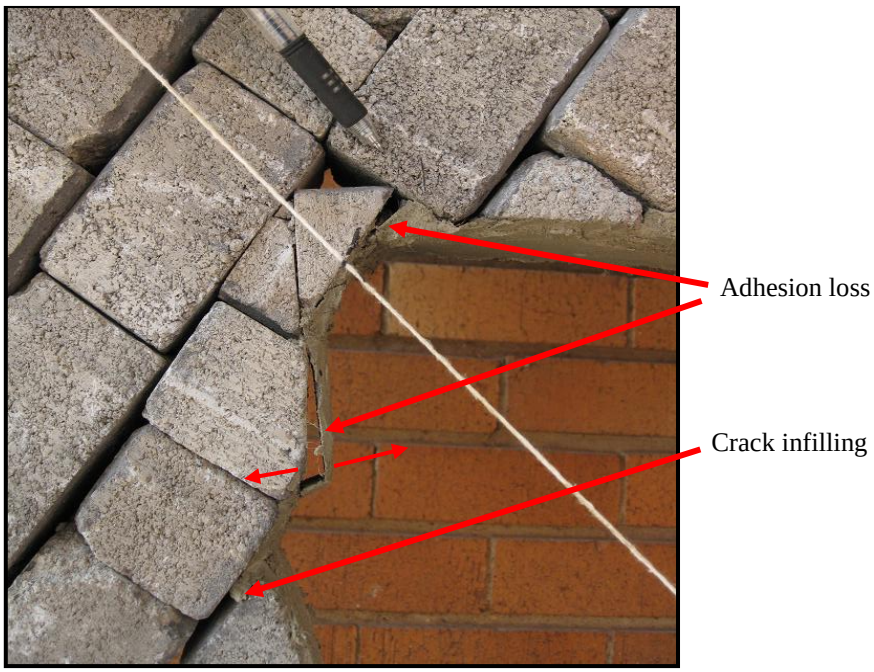


**Figure 4. 3 Adhesion loss at the corner of the tunnel**

Figure 4.4 a) and b) show the types of adhesion failure that were observed. Liner A experienced adhesion failure more frequently than the other liners and that could have been due to the quality of the liner, which fell into the weak category. However, despite adhesion loss in some highly stressed areas, the liner continued to offer support to the model tunnel. As Ozturk and Tannant (2010) pointed out, where adequate adhesion strength exists, the liners have the potential to carry the load into the surrounding stable rock.

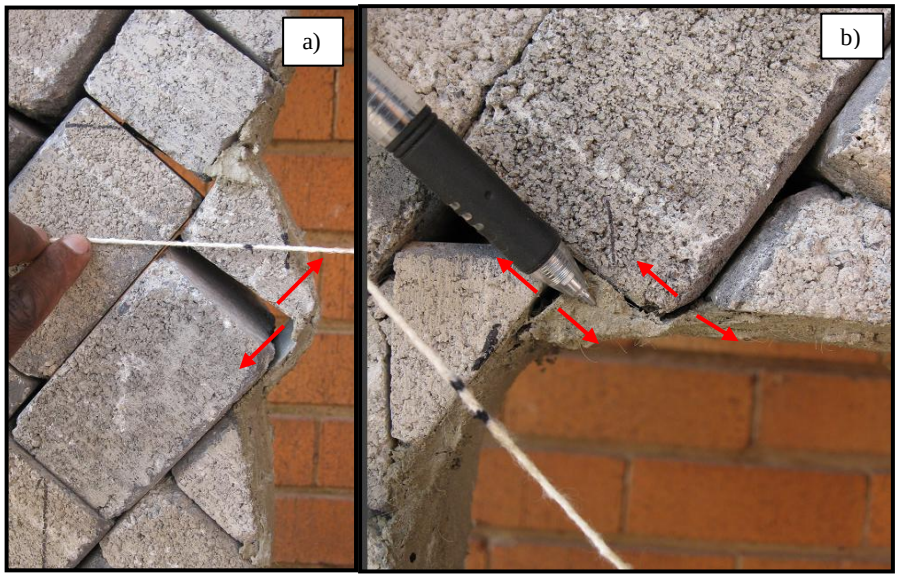


**Figure 4. 4 Adhesion failure of the liner a)on the sidewall b) at the corner of the Tunnel**

### 4.4.1.2 Shear Failure

Figure 4.5 a) shows direct shearing on the left hand side corner of the tunnel roof. Figure 4.5 b) indicates shearing resulting in shear bond loss between the liner and the block.

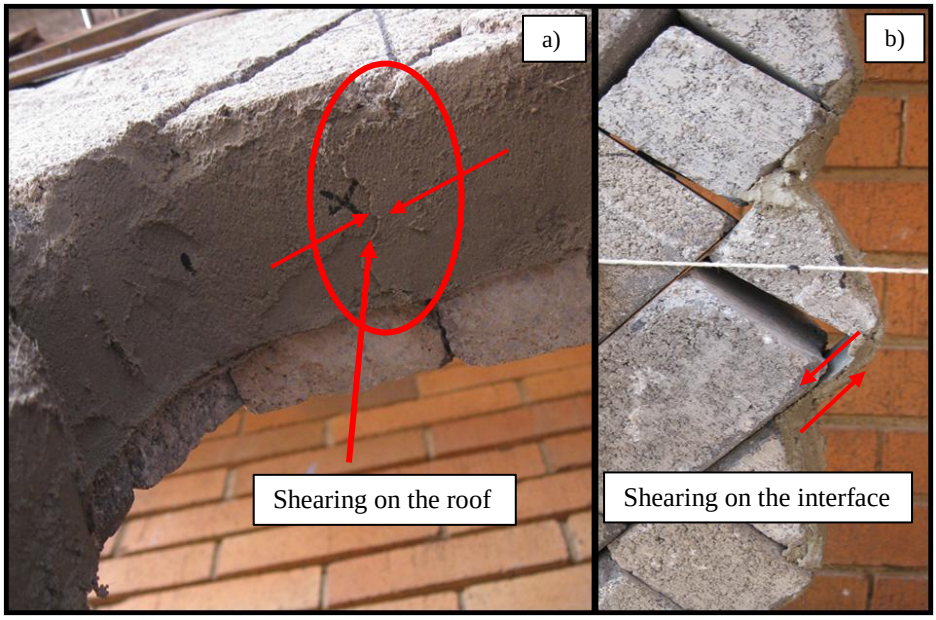


**Figure 4. 5 a) Shear failure at the top right hand corner of the tunnel b) Shear bond failure**

Figure 4.6 a) and b) show direct shearing on the right hand side of the tunnel corners. At the bottom of Figure 46b) the liner managed to resist shearing along the surface of the blocks giving rise to inward bending of the sidewall of the tunnel. Shearing was observed to be the result of concentrated loading on the liner by the movement of the blocks in opposing directions. Barrett and McCreath (1995) mentioned that direct shear only occurs when a strong adhesion bond is maintained. A "basket" was formed as described by Stacey (2001).

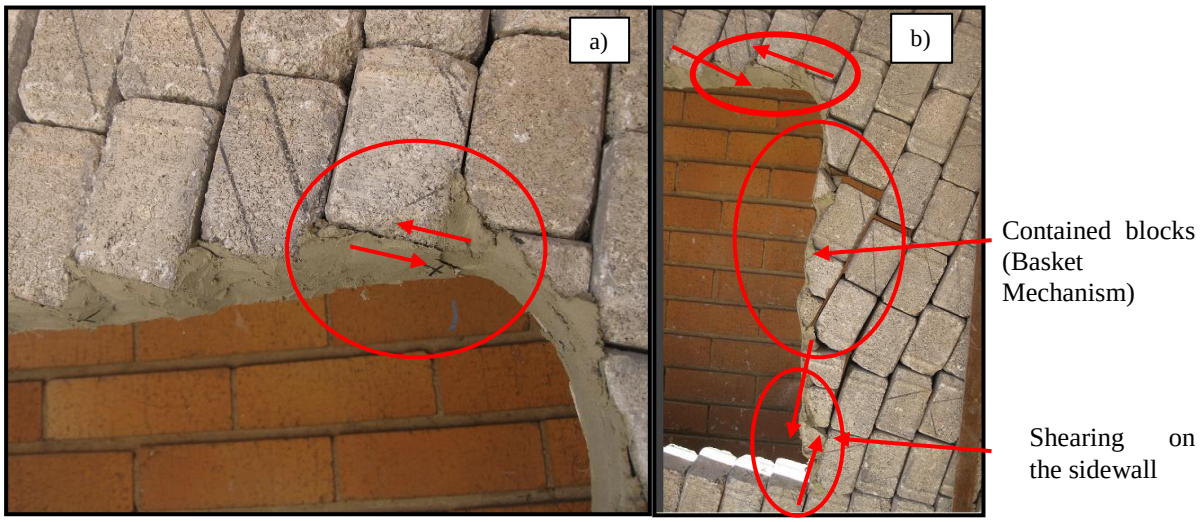


**Figure 4. 6 Shearing of the liner at the right hand corner a) and b)**

Also observed to be associated with shear were broken blocks that were located at the corner of the tunnel. Broken blocks were due to high horizontal loading above the tunnel (Figure 4.7b).

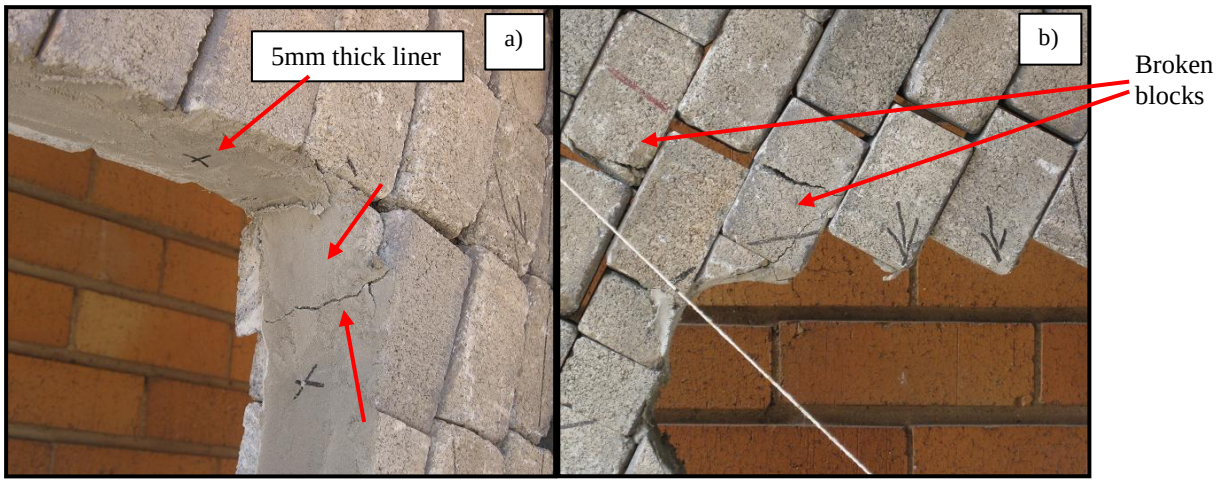


**Figure 4. 7 a)Shearing and flexure at the right corner b) Block crushing at the left corner**

### 4.4.1.3 Compression failure

Figure 4.8 shows compression failure of the liner at the corner of the tunnel. This results from the squeezing of the tunnel sidewalls which induces compressive forces on the liner

at the corners. This mechanism occurs at the haunches of the excavation as described by Stacey (2001) when strong adhesion strength is present between the liner and the blocks.

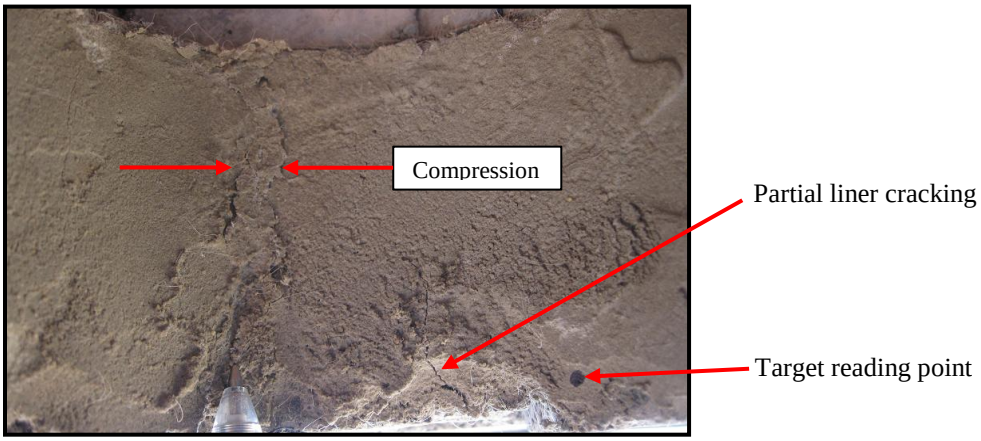


**Figure 4. 8 Compression failure of the liner at the corner**

#### 4.4.1.4 Flexural Failure

Flexural failure was manifest as a beam or basket of loose blocks resting on the liner. Two modes of flexural failure were observed. The first occurred on the sidewall of the tunnel as a result of excessive deformation as shown in Figure 4.9 a) and b). For sidewall flexural failure to occur, the liner has to prevent shear failure near the floor and roof of the tunnel so that the blocks in these regions are held in place. The overall failure mode of the sidewall blocks was toppling failure.

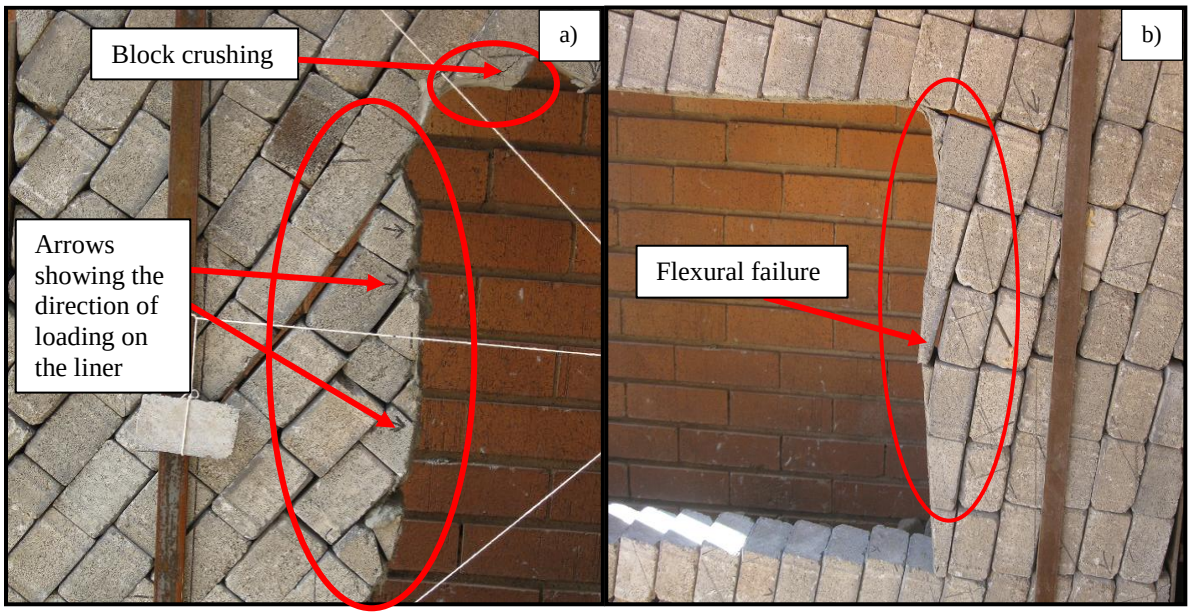


**Figure 4. 9 Flexural failure a) on the left sidewall for $60^0$ b) on the sidewall for $80^0$ orientation**

The second mode of flexural failure occurred in the roof of the tunnel. This mode of failure occurred when there was partial loss of adhesion at the centre of the tunnel, which could be a result of the squeezing of the tunnel, and adhesion being maintained at the corners as shown in Figure 4.10 a) and b). Roof flexural failure was observed to be a function of the orientation of the blocks. The orientation in Figure 4.10 a) fails earlier than the one in Figure 4.10 b). This could be caused by increased clamping between the blocks due to applied load across the tunnel (Figure 4.10 b) while in Figure 4.10 a) there is early failure as a result of higher shear stresses and sliding of blocks.

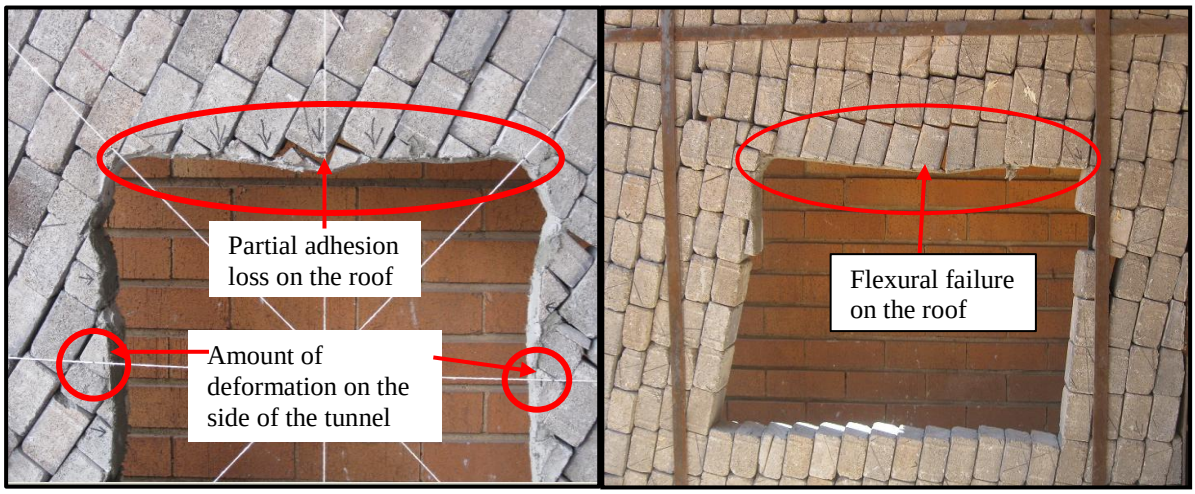


**Figure 4.10 Flexural failure at the roof of the tunnel a) for $60^0$ orientation b) for $80^0$ Orientation**

### 4.4.1.5 Tensile Failure

Figure 4.11 illustrates the tensile failure of the liner resulting from the distributed loading from the blocks on the liner. For this failure mechanism to occur it was observed that good adhesion existed between the blocks and the liner and that there was penetration of the liner into the cracks to prevent shear punching.




**Figure 4.11 Tunnel squeezing before sidewall collapse**

Figure 4.12 a) and b) illustrate the direct tensile failure of the liner observed. The liner fails as a result of gravitational loading of the blocks that slide downwards on the right hand side of the tunnel thereby transferring the load to the liner. In Figure 4.12b) it was a result of the initial shear failure at the base of the tunnel leading to rotation of blocks and downward sliding. Tensile failure of the liner was observed to be in areas where there was no liner in the cracks.

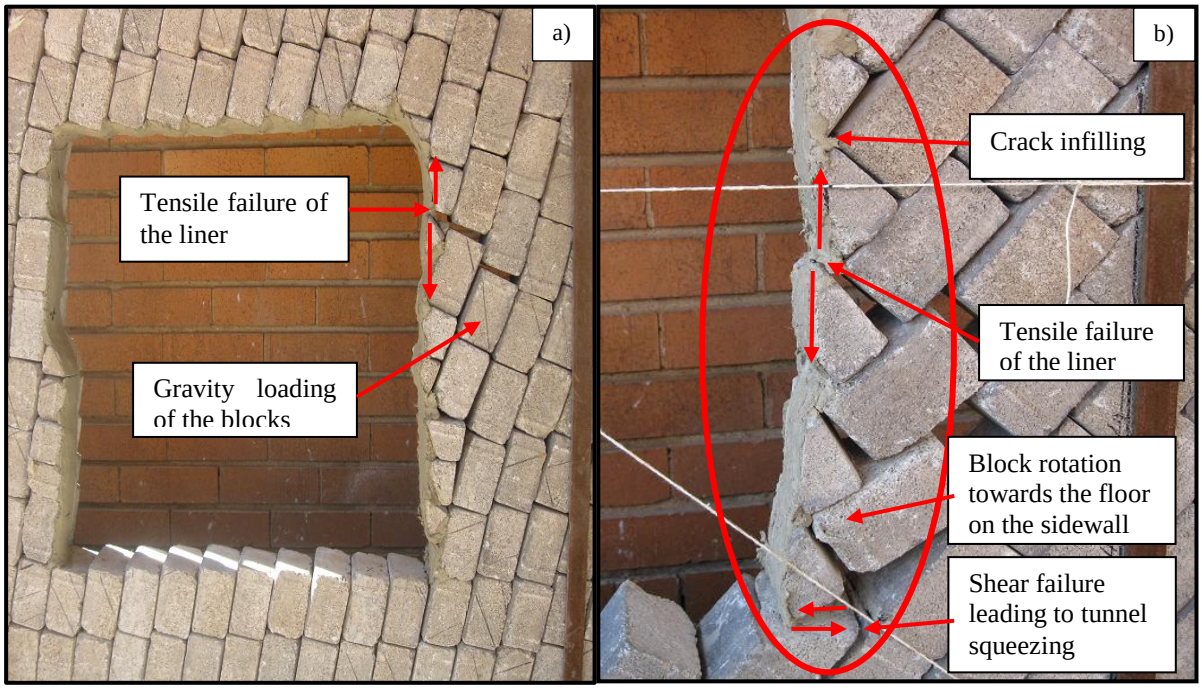


**Figure 4.12 a) Tensile failure on the sidewall b) Tensile failure on the sidewall near the footwall**

TSL A acting as a bridge in Figure 4.13, supporting failed blocks following shaking of the frame to destroy the model at the end of the test run. This Figure shows the ability of the liner material to offer support in squeezing conditions and to hold loose blocks together.

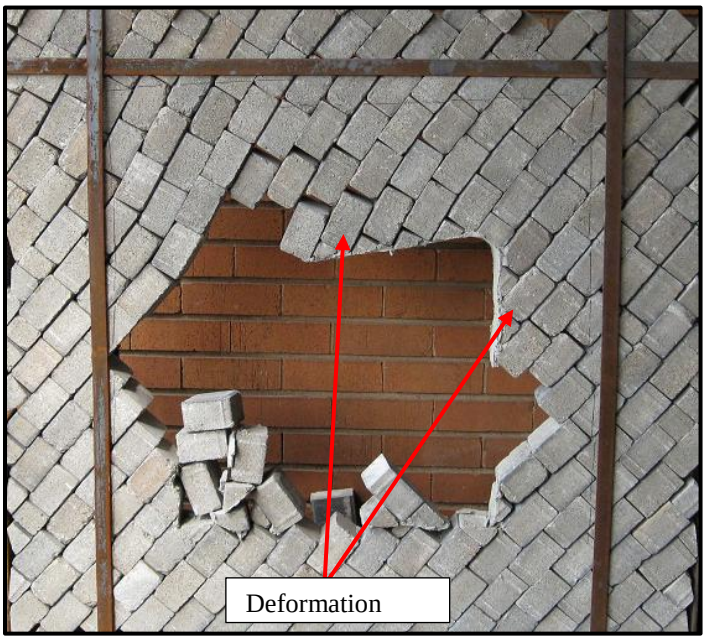


**Figure 4. 13 Liner A supporting loose block in the roof of the tunnel at the end of test**

### 4.4.2 Liner Support Performance and Practical Implications

The amount of deformation incurred in the model tunnel in relation to the applied deformation to the blocks, and the liner failure modes, were used to compare the results (Figure 4.14 to 4.22). The range of values of the applied deformation used for the comparisons of the sprayed liner performances are: 0 - 3mm, 3 – 6mm, 6 - 9mm, 9 – 12mm, and 12+mm for the liner performance (Table D.1).

#### 4.4.2.1 Performance of TSL A at $45^0$ Orientation

Liner A for this orientation appeared to support the tunnel after the internal steel support frame was removed and no cracking was observed on the side of the tunnel before loading was applied. Cracking at the centre of the side walls and the roof was observed after applied deformation was in the range of about 3mm to 6mm on both sides of the test frame. Collapse occurred when applied deformation was in the range 6mm to 9mm as shown in Figure 4:14 a), b) and c). Crack configuration as mentioned before was parallel to jointing and occurred near the joints.

The applied liner shows that, it has the ability to support the tunnel to some extent after cracking has occurred. However, it fails easily following continued loading. The liner failure modes observed were a combination of tensile failure, adhesion failure and bending failure.




a)**TSL A 45$^0$** 0 – 3mm b)**TSL A 45$^0$** 3 – 6mm c)**TSL A 45$^0$** 6 – 9mm

**Figure 4.14 Loading Stages of the Tunnel Model for TSL A at 45$^0$ orientation a), b) and c)**

### 4.4.2.2 Performance of TSL A at 60$^0$ Orientation

The 60$^0$ orientation appeared to be the most unstable for TSL A. Cracking occurred at the centre of the sidewalls and the roof of the excavation upon removal of the tunnel internal steel support frame and was unable to withstand gravity loading, resulting in collapse of the roof and the right hand side of the tunnel. The mechanisms of failure observed were predominantly tensile failure and bending failure.

Patches of the liner remained supporting the blocks on the right hand side top corner and left hand side of the tunnel. These collapsed when deformation applied was in the range 9mm to 12mm. Figure 4:15 a), b) and c) show the stages of loading and tunnel failure.

The practical implications are that loading of the liner is dependent on the orientation of jointing and that weak liners like TSL A do not offer significant support in this regard.

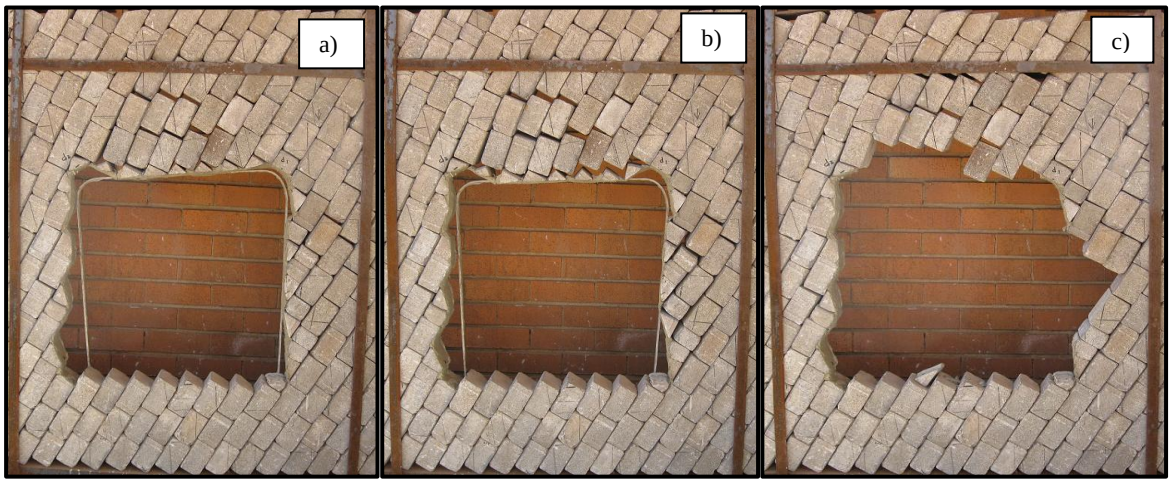


**a)TSL A 60$^0$** 0 – 3mm b) **TSL A 60$^0$** 3 – 6mm c) **TSL A 60$^0$** 6 – 9mm

**Figure 4.15 Loading Stages of the Tunnel Model for TSL A at 60$^0$ orientation a), b) and c)**

### 4.4.2.3 Performance of TSL A at 80$^0$ Orientation

The 80$^0$ orientation was the most stable of the three geometries. The reason for the stability of this orientation is that once the roof is prevented from collapse then clamping of the blocks occurs in the roof and sidewalls. As a result, the test set up remained stable when the internal steel support frame was removed. Significant deformation had to be applied before collapse occurred. The predominant mode of tunnel failure was slabbing of the sidewall as shown in Figure 4.16 a), b), c), d) and e). The mechanism of support observed was promotion of block interlock, basket mechanisms on the roof, and slab enhancement on the sidewalls. The mechanism by which the liner was loaded was key block loading on the right hand sidewall and on the roof with squeezing at the corners of the tunnel. The liner failure modes observed were predominantly tensile and bending failure on the sidewalls and shear failure near the floor.

Due to the orientation of the blocks insignificant shearing occurred resulting in block lockup above the roof and below the floor. Total collapse of the tunnel occurred when applied deformation was more than 12mm. The maximum applied deformation was 37mm for 80$^0$ orientation.

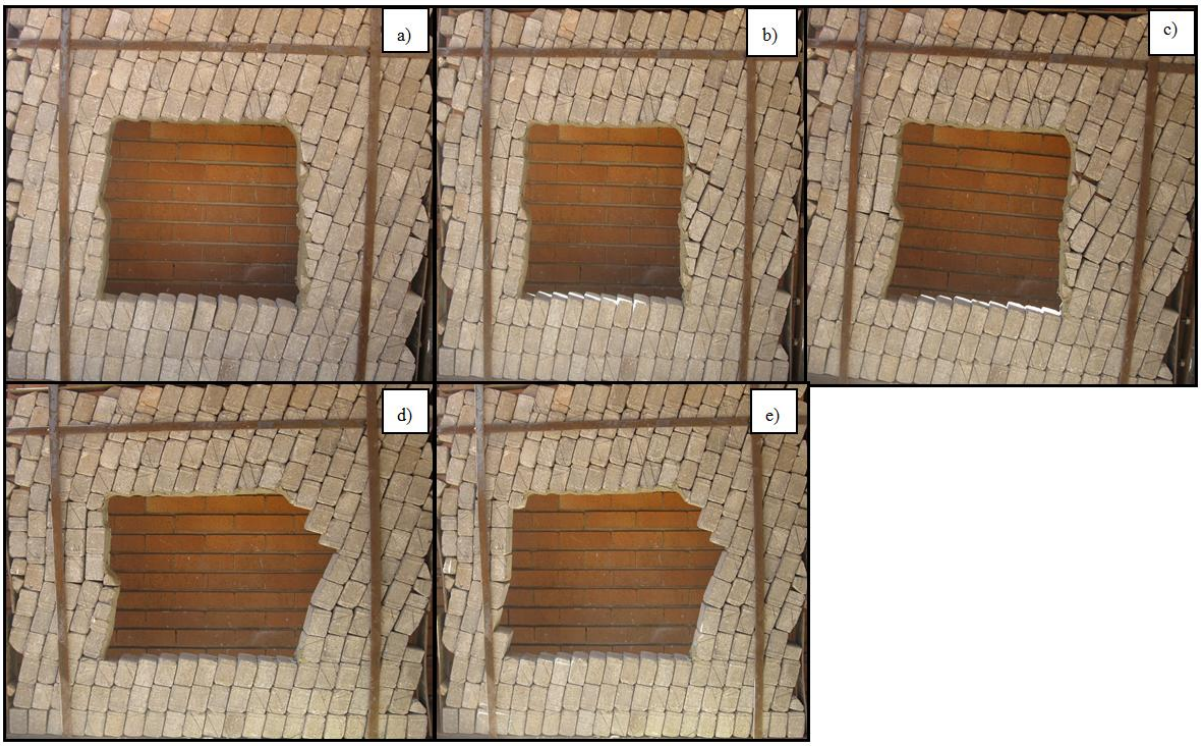


a)TSL A $80^0$ 0 – 3mm b)TSL A $80^0$ 3 – 6mm c)TSL A $80^0$ 6 – 9mm d)TSL A $80^0$ 9 – 12mm e)TSL A $80^0$ 12 +mm

**Figure 4.16 Loading Stages of the Tunnel Model for TSL A at $80^0$ orientation a), b) c), d) and e)**

### 4.4.2.4 Performance of TSL B at $45^0$ Orientation

It was observed that for TSL B $45^0$ orientation, unlike TSL A, cracking did not occur when the internal steel support frame was removed. The structure remained stable, however, cracking started on the right hand sidewall and roof collapse when applied deformation was in the range of 0mm to 3mm as shown in Figure 4.17. Sidewall collapse occurred when deformation was in the range 3mm to 6mm and total collapse when applied deformation was 9mm to 12mm. Compared with TSL A, it was observed that there was an increase in applied deformation before the first collapse occurs with TSL B.

Similar modes of liner loading and failure were observed for TSL A and B, as well as the practical implications.



TSL B $45^0$ 0 – 3mm

**Figure 4.17 Loading Stages of the Tunnel Model for TSL B at $45^0$ Orientation**

### 4.4.2.5 Performance of TSL B at $60^0$ Orientation

The $60^0$ orientation for TSL B displayed performance results that were better compared to TSL A for the same orientation. It was observed that no cracking on the roof and the sidewalls of the tunnel when the internal steel support frame was removed and stability was maintained. Cracking on the roof and sidewall occurred when applied deformation was in the range 3mm to 6mm. Roof collapse occurred when applied deformation was in the range of 3mm to 6mm on both sidewalls as shown in Figure 4. 18 a), b) and c).

Where adhesion was maintained a basket mechanism Stacey (2001) was displayed on the roof in the form of a beam. This mechanism was formed by partial adhesion loss between the liner and corners of the main blocks in between the wedge blocks. The main material failure mode was observed to be bending failure.

The maximum deformation recorded before total collapse inside the tunnel was 18mm at the centre of the sidewalls. It was observed that the deformation of the diagonals up to

collapse for TSL B liner for the $45^0$ and $80^0$ orientations underwent more squeezing compared with TSL A and C for the same orientations.

The practical implications indication that TSL B when used in hard rock low stress fields can be a better surface support as compared to TSL A and C.

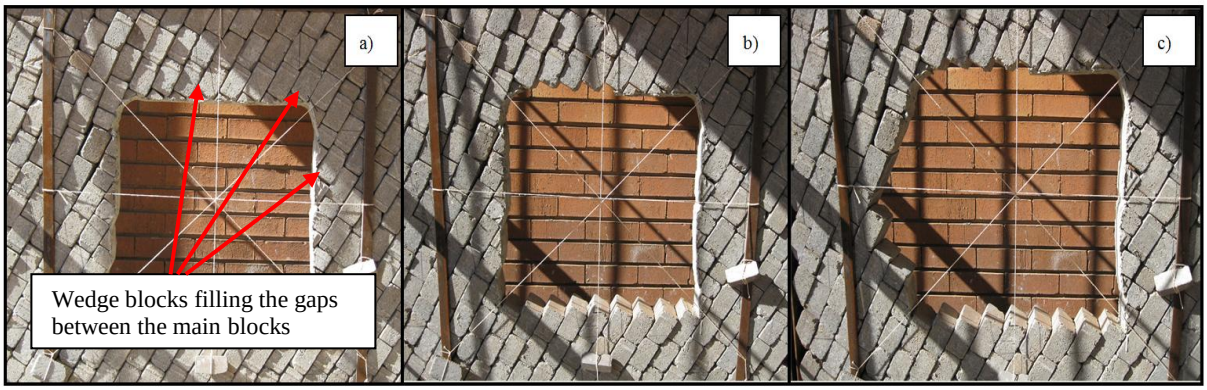


a)TSL B $60^0$ 0 – 3mm b)TSL B $60^0$ 3 – 6mm c)TSL B $60^0$ 6 – 9mm

**Figure 4.18 Loading Stages of the Tunnel Model for TSL B at $60^0$ orientation a), b) and c)**

### 4.4.2.6 Performance of TSL B at $80^0$ Orientation

Similar trends as those observed for TSL A $80^0$ orientation were observed except that sidewall collapse started on the left hand side of the tunnel when applied deformation was in the range 3mm to 6mm. Total collapse of the sidewall occurred when the applied deformations were in the range of 6mm to 11mm on both sides. Figure 4.19 a) b) and c) show the stages during load application up to failure.

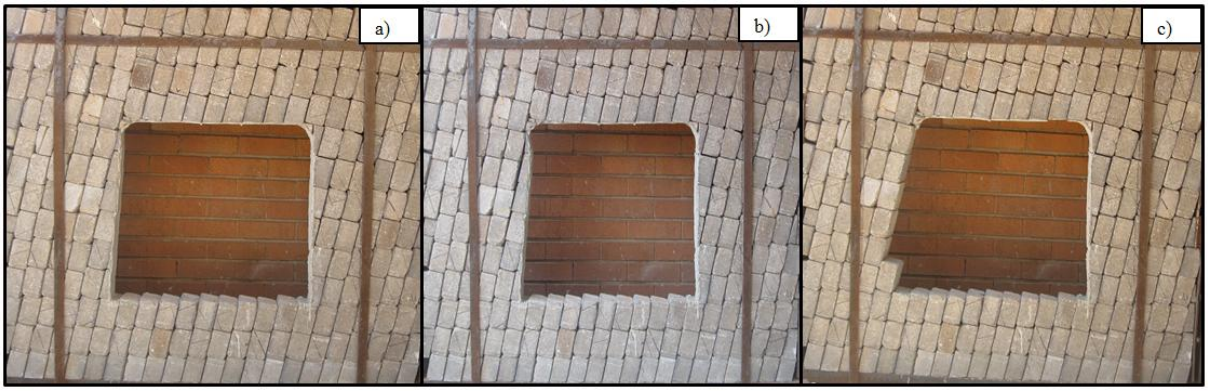


a)TSL B $80^0$ 0 – 3mm b)TSL B $80^0$ 3 – 6mm c)**TSL B $80^0$** 6 – 9mm

**Figure 4.19 Loading Stages of the Tunnel Model for TSL B at $80^0$ orientation a), b) and c)**

### 4.4.2.7 Performance of TSL C at $45^0$ Orientation

TSL C liner for this orientation remained stable without any signs of cracking when the internal steel support frame was removed. The results are similar to those obtained from TSL A and B. They support the investigation done by Mason and Stacey (2008) for a cylindrical tunnel model supported by a sprayed liner, which suggested that a stiffer liner is better at preventing initial fracturing and movement on the surface of the excavation. The maximum applied deformation required to induce cracking on the liner was in the range 3mm to 6mm on both sides of the model. The values obtained for TSL C and A are in the range 0mm to 6mm required to induce initial cracking, while for TSL B the range was 0mm to 3mm. Crack configuration is the same for all three liners.

It was observed that much higher values of applied deformation were required before collapse of the roof. The range was 6mm to 9mm on both sides of the model, which is higher than for TSL A, but the same range as for TSL B. The failure mode of the roof for TSL C was the same as that of TSL B for $45^0$ and $60^0$ orientations, but differs from that of TSL A. The liner failure mode on the roof for TSL C was due to squeezing unlike TSL A, which was driven by gravity loading.

Total collapse of the sidewalls occurred when the applied deformation was in the range 12+mm on both sides of the tunnel with a maximum value of 25mm. Figure 4.20 a), b). c)

and d) show the stages of tunnel deformation. The liner failure mode that was observed on the sidewalls was a combination of tensile failure and bending failure.

The implication of using this liner are that the liner continues to offer support after cracking has occurred and that crack infilling bonds small loose blocks together, inhibiting shear between joints and thereby promoting stability.

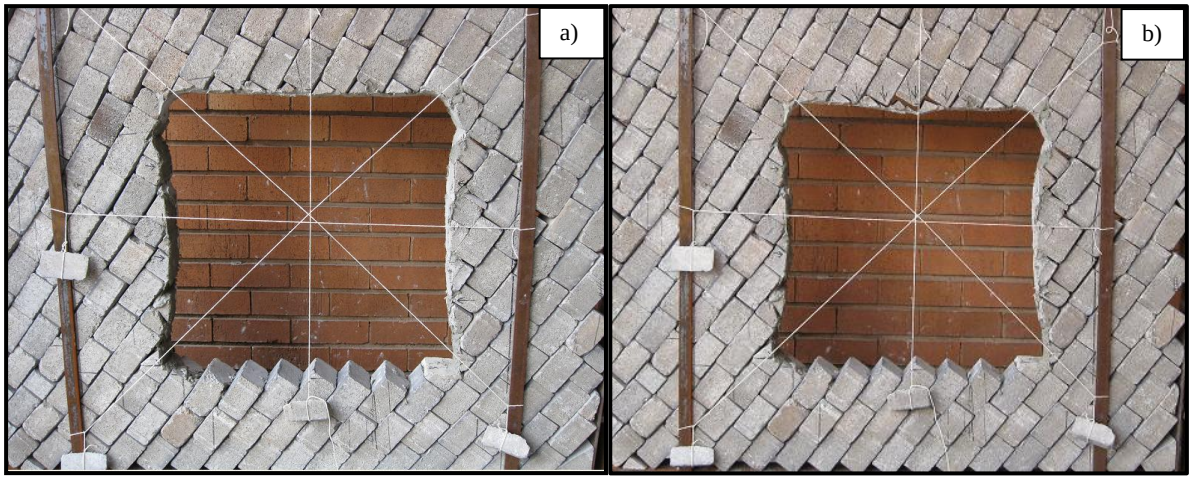


**a)TSL C 45$^0$** 0 – 3mm b)**TSL C 45$^0$** 3 – 6mm

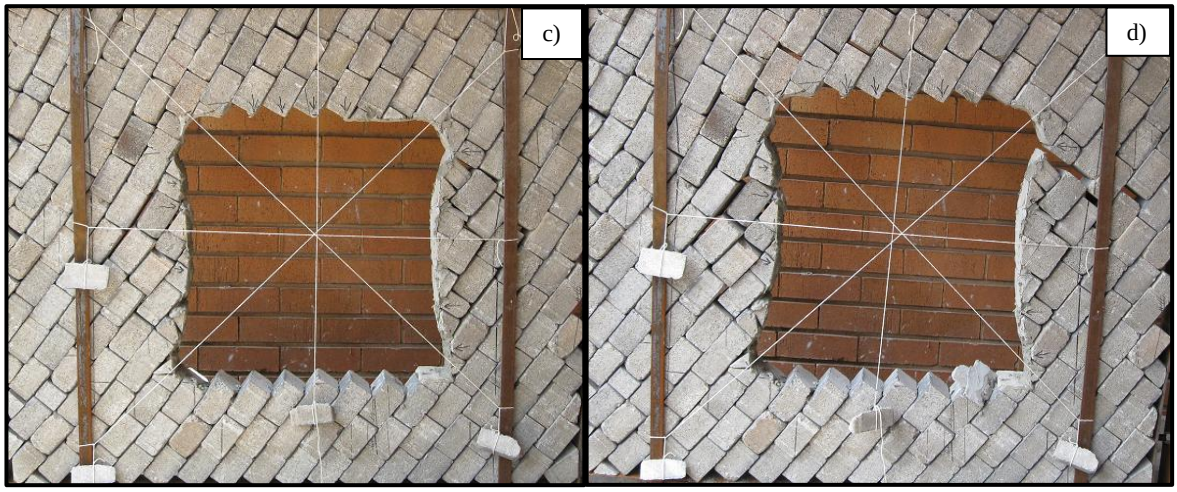


**c)TSL C 45$^0$** 6 – 9mm d)**TSL C 45$^0$** 9 – 12mm

**Figure 4.20 Loading Stages of the Tunnel Model for TSL C at 45$^0$ orientation a), b1), b2) and c)**

### 4.4.2.8 Performance of TSL C at $60^0$ Orientation

Similar applied deformation range as for TSL B was observed with a range between 3mm to 6mm was required to induce initial cracking on the sidewall and the roof, while TSL A cracked due to gravity loading. However, roof collapse for TSL C occurred in the same range, 3mm to 6mm, compared with 9mm to 12mm for TSL B Figure 4.21 a), b) and c). The tunnel failure mode for TSL C $60^0$ is similar to that of TSL B $60^0$, which started on the roof, followed by the sidewalls. Failure of TSL A model started on the roof and sidewalls simultaneously. This could be as a result of the weak nature of TSL A, which allowed sliding and shearing of the blocks to occur. The practical implication of TSL C is that a stiff liner prevents the initial movement of in jointed rock masses thereby promoting stability. However, if deformation exceeds the strength of the liner instability occurs.

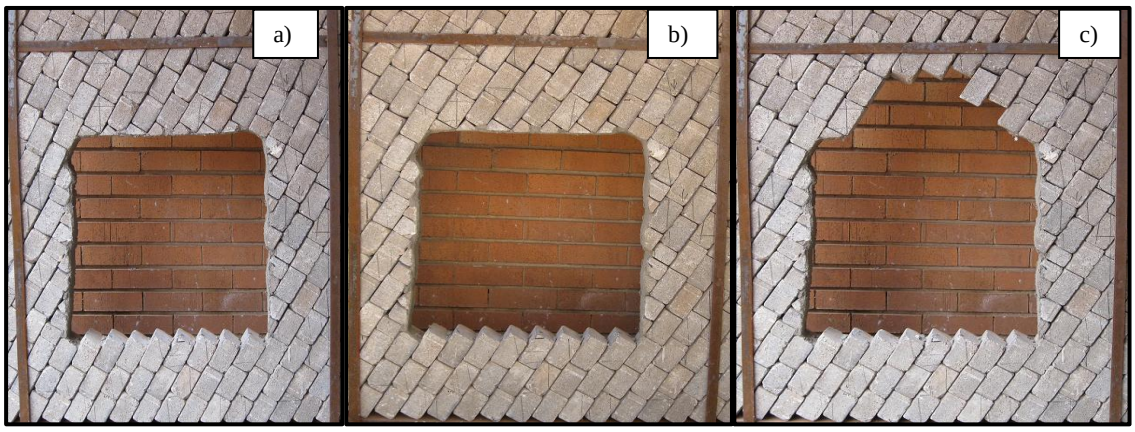


a)TSL C $60^0$ 0 – 3mm b)TSL C $60^0$ 3 – 6mm c)TSL C $60^0$ 6 – 9mm

**Figure 4.21 Loading Stages of the Tunnel Model for TSL C at $60^0$ orientation a), b) and c)**

### 4.4.2.8 Performance of TSL C at $80^0$ Orientation

A similar trend was displayed as that experienced for TSL A and B, with the dominant mode of failure being slabbing of the sidewalls Figure 4.22 a), b), c) and d). The difference is in the location of initial sidewall failure of the tunnel. As a result of the clamping of the blocks, higher loads are obtained which do not necessarily reflect the performance of the liners, making comparison of the sprayed liners difficult.

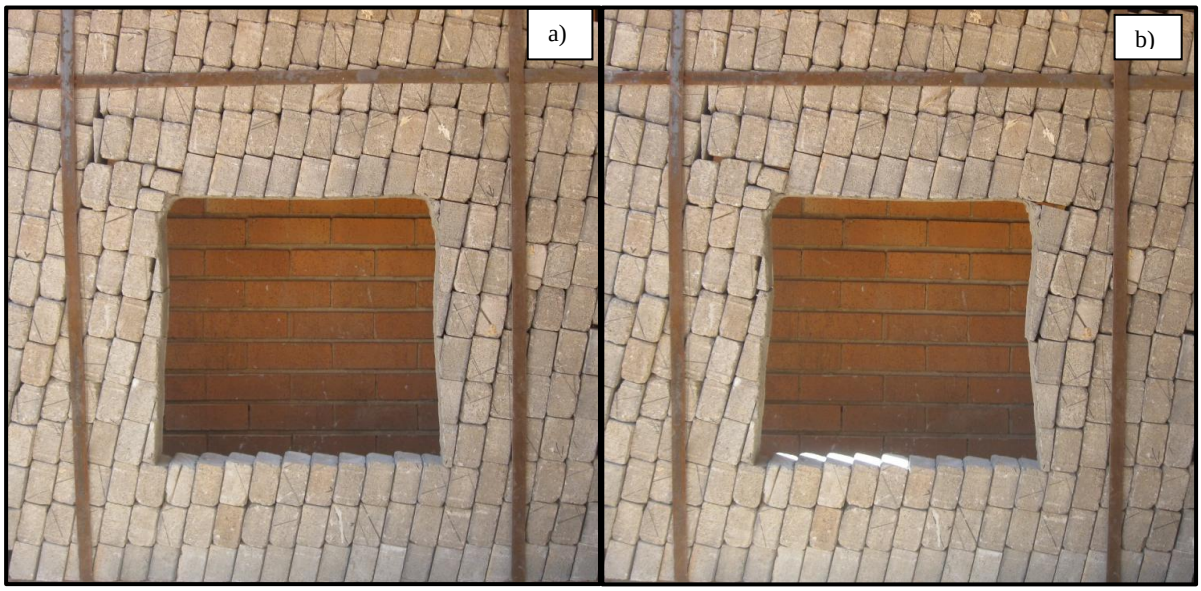


a)TSL C $80^0$ 0 – 3mm b)TSL C $80^0$ 3 – 6mm

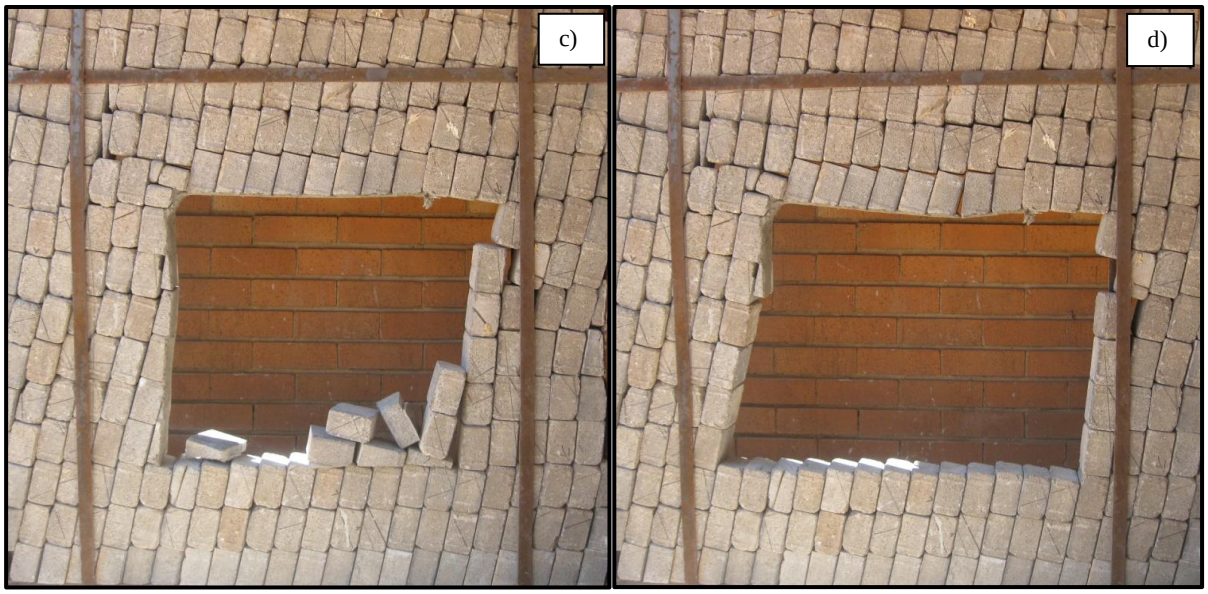


a)TSL C $80^0$ 6 – 9mm b)TSL C $80^0$ 9 – 12mm

**Figure 4.22 Loading Stages of the Tunnel Model for TSL C at $80^0$ orientation a), b), c) and d)**

## 4.5 Comparison of Test Procedures

The results for the four test procedures for evaluating the sprayed liners were consistent and showed closely related trends in terms of the performance of the sprayed liners. The ranking that was carried out for the Brazilian strength test results was confirmed by the compression, bending and the physical model test results. In all tests TSL C showed superior performance compared to TSL B and A. The 3-point bending test results showed poor performance for TSL A, B and C, but better performance of TSL D which is a better quality (stronger) liner. This behaviour suggests the limitation of the usefulness of TSL A, B and C in soft sandstone rocks. The results for TSL D are at variance with the findings by Tannant (2001) who indicates that liners have never been used successfully on weak rocks.

The laboratory test methodologies revealed different mechanisms of behaviour provided by the sprayed liners, but all of which reflect the qualities of the liners. The Brazilian test method displayed promotion of block interlock and basket mechanisms. Stacey (2001) indicated that the basket and the promotion of block interlock mechanisms rely on the liner's strong bond, to arrest and contain fracturing Figure 4.23 a) and b).

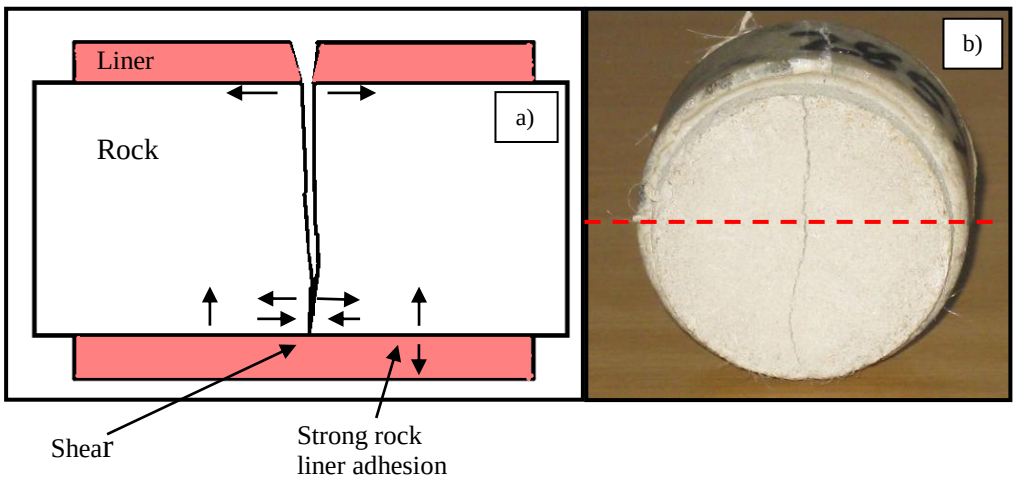


**Figure 4.23 a) Basket and promotion of block interlock b) Section line on a Brazilian disc**

The compression test was aimed at displaying the structural arch support mechanism potential. The results obtained from this test compare well with those obtained from the Brazilian indirect strength test in reflecting the properties of the liners.

The bending test displayed the slab and beam enhancement mechanism (Stacey, 2001). The application of the liner provides resistance to buckling and reduces the likelihood of formation of tensile cracking due to bending. The results showed strong dependence on the quality of the liner used and that weak liners may reduce the bending resistance of weak rocks. This behaviour was not displayed by the other test methods.

The physical model displayed all the mechanisms of support encountered in the Brazilian, compression and the bending test, but not all that were described in the literature. The model played a major role in linking the mechanisms of behaviour provided by the sprayed liners from the other tests. Despite the differences in the mechanisms of behaviour of the sprayed liners from the different test methodologies, the tests reliably demonstrated the real situations that are encountered in underground static loading conditions. Hence, they may be considered useful in assessing the performance of sprayed liners.

## 4.6 Conclusions

The results presented in this chapter for the coated rock samples and material test showed the mechanisms of behaviour of the TSLs. The results provided a measure of the performance of the liner and allowed comparison of the sprayed liners to be made. The performance enhancement provided by the sprayed liners is responsible for providing additional strength to the rock, increasing the load at which failure initiates, and controlling the post failure behaviour. For Brazilian rock discs the higher load is a result of the combination of liner adhesion and tensile strength properties that create the resisting force across the potential fracture surface, delaying fracturing. Bending test results showed that TSL A, B and C weaken the sandstone rock beams upon application for up to seven days curing time, and display poor performance. In view of the fact that

the liner for the demonstrational physical model was applied in isolation without other support elements and in two dimensions, all mechanisms of rock support provided by sprayed liners were not identified. However, the tunnel model provided a means of observing and comparing sprayed liners on a small model that can be compared with in-situ conditions.

# CHAPTER 5

# Conclusions and Recommendations

The study of the properties and performance of TSLs for rock support described in this research provides a clear conceptual understanding of mechanical behaviour of the liners. The literature survey identified mechanisms that are most appropriate for rock support provided by TSLs. The proposed test methodologies provided means for comparison between different liner products by carrying out laboratory tests. A number of conclusions can be drawn regarding the performance of the liner materials and the mechanisms of behaviour of rock support provided by the sprayed liners:

**Brazilian Test**

- The test provided a method for evaluating and comparing the various liner products performances in terms of strength. As could be expected, different liner products were found to have different performances, which depended on the physical properties of the individual liner materials.

- Application of a liner, in general, enhances the resistance of the rock to tensile failure. The better the quality, tensile strength and adhesion strength of the liner material, the greater the enhancement. Application of a weak liner to anorthosite rock does not significantly change the load at which failure occurs. The contribution of the liner performance was an improvement from violent to less violent rock failure behaviour.

- The liner failure modes that were observed were tensile bonding failure and shear bonding failure. The mechanisms of rock support were found to be promotion of block interlock, a result of strong tensile and shear bond between the liner and the rock, and a basket mechanism through the tensile strength of the liner. These

mechanisms will also be applicable in high stress environments where dog-earing occurs.

**Compression Test**

- The compression test enabled comparison of the TSL material properties to be made in isolation. The material properties provide a quick assessment of the behaviour of the TSL which reflects the performance of the liner as well as being useful for quality control purposes. The results displayed depended on the curing time as was anticipated.

- The test allowed the isolated properties to be compared with the performance of the liner from other tests so that an informed decision on the selection process for a suitable sprayed liner can be made.

- The mechanism of support appropriate to this test is the structural arch, where the liner utilizes its rigidity. This mechanism is particularly applicable at the haunches of the excavation.

**3-Point Bending Test**

- Comparisons of the peak load at which failure initiates for coated beams show that there is no statistical difference between the strengths of coated and uncoated flexural beams for TSL A, B and C. The results showed poor performance of the liners for the first seven days of curing time. It was noted that these liners offered little post-fracture control of deformation, hence rupture occurred under the small amounts of deformation. The liners would be unable to provide appreciable containment of bending failure for the 28 day curing times. It is probable that water contained in the liners may have had some effect in reducing the strength of the sandstone rock used for the tests.

- Weak liners are unsuitable as surface support for weak rocks such as sandstone, and alternative strong liners should be considered. Tests carried out revealed that TSL D, a strong liner, provided significant support to the weak rocks.

- The mechanisms of rock support identified were slab and beam enhancement.

**Physical Model**

- The physical model of the tunnel supported with the liners opened new avenues for investigating surface support in terms of rock support in underground situations. The results indicate that the test procedure produced sufficiently repeatable results as seen by similar trends in the applied deformation for all orientations. However, it was expected that some variability would occur as a result of the scale and nature of the experiment. The tunnel model results were able to differentiate between the candidate liners in terms of their performance. It was possible from the model results to conclude that TSL C provided better support than TSL B and TSL A and the results therefore compared well with those of other test procedures.

- The results showed that the performance of the liners was dependant on the orientation of jointing and significant failure was observed at for the $60^0$ bedding orientation. Liners responded in a way that revealed their strength.

- The performance enhancement properties of liners were brought about by the interaction between the liner and the substrate through the bond strength, tensile strength and shear strength. The types of liner failure observed to have been involved in the test method were direct shear failure, tensile failure, bending failure and adhesion failure. Shearing occurred at the corners of the tunnel where the roof was deforming in the upward direction and the sidewalls deforming inwards. Tensile failure occurred on the sidewalls in combination with bending failure of the liner, while adhesion failure occurred on the sidewall and in the roof near the corners of the excavation.

- The mechanisms of support offered by the liners were observed to be the basket mechanism, the promotion of block interlock, slab and beam enhancement and, because of the scale effect of the experiment, the structural arch mechanism was identified.

**General**

Although the test procedures identified different mechanisms of support they gave consistent, reliable and realistic results that allowed comparison of the relative capabilities of the selected liners for rock support, as well as a comparison between the test procedures. The Brazilian and the three-point bending tests on coated rock specimen are "new" tests for evaluation of TSLs.

The selected liner products were found to vary in their ability to control imposed deformation. TSL A, B and C were classified as weak and medium strength liners according to the Brazilian strength ranking. The strength ranking was supported by compression strength tests, bending strength tests and the physical model tests, and was confirmed through the mechanisms of behaviour of support provided by the liners.

The following are the recommendations for further study:

- Weak and medium strength liners were used in this research; however the tests could be repeated using strong liners in order to improve our understanding of the mechanism of support of sprayed liners.

- The research work carried out on the physical model used a 5mm thickness of the liners and seven days curing time only. Various thicknesses such as 1mm and 3mm and different curing times should be used to see how the model behaves. In addition, the influence of filling the "valleys" on the joints for rock support should be investigated as well the combination of the sprayed liners with bolts to improve the understanding of the mechanisms of behaviour associated with the interaction of the two types of support.

- On the physical model, plain shotcrete and fibre-reinforced shotcrete should be applied so that the mechanisms of rock support provided by shotcrete may be compared with those of liners. Video monitoring of physical models is recommended so that important mechanisms, which may occur suddenly and rapidly can be associated with the results obtained.

# References

Chamber of Mines of South Africa Annual Report 2007-2008. (2008).

AMIN, M. F. M, SIANG, K and CHON, C. H. (2004). Reinforcement Mechanisms of Rock Bolt: A Laboratory Investigation. *Jurnal Kejuruteraan Awam, 16 (1)*, pp 1-12.

ARCHIBALD, J. F. (2001). Assessing Acceptance Criteria for and Capabilities of Liners for Mitigating Ground Fallls. *Mining Health and Safety Conference*.

ARCHIBALD, J. F, BAIDOE, J. P and KATSABANIS, P. T. (2004 B). Rockburst Damage Mitgation Benefits Deriving from Use of Spray-on Rock Linings. In Y. POTVIN, D. STACEY, & J. HADJIGEORGIOU, *Surface Support in Mining.* Australian Centre for Geomechanics, pp 169-178.

ARCHIBALD, J. F, BAIDOE, J. P and KATSABANIS, P. T. (2004 A). Comparative Assessment of Conventional Support Systems and Spray-on Rock Linings in a Rockburst Prone Environment. In Y. POTVIN, D. STACEY, & J. HADJIGEORGIOU, *Surface Support in Mining.* Australian Centre for Geomechanics, pp 179-185.

ARCHIBALD, J. F, ESPLEY, S. J and DeGAGNE, D. O. (2000). Economic and Productivity Comparison of Bolt and Screen, Shotcrete and Spray-on Liner Rock Support Methods. *Proceedings 102nd Annual General Meeting of the Canadian Institute of Mining Metallurgy and Petroleum, Torornto, Ontario. (CD-ROM Publication).*

ARCHIBALD, J. F. (2004). Canadian Laboratory and Field Testing. In Y. POTVIN, D. STACEY, & J. HADJIGEORGIOU, *Surface Support in Mining.* Australian Centre for Geomechanics, pp 73-88.

ARCHIBALD, J. F; DEGAGNE, D. O. (2000). Recent Canadian Advances in the Application of Spray-on Polymeric Linings. *Mining Health and Safety Conference*.

BARRETT, S. V. L and McCREATH, D. R. (1995). Shotcrete Support Design in Blocky Ground: Towards a Deterministic Approach. *Tunnelling and Underground Space Technology, Vol 10 No. 1*, pp 79-89.

BARTLETT, P. J and NESBITT, K. (2000). Durability of Kimberlite and its Effect on Drilling and Support in Tunnels, Proc. AITES-ITA World Tunnel Congress, Tunnels Under Pressure, Durban, South Africa. *South African Institute of Mining and Metallurgy*, pp 37-45.

BRADY, B. H.G and BROWN, E. T. (1985). *Rock Mechanics for Underground Mining.* London: George Allen & Unwin.

CARSWELL, T. S and NASON, H. K. (1944). Modern Plastics. *21*, 121.

COATES, D. (1970). *Rock Mechanics principles.* Canada: Mines Branch Monograph 874, Department of Energy, Mines Resources.

COOPER, G. A. (1977). Optimization of the Three-point Bend Test for Fracture Energy Measurement. *Journal of Materials Science, Vol 12*, pp 277-289.

CRISTESCU, N and DUDA, I. (1989). A Tunnel Support Analysis Incorporating Rock Creep and the Compressibility of a Broken Rock Stratum. *Computers and Geotechnics, 7*, pp 239-254.

DAEHNKE, A, ACHEAMPONG, E, REDDY, N, Le BRON, K. B and HAILE, A.T. (2000). Support Technologies to Cater for Rockbursts and Falls of Ground in the Immediate Face Area. Vol 1. *Safety in Mines Research Advisory Committee, Project Number GAP 606*.

DAEHNKE, A, van ZYL, M and ROBERTS, M.K.C. (2001). Review and Application of Stope Support Design Criteria. *The Journal of the South African Institute of Mining and Metallurgy, Vol 101*, pp 135-164.

DAEHNKE, A, WATSON, B. P, ROBERTS, D, ACHEAMPONG, E and van ZYL, M. (2000B). The Impact of Soft Loading Conditions on the Performance of Elongate Support Elememts. *Safety in Mines Research Advisory Committee, Final Project Report GAP 613*.

DE SOUZA, E. (2002). A Centrifuge for Solving Mining Problems. In R. PHILLIPS, P. J. GUO, & R. POPESCU, *Physical Modelling in Geotechnics- ICPMG '02.* Canada: A. A. Balkema, pp 49-54.

DIEDERICHS, M. S. (1999). Instability of Hard Rockmasses: The Role of Tensile Damage and Relaxation. *PhD Thesis. University of Waterloo, Ontario, Canada.*

DUBE, J. (2009). *Investigations Into The Mechanisms Of Rock Support Provided By Sprayed Liners.* University of Witwatersrand, Johennesburg: MSc Dissertation.

DYSON, R. W. (1990). *Engineering Polymers.* New York USA: Chapman and Hall.

ESPLEY, S., GUSTAS, R., HEILIG, J. and MOREAU, L.H. (2001). Thin spray-on liner research & field trials at Inco. *1st International seminar on Surface Support Liners: Membranes,Shotcrete and Mesh, Australian Centre for Geomechanics , Australia.*

ESPLEY, S; TANNANT, D. D; BAIDEN, G and KAISER, P. K. (1999). Design Criteria for Thin Spray-on Membrane Support for Underground Hardrock Mining. *Canadian Institute of Mining and Metallurgy Annual Meeting, Calgary*.

ESPLEY-BOUDREAU, S. (1999). *Thin Spray-on Liner Support and Implementation in the Hardrock Mining Industry.* MSc Thesis, Laurentian University, Department of Mining Engineering, Sudbury, Ontario.

EXADAKTYLOS, G. E; VARDOULAKIS, I and KOURKOULIS, S. K. (2001). Influence of nonlinearity and Double Elasticity on Flexure of Rock Beams - I . Technical Theory. *International Journal of Solids and Structures, 38*, pp 4091-4117.

FAIRHURST, C. (1964). On the Validity of the Brazilian Test for Brittle Materials. *International Journal of Rock Mechanics and Mining Sciences, Vol 1*, pp 535-546.

FINN, D. J, TEASDALE, P and WINDSOR, C. R. (1999). In-situ Trials and Field Testing of Two Polymer Restraint Membranes. Proceedings of Rock Support and Reinforcement Practice in Mining, E. Villaescusa, C. R, Windsor A. G, Thompson (ed.), Kalgoorlie , Australia, A.A. Balkema, pp 139-153.

FINN, D. J. (2004). Thin Spray-on Liners. In Y. POTVIN, D. STACEY, & J. HADJIGEORGIOU, *Surface Support in Mining.* Australian Centre for Geomechanics, pp 89-95.

GOODMAN, R. E. (1980). *Introduction to Rock Mechanics.* New York: John Wiley and Sons.

GREEN, G and SMRCEK, L. (2006). On the Developing Role of Physical Models in Engineering Design Education. *European Journal of Engineering Education, Vol 31*(No. 2), pp 191-200.

GULER, G, KUIJPERS, J. S, WOJNO, L, MILEV, A and HAILE, A. (2001). Determine the effect of repeated dynamic loading on the performance of tunnel support systems. *Safety in Mines Research Advisory Committee, Johannesburg, South Africa, Final Project Report GAP 616*.

HALL. C. (1981). *Polymer Materials An Introduction for Technologist and Scientists.* London: The MacMillan Press Ltd.

HENNING, P and FERREIRA, P. (2010). In-stope Bolting for a Safer Working Environment. *The Journal of The Southern African Institute of Mining and Metallurgy, Vol 110,* pp 47-52.

HOEK, E. (2006). Practical Rock Engineering, Course Notes. *http://www.scribd.com/doc/29745308/Practical-Rock-Engineering-by-HOEK. Cited 17 August 2011*.

HOEK, E. (2011). Shotcrete Support. INTERNET (http :// download. rocscience.com /hoek/pdf/ 16_Shotcrete_support. pdf) Cited 27 January 2011.

HOEK, E and BROWN, E. T. (1980). *Underground Excavations in Rock.* London, England: The Institute of Mining and Metallurgy.

HOEK, E, KAISER, P. K and BAWDEN, W. F. (1995). *Support of Underground Excavations in Hard Rock.* A. A. Balkema, Rotterdam.

HUDSON, J. A, BROWN, E. T and RUMMEL, F. (1972). The Controlled Failure of Rock Disc and Ring Loaded in Diametral Compression. *International Journal of Rock Mechanics and Mining Sciences, Vol 9*, pp 241-248.

Internet. (2000). http://www.madsci.org/posts/archives/2000-09/969072644.Sh.r.html. Cited 5 August 2009.

IVANICOVA, L. (2004). Statistical Evaluation of Model Rock Compressive Strength at Branisko Exploratory Tunnel Excavation. *Acta Montanistica Slovaca*, *Rocnik 9, cislo 4*, pp 360-363.

JANSSON, A and THUVANDER, F. (2004). Influence of Thickness on the Mechanical Properties for Starch Films, pp 499–503.

JOUGHIN, W.C; THOMPSON, J; LEACH, A. R; Le BRON, K. B; HOWELL, G .C; DUBE, J; and VENTER, J. (2010). Evaluation of the Performance of Shotcrete With and Without Fibre Reinforcement Under Dynamic and Quausi-Static Loading Conditions. *Safety in Mines Research Advisory Committee, MHSC (UNPUBLISHED PRESENTATION), Vol 1*.

KIRSTEN, H. A. D and LABRUM, P. R. (1990). The Equivalence of Fibre and Mesh Reinforcement in the Shotcrete Used in Tunnel-support Systems. *The Journal of the South African Institute of Mining and Metallurgy, Vol 90*(no 7), pp 153-171.

KIRSTEN, H. A. D. (1998). System Ductility of Long Fibre Reinforced Shotcrete. *The Journal of the South African Institute of Mining and Metallury, Vol 98*(no 3), pp 93-104.

KÖNIG, D. (2002). Modelling of Deep Excavations. In R. PHILLPS, P. J. GUO, & R. POPESCU, *Physical Modelling in Geotechnics-ICPMG '02.* Canada: A. A. Balkema, pp 83-88.

KUIJPERS, J. (2001). Evaluation of Membrane Support Behaviour. *Surface Support Liners: Membranes, Shotcrete and Mesh. Australian Centre for Geomechanics, Perth*.

KUIJPERS, J. S and TOPER, Z. (2002). Towards a Better Understanding of the Support Function of Thin Sprayed Liners. *2nd International Seminar on Surface Support Liners: Thin Sprayed Liners, Shotcrete, Mesh and Lace, Sandton, South Africa. South African Institute of Mining and Metallurgy*.

KUIJPERS, J. S, MILEV, A. M, JAGER, A. J and ACHEAMPONG, E. (2002). Performance of Various Types of Containment Support Under Quasi-static and Dynamic Loading Conditions. Part 1. *Safety in Mines Research Advisory Committee, Project Number GAP 810*.

KUIJPERS, J. S, RANGASAMY, T and SELLERS, E. J. (2004 B). Performance and Design of Thin Sprayed Liners as Rock Support in Mine Tunnels. *1st Proceeding, SANCOT*, pp 1-15.

KUIJPERS, J. S. (2004). Evaluation of Thin Spray-on Liners Support Behaviour. In Y. POTVIN, D. STACEY, & J. HADJIGEORGIOU, *Surface Support in Mining.* Australian centre for Geomechanics.pp 103-112.

KUIJPERS, J. S; SELLERS, E. J; TOPER, A. Z; RANGASAMY, T; WARD, T; van RENSBURG, A. J; YILMAZ, H and STACEY, R. (2004). Required Technical Specifications and Standard Testing Methodology for Thin Sprayed Linings. *Safety in Mines Research Advisory Committee, Project Number SIM 020206*.

KULATILAKE, P. H. S. W, HE, W, UM, J and WANG, H. (1997). A Physical Model Study of Jointed Rock Mass Strength Under Uniaxial Compressive Loading. *International Journal of Rock Mechanics and Mining Sciences, 34*(No. 3-4).

LAU, V, SAYDAM, S, CAI, Y and MITRA, R. (2008). Laboratory Investigation of Support Mechanism for Thin Spray-on Liners. *The 12th International Conference of International Association for Computer Methods and Advances in Geomechanics (IACMAG),* pp 1381-1388.

LAUBSCHER, D. H. (1990). A Geomechanics Classification System for the Rating of Rock Mass in Mine Design. *The Journal of the South African Institute of Mining and Metallurgy, Vol 90,* pp 257-273.

LEWIS, B. (2001). Mondi Rock-Hold, the Development of this Structural Membrane Support. *1st International Seminar on Surface Support Liners: Membranes, Shotcrete and Mesh, Australian Centre for Geomechanics, Australia.*

LIGHTFOOT, N and MACCELARI, M. J. (2000). *Numerical Modelling of Mine Workings, 2nd Edition, Vol 1.* Safety In Mines Research Advisory Committee, Project Report GAP 728.

MALAN, D. F and BASSON, F. R. P. (1998). Ultra-Deep Mining: The Increased Potential for Squeezing Conditions. *The Journal of the South African Institute of Mining and Metallurgy, Vol 98*(No. 7), pp 353-364.

MALMGREN, L, NORDLUND, E and ROLUND, S. (2005). Adhesion Strength and Shrinkage of Shotcrete. *Tunnelling and Underground Space Technology, Vol 20*(No. 1), pp 33-48.

MASON, D. P and STACEY, T. R. (2008). Support of Rock Excavation Provided by Sprayed Liners. *International Journal of Rock Mechanics and Mining Sciences, 45*, pp 773-788.

NAISMITH, W.A. and STEWARD, N.R. (2002). Comparative Performance Testing of Ultra-Thin Structural Liners. *2nd Proceeding Intrenational Seminar on Surface Support Liners. South African Institute of Mining and Metallurgy*.

NAPIER, J. A. L, HILDYARD, M. W, KUIJPERS, J. S, DAEHNKE, A, SELLERS, E. F, MALAN, D. F, SIEBRITS, E, OZBAY, M.U, DEDE, T and TURNER, P.A. (1995). Develop a Quantitative Understanding of Rockmass Behaviuor Near Excavations in Deep Mines. Part 2. Chapters 3-6. *Safety In Mines Research Advisory Committee, Project Number GAP 029*.

NDLOVU, X. (2007). *Three Dimensional Analysis of Stress and Strain Distributions Around Bord and Pillar Geometries.* University of Witwatersrand, Johannesburg: MSc Dissertation.

NIELSEN, L. E. (1962). *Mechanical Properties of Polymers.* New York USA: Reinhold Publishing Corporation, Chapman and Hall Ltd, London.

ORTLEPP, W. D and STACEY, T. R. (1997). Testing of Tunnel Support: Dynamic Load Testing of Rock Support Containment Systems (eg Wire Mesh). *Safety In Mines Research Advisory Committee*.

OZTURK, H and TANNANT, D. D. (2010). Thin Spray-on Liner Adhesive Strength Test Method and Effect of Liner Thickness on Adhesion. *International Journal of Rock Mechanics and Mining Sciences, Vol 47*(No. 5), pp 808-815.

PALMSTROM, A and BROCH, E. (2006). Use and Misuse of Rock Mass Classification Systems with Particular Reference to the Q-System. *Tunnelling and Underground Space Technology, 21*, pp 575-593.

PAPPAS, D. M, BARTON, T.M and WEISS, E.S. (2004). The Long-term Performance of Surface Support Liners for Ground Control in an Underground Limestone Mine. In Y. POTVIN, D. STACEY, & J. HADJIGEORGIOU, *Surface Support in Mining.* Australian Centre for Geomechanics, pp 157-166.

PARK, D. W and KICKER, D. C. (1985). Physical Model Study of a Longwall Mine. *Mining Science and Technology, 3*, pp 51-61.

POTVIN, Y; STACEY, D and HADJIGEORGIOU, J. (2004). *Surface Support in Mining.* Australian Centre for Geomechanics.

RYDER, J. A and JAGER, A. J. (2002). *A Text Book on Rock Mechanics for Tabular Hard Rock Mines.* Safety In Mines Research Advisory Committee, Johannesburg.

SAYDAM, S; YILMAZ, H and STACEY, T. R. (2003). A New Testing Approach for Thin Spray-on Liners: Double Sided Shear Strenght. *3rd International Seminar on Surface Support Liners: Thin Spray-on Liners, Shotcrete and Mesh*.

SEYMOUR, B, MARTIN, L, CLARK, C, STEPAN, M, JACKSHA, R, PAKALNIS, R, ROWORTH, M and CACERES, C. (2010). A Practical Method of Measuring Shotcrete Adhesion Strength. *SME - Annual Meeting and Exhibit*, pp 653 - 661.

SINGH, M and RAO, K. S. (2005). Empirical Methods to Estimate the Strength of Jointed Rock Masses. *Engineering Geology, Vol 77*, pp 127-137.

SINGH, M, SINGH, B and CHOUDHARI, J. (2007). Critical Strain and Squeezing of Rock Mass in Tunnels. *Tunnelling and Underground Space Technology, Vol 22,* pp 343-350.

SINGH, T. N and FARMER, I. W. (1985). A Physical Model of Underground Coal Mine Prototype. Technical Note. *International Journal of Mining Engineering, Vol 3*, pp 319-326.

SPEARING, A. J. S. (2001). MBT's approach to Thin Support Membranes in Mines. Underground Construction Group MBT International. *Unpublished PowerPoint Presentation*.

SPEARING, A. J. S and GELSON, J. (2002). Developments and the Future of Thin Reactive Liners Since the Previous Conference in Australia. *2nd International Seminar on Surface Support Liners: Thin Sprayed Liners, Shotcrete, Mesh. South African Institute of Mining and Metallurgy. Sec 13. Sandton South Africa*, pp 1-10.

SPEARING, A. J. S and HAGUE, I. (2003). The Application of Underground Support Liners Reaches Maturity. *International Society for Rock Mechanics and South African Institute of Mining and Metallurgy*, pp 1127-1132.

SPEARING, A. J. S; CHAMPA, J. T and HULVEY, B. S. (2004). Recent Developments With the Use of Fibres in Sprayed Concrete. In *Surface Support in Mining.* POTVIN, Y; STACEY, D and HADJIGEORGIOU, J Eds.Australian Centre for Geomechanics, pp 267-270.

SPEARING, A.J.S, OHLER, J and ATTIOGBE, E. (2001). The Effective Testing of Thin Support Membranes (Superskins) For Use in the Underground Mines. *Surface Support Liners: Membranes, Shotcrete and Mesh. Australian Centre for Geomechanics.*

STACEY, T. R. (1974). 2. The Behaviour of Two- and Three-Dimensional Model Rock Slopes: Technical Note. *Q. Journal of Engineering Geology, Vol 8*, pp 67-72.

STACEY, T. R and KASANGULA, K. (2003). Results from Testing of TSLs Using a Simple, Low Cost Laboratory Test. *3rd International Seminar on Surface Support Liners: Thin Spray-on Liners, Shotcrete and Mesh, Quebec City, Canada. Section 17*.

STACEY, T. R and YU, X. (2004). Investigation Into the Mechanisms of Rock Support Provided by Sprayed Liners. In *Ground Support in Mining and Underground Construction, ed. E, VILLAESCUSA; Y, POTVIN*. London: Taylor and Francis Group, pp 565 - 569.

STACEY, T. R. (2001). Review of Membrane Support Mechanisms, Loading Mechanisms, Desired Membrane Peformance and Appropriate Test Methods. *The Journal of the South African Institute of Minining and Metallurgy, Vol 101*(No 7), pp 343 - 351.

STACEY, T. R. (2004). Shotcrete in Mines- State-of-the-Art in South Africa. In *Surface Support in Mining.* Potvin,Y; Stacey, D and Hadjigeorgiou, J Eds. Perth, Australia, pp 247-253.

SWAN, G and HENDERSON, A. (2001). Water-Based Spray-on Liner Implimentation at Falconbridge Limited. *Proceeding of Surface Support Liners: Membranes, Shotcrete and Mesh. Australian Centre for Geomechanics.*

TANNANT, D. D. (1997). *Large-scale Pull Test on Mineguard Spray-on Liner.* Report to INCO Limited. Geomechanics Centre, Sudbury, Ontario, Canada.

TANNANT, D. D and OZTURK, H. (2003). Evaluation of Test Methods for Measuring Adhesion Between Liner and Rock. *3rd Intenational Seminar on Surface Support Liners: Thin Sprayed Liners, Shotcrete and Mesh, Universit'e Laval, Quebec City, Canada.*

TANNANT, D. D; SWAN, G; ESPLEY, S; GRAHAM, C. (1999). Laboratory Procedures for Validating the Use of Thin Spray-on Liners for Mesh Replacement. *Canadian Institute of Mining and Metallurgy Annual Meeting, Calgary, Published on CD-Rom, pp 1-8.*

TANNANT, D.D. (2001). Thin Spray-on Liners for Underground Rock Support. *17th International Mining Congress and Exhibition of Turkey. Ankara, Turkey*, pp 57-73.

TARR, K, ANNOR, A and FYNN, D. (2006). Laboratory Testing Procedures for Evaluating Thin, Spray-on Membrane Liners. *CANMET Mining and Mineral Sciences Laboratories, Natural Resources Canada, Sudbury, Ontario*, pp B231-B244.

THOMPSON, A. G. (2004). Rock Support Action of Mesh Quantified by Testing and Analysis. In *Surface Support in Mining.* POTVIN, Y; STACEY, D; HADJIGEORGIOU, J eds. Australian Centre for Geomechanics, pp 391-398.

VANDEWALLE, M. (1998). The Use of Steel Fibre Reinforced Shotcrete for the Support of Mine Openings. *The Journal of the South African Institute of Mining and Metallurgy, Vol 98*(No. 3), pp 113-120.

VENTER, D. P and GARDNER, L. J. (1998). Application of Shotcrete at Oryx Mine. *The Journal of the South African Institute of Mining and Metallurgy*, pp 121-126.

VESELY, V. (2007). Experimental Tests for the Determination of Fracture- Mechanical Parameters of Concrete. *Centre for Intergrated Design of Advanced Structures. Brno University of Technology*.

VISWANATHAN, V. K and LINSEY, J. S. (2009). Enhancing Student Innovation: Physical Models in the Idea Generation Process. *39th ASEE/IEEE Frontiers in Education Conference, M1J-1*.

VORSTER, B and FRANKLIN, D. (2008). Immediate Ground Support, After Development or Exposure, Can Prevent Falls Of Ground. *The Journal of The South African Institute of Mining and Metallurgy,* pp 1-20.

WALLIMAN, N. (2004). *Your Undergraduate Dissertation: The Essential Guide for Success.* London: SAGE Publications Ltd.

YILMAZ, H. (2010). Tensile Strength Testing of Thin Spray-on Liner Products (TSLs) and Shotcrete. *The Journal of the South African Institute of Mining and Metallurgy, Vol 110*(No 10), pp 559-569.

YILMAZ, H. (2007). Shear-Bond Strength Testing of thin Spray-on Liners. *The Journal of the South African Institute of Mining and Metallurgy, Vol 107*.

YILMAZ, H. SAYDAM, S. and HENDERSON, D. (2003). Torque Testing of Thin Spray-on Liners Coated Cores. *Proceeding of 3rd International Seminar on Surface Support Liners, The Journal of the South African Institute of Mining and Metallurgy*.

# Appendix A Brazilian Tests

**Table A.1 Brazilian Indirect Tensile Strength used on 1mm thickness for TSL A**

| TSL A 1mm | Sample No | Def (mm) | Load (kN) | Stress (MPa) | Energy (Joules) | TSL (mm) |
|---|---|---|---|---|---|---|
| Control | BC1 | 0.191 | 5.853 | 5.608 | 0.444 | |
| | BC2 | 0.229 | 7.148 | 6.553 | 0.615 | |
| | BC3 | 0.206 | 6.959 | 6.667 | 0.550 | |
| | BC4 | 0.206 | 6.652 | 6.366 | 0.513 | |
| | BC5 | 0.213 | 7.603 | 6.973 | 0.613 | |
| | BC6 | 0.202 | 5.857 | 5.654 | 0.453 | |
| | BC7 | 0.198 | 6.921 | 6.499 | 0.529 | |
| | BC8 | 0.225 | 7.455 | 7.057 | 0.635 | |
| | BC9 | 0.193 | 5.984 | 5.693 | 0.465 | |
| | BC10 | 0.204 | 7.283 | 6.928 | 0.591 | |
| | **Average** | **0.207** | **6.772** | **6.400** | **0.541** | |
| Curing Time 1 Day | LA111 | 0.263 | 7.055 | 6.815 | 0.638 | 1.18 |
| | LA112 | 0.249 | 8.227 | 7.734 | 0.771 | 1.40 |
| | LA113 | 0.226 | 6.074 | 5.756 | 0.519 | 1.18 |
| | LA114 | 0.219 | 5.857 | 5.605 | 0.482 | 1.29 |
| | LA115 | 0.227 | 6.842 | 6.526 | 0.597 | 1.11 |
| | **Average** | **0.237** | **6.811** | **6.487** | **0.602** | **1.23** |
| Curing Time 7 days | LA711 | 0.356 | 7.507 | 7.054 | 0.771 | 1.31 |
| | LA712 | 0.251 | 9.022 | 8.464 | 0.883 | 1.46 |
| | LA713 | 0.223 | 7.341 | 6.898 | 0.617 | 1.17 |
| | LA714 | 0.233 | 9.146 | 8.389 | 0.784 | 1.52 |
| | LA715 | 0.245 | 7.224 | 6.917 | 0.611 | 1.45 |
| | **Average** | **0.262** | **8.048** | **7.544** | **0.733** | **1.38** |
| Curing Time 14 days | LA1411 | 0.256 | 7.961 | 7.660 | 0.700 | 1.30 |
| | LA1412 | 0.242 | 10.131 | 9.297 | 0.908 | 1.03 |
| | LA1413 | 0.213 | 6.942 | 6.607 | 0.570 | 1.08 |
| | LA1414 | 0.218 | 7.562 | 6.891 | 0.659 | 1.29 |
| | LA1415 | 0.230 | 7.641 | 7.332 | 0.649 | 1.03 |
| | **Average** | **0.232** | **8.047** | **7.557** | **0.697** | **1.15** |
| Curing Time 28 days | LA2811 | 0.294 | 7.968 | 7.625 | 0.751 | 1.08 |
| | LA2812 | 0.275 | 8.330 | 7.664 | 0.793 | 1.05 |
| | LA2813 | 0.271 | 9.029 | 8.543 | 0.820 | 1.22 |
| | LA2814 | 0.296 | 8.003 | 7.629 | 0.761 | 1.09 |
| | LA2815 | 0.266 | 8.244 | 7.885 | 0.729 | 1.05 |
| | **Average** | **0.280** | **8.315** | **7.869** | **0.771** | **1.10** |

**Table A.2 Brazilian Indirect Tensile Strength used on 3mm thickness for TSL A**

| TSL A 3mm | Sample No | Def (mm) | Load (kN) | Stress (MPa) | Energy (Joules) | TSL (mm) |
|---|---|---|---|---|---|---|
| Curing Time 1 Day | LA131 | 0.287 | 7.689 | 7.067 | 0.694 | 3.26 |
| | LA132 | 0.225 | 6.770 | 6.464 | 0.572 | 3.40 |
| | LA133 | 0.238 | 7.124 | 6.938 | 0.584 | 3.51 |
| | LA134 | 0.214 | 7.300 | 6.955 | 0.597 | 3.15 |
| | LA135 | 0.202 | 6.742 | 6.483 | 0.518 | 3.44 |
| | **Average** | **0.233** | **7.125** | **6.782** | **0.593** | **3.35** |
| Curing Time 7 days | LA731 | 0.232 | 6.546 | 6.264 | 0.610 | 3.33 |
| | LA732 | 0.223 | 7.197 | 6.857 | 0.631 | 3.62 |
| | LA733 | 0.213 | 7.910 | 7.561 | 0.683 | 3.55 |
| | LA734 | 0.260 | 7.572 | 7.286 | 0.735 | 3.56 |
| | LA735 | 0.248 | 9.022 | 8.320 | 0.863 | 3.31 |
| | **Average** | **0.235** | **7.649** | **7.258** | **0.704** | **3.47** |
| Curing Time 14 days | LA1431 | 0.202 | 6.670 | 6.185 | 0.544 | 3.35 |
| | LA1432 | 0.213 | 6.215 | 5.935 | 0.539 | 3.2 |
| | LA1433 | 0.236 | 9.043 | 8.372 | 0.817 | 3.21 |
| | LA1434 | 0.205 | 6.132 | 5.875 | 0.495 | 3.17 |
| | LA1435 | 0.239 | 8.075 | 7.418 | 0.723 | 3.4 |
| | **Average** | **0.219** | **7.227** | **6.757** | **0.624** | **3.23** |
| Curing Time 28 days | LA2831 | 0.211 | 6.969 | 6.695 | 0.599 | 3.76 |
| | LA2832 | 0.250 | 6.167 | 5.828 | 0.534 | 3.16 |
| | LA2833 | 0.222 | 6.253 | 6.090 | 0.538 | 3.66 |
| | LA2834 | 0.223 | 7.386 | 7.000 | 0.666 | 3.55 |
| | LA2835 | 0.199 | 6.938 | 6.795 | 0.551 | 3.67 |
| | **Average** | **0.221** | **6.743** | **6.482** | **0.577** | **3.53** |

**Table A.3 Brazilian Indirect Tensile Strength used on 5mm thickness for TSL A**

| TSL A 5mm | Sample | Def | Load | Stress | Energy | TSL |
|---|---|---|---|---|---|---|
| | No | (mm) | (kN) | (MPa) | (Joules) | (mm) |
| Curing Time 1 Day | LA151 | 0.209 | 7.131 | 6.788 | 0.568 | 5.10 |
| | LA152 | 0.207 | 6.749 | 6.361 | 0.548 | 5.27 |
| | LA153 | 0.232 | 7.979 | 7.627 | 0.684 | 5.16 |
| | LA154 | 0.229 | 8.171 | 7.467 | 0.682 | 5.03 |
| | LA155 | 0.242 | 8.674 | 8.337 | 0.763 | 5.08 |
| | **Average** | **0.224** | **7.741** | **7.316** | **0.649** | **5.13** |
| Curing Time 7 days | LA751 | 0.250 | 7.035 | 6.750 | 0.678 | 4.33 |
| | LA752 | 0.266 | 8.829 | 8.426 | 0.856 | 5.41 |
| | LA753 | 0.240 | 8.096 | 7.397 | 0.769 | 5.57 |
| | LA754 | 0.224 | 7.820 | 7.463 | 0.698 | 5.13 |
| | LA755 | 0.220 | 7.503 | 7.153 | 0.658 | 5.45 |
| | **Average** | **0.240** | **7.857** | **7.438** | **0.732** | **5.18** |
| Curing Time 14 days | LA1451 | 0.263 | 7.018 | 6.450 | 0.655 | 5.02 |
| | LA1452 | 0.231 | 7.923 | 7.229 | 0.704 | 4.70 |
| | LA1453 | 0.227 | 7.383 | 7.108 | 0.632 | 4.89 |
| | LA1454 | 0.231 | 9.022 | 8.293 | 0.787 | 4.68 |
| | LA1455 | 0.195 | 5.815 | 5.605 | 0.452 | 4.85 |
| | **Average** | **0.229** | **7.432** | **6.937** | **0.646** | **4.83** |
| Curing Time 28 days | LA2851 | 0.200 | 7.042 | 6.858 | 0.573 | 5.26 |
| | LA2852 | 0.204 | 7.579 | 7.391 | 0.641 | 5.73 |
| | LA2853 | 0.256 | 8.068 | 7.719 | 0.787 | 6.17 |
| | LA2854 | 0.278 | 8.609 | 8.384 | 0.930 | 5.49 |
| | **Average** | **0.235** | **7.824** | **7.588** | **0.733** | **5.66** |

**Table A.4 Brazilian Indirect Tensile Strength used on 1mm thickness for TSL B**

| TSL B 1mm | Sample No | Def (mm) | Load (kN) | Stress (MPa) | Energy (Joules) | TSL (mm) |
|---|---|---|---|---|---|---|
| Curing Time 1 Day | T111 | 0.233 | 7.396 | 7.090 | 0.665 | 1.31 |
| | T112 | 0.245 | 7.607 | 7.174 | 0.683 | 1.15 |
| | T113 | 0.250 | 8.771 | 8.430 | 0.826 | 1.23 |
| | T114 | 0.243 | 7.775 | 7.482 | 0.718 | 1.32 |
| | T115 | 0.222 | 7.066 | 6.866 | 0.608 | 1.81 |
| | **Average** | **0.239** | **7.723** | **7.408** | **0.700** | **1.36** |
| Curing Time 7 days | T711 | 0.254 | 7.241 | 6.941 | 0.614 | 1.13 |
| | T712 | 0.237 | 8.399 | 7.960 | 0.730 | 1.38 |
| | T713 | 0.231 | 8.020 | 7.696 | 0.685 | 1.29 |
| | T714 | 0.285 | 8.643 | 8.280 | 0.757 | 1.39 |
| | T715 | 0.209 | 6.776 | 6.419 | 0.538 | 1.38 |
| | **Average** | **0.243** | **7.816** | **7.459** | **0.665** | **1.31** |
| Curing Time 14 days | T1411 | 0.251 | 9.573 | 8.680 | 0.868 | 1.06 |
| | T1412 | 0.227 | 5.760 | 5.530 | 0.618 | 1.33 |
| | T1413 | 0.252 | 7.272 | 6.704 | 0.477 | 1.43 |
| | T1414 | 0.227 | 8.537 | 8.268 | 0.714 | 1.28 |
| | T1415 | 0.228 | 8.612 | 7.931 | 0.762 | 1.28 |
| | **Average** | **0.237** | **7.951** | **7.423** | **0.688** | **1.28** |
| Curing Time 28 days | T2811 | 0.296 | 9.098 | 8.631 | 0.885 | 1.63 |
| | T2812 | 0.272 | 8.822 | 8.425 | 0.811 | 1.28 |
| | T2813 | 0.259 | 8.488 | 8.070 | 0.743 | 1.19 |
| | T2814 | 0.250 | 8.664 | 8.273 | 0.750 | 1.55 |
| | T2815 | 0.346 | 8.416 | 8.129 | 0.769 | 1.51 |
| | **Average** | **0.284** | **8.698** | **8.306** | **0.792** | **1.43** |

**Table A.5 Brazilian Indirect Tensile Strength used on 3mm thickness for TSL B**

| TSL B 3mm | Sample No | Def (mm) | Load (kN) | Stress (MPa) | Energy (Joules) | TSL (mm) |
|---|---|---|---|---|---|---|
| **Curing Time 1 Day** | T131 | 0.237 | 8.316 | 7.818 | 0.749 | 3.76 |
| | T132 | 0.227 | 7.148 | 6.804 | 0.620 | 3.77 |
| | T133 | 0.216 | 7.235 | 6.897 | 0.596 | 3.43 |
| | T134 | 0.211 | 6.604 | 6.341 | 0.527 | 3.15 |
| | T135 | 0.220 | 7.241 | 6.922 | 0.632 | 3.43 |
| | **Average** | **0.222** | **7.309** | **6.956** | **0.625** | **3.51** |
| **Curing Time 7 days** | | | | | | |
| | | | | | | |
| | T731 | 0.215 | 6.952 | 6.493 | 0.597 | 3.56 |
| | T732 | 0.220 | 6.725 | 6.414 | 0.574 | 3.69 |
| | T733 | 0.241 | 8.757 | 8.294 | 0.832 | 3.61 |
| | **Average** | **0.226** | **7.478** | **7.067** | **0.668** | **3.62** |
| **Curing Time 14 days** | T1431 | 0.326 | 7.999 | 7.716 | 0.862 | 3.67 |
| | T1432 | 0.279 | 7.789 | 7.575 | 0.761 | 4.10 |
| | T1433 | 0.219 | 6.842 | 6.546 | 0.599 | 3.85 |
| | T1434 | 0.232 | 8.526 | 7.859 | 0.769 | 3.47 |
| | T1435 | 0.221 | 7.400 | 7.138 | 0.634 | 3.79 |
| | **Average** | **0.256** | **7.711** | **7.367** | **0.725** | **3.77** |
| **Curing Time 28 days** | T2831 | 0.369 | 6.615 | 6.372 | 0.841 | 4.17 |
| | T2832 | 0.269 | 8.254 | 7.833 | 0.834 | 3.72 |
| | T2833 | 0.325 | 9.315 | 8.876 | 1.058 | 3.94 |
| | T2834 | 0.261 | 8.764 | 8.185 | 0.859 | 4.05 |
| | T2835 | 0.260 | 7.390 | 6.820 | 0.662 | 3.79 |
| | **Average** | **0.297** | **8.067** | **7.617** | **0.851** | **3.93** |

**Table A.6 Brazilian Indirect Tensile Strength used on 5mm thickness for TSL B**

| TSL B 5mm | Sample No | Def (mm) | Load (kN) | Stress (MPa) | Energy (Joules) | TSL (mm) |
|---|---|---|---|---|---|---|
| Curing Time 1 Day | T151 | 0.223 | 6.869 | 6.628 | 0.598 | 4.36 |
| | T152 | 0.223 | 7.238 | 6.797 | 0.590 | 4.98 |
| | T153 | 0.225 | 8.254 | 7.642 | 0.726 | 5.24 |
| | T154 | 0.226 | 7.148 | 6.893 | 0.622 | 5.21 |
| | T155 | 0.227 | 7.310 | 6.905 | 0.624 | 4.89 |
| | **Average** | **0.225** | **7.364** | **6.973** | **0.632** | **4.94** |
| Curing Time 7 days | T751 | 0.230 | 8.540 | 8.387 | 0.759 | 5.37 |
| | T752 | 0.252 | 8.199 | 7.765 | 0.752 | 5.15 |
| | T753 | 0.297 | 7.675 | 7.567 | 0.769 | 5.17 |
| | T754 | 0.234 | 8.113 | 7.614 | 0.756 | 5.10 |
| | T755 | 0.245 | 8.740 | 7.962 | 0.835 | 5.26 |
| | **Average** | **0.252** | **8.253** | **7.859** | **0.774** | **5.21** |
| Curing Time 14 days | T1451 | 0.223 | 7.272 | 7.005 | 0.617 | 5.60 |
| | T1452 | 0.221 | 7.348 | 7.030 | 0.623 | 5.49 |
| | T1453 | 0.207 | 7.410 | 7.148 | 0.605 | 5.35 |
| | T1454 | 0.214 | 7.238 | 6.943 | 0.604 | 5.28 |
| | T1455 | 0.211 | 8.106 | 7.808 | 0.678 | 5.61 |
| | **Average** | **0.215** | **7.475** | **7.187** | **0.625** | **5.43** |
| Curing Time 28 days | T2851 | 0.243 | 7.796 | 7.408 | 0.708 | 5.84 |
| | T2852 | 0.246 | 7.662 | 7.320 | 0.692 | 5.69 |
| | T2853 | 0.258 | 8.702 | 8.359 | 0.819 | 5.25 |
| | T2854 | 0.248 | 8.282 | 8.032 | 0.763 | 5.50 |
| | T2855 | 0.244 | 7.751 | 7.570 | 0.727 | 5.66 |
| | **Average** | **0.248** | **8.038** | **7.738** | **0.742** | **5.57** |

**Table A.7 Brazilian Indirect Tensile Strength used on 1mm thickness for TSL C**

| TSL C 1mm | Sample No | Def (mm) | Load (kN) | Stress (MPa) | Energy (Joules) | TSL (mm) |
|---|---|---|---|---|---|---|
| Curing Time 1 Day | N111 | 0.272 | 7.968 | 7.576 | 0.741 | 1.07 |
| | N112 | 0.226 | 6.721 | 6.460 | 0.587 | 1.06 |
| | N113 | 0.346 | 7.417 | 7.121 | 0.831 | 1.09 |
| | N114 | 0.215 | 6.532 | 6.254 | 0.548 | 1.10 |
| | N115 | 0.299 | 8.781 | 8.524 | 0.872 | 1.61 |
| | **Average** | **0.272** | **7.484** | **7.187** | **0.716** | **1.19** |
| Curing Time 7 days | N711 | 0.248 | 6.584 | 6.173 | 0.610 | 1.41 |
| | N712 | 0.254 | 9.036 | 8.577 | 0.791 | 1.28 |
| | N713 | 0.242 | 9.098 | 8.509 | 0.799 | 1.15 |
| | N714 | 0.223 | 8.702 | 8.332 | 0.749 | 1.3 |
| | N715 | 0.237 | 8.940 | 8.536 | 0.782 | 1.2 |
| | **Average** | **0.241** | **8.472** | **8.025** | **0.746** | **1.27** |
| Curing Time 14 days | N1411 | 0.205 | 5.981 | 5.680 | 0.451 | 1.18 |
| | N1412 | 0.270 | 8.395 | 8.012 | 0.788 | 1.52 |
| | N1413 | 0.259 | 9.969 | 9.138 | 0.911 | 1.35 |
| | N1414 | 0.275 | 8.426 | 8.086 | 0.787 | 1.93 |
| | N1415 | 0.338 | 8.912 | 8.148 | 0.942 | 1.55 |
| | **Average** | **0.269** | **8.337** | **7.813** | **0.776** | **1.51** |
| Curing Time 28 days | N2811 | 0.268 | 6.863 | 6.536 | 0.581 | 1.04 |
| | N2812 | 0.289 | 7.755 | 7.523 | 0.709 | 1.48 |
| | N2813 | 0.310 | 11.878 | 11.036 | 1.205 | 1.44 |
| | N2814 | 0.330 | 10.197 | 9.416 | 1.161 | 1.44 |
| | N2815 | 0.278 | 8.843 | 8.135 | 0.852 | 1.47 |
| | **Average** | **0.295** | **9.107** | **8.529** | **0.902** | **1.37** |

**Table A.8 Brazilian Indirect Tensile Strength used on 3mm thickness for TSL C**

| TSL C 3mm | Sample No | Def (mm) | Load (kN) | Stress (MPa) | Energy (Joules) | TSL (mm) |
|---|---|---|---|---|---|---|
| Curing Time 1 day | N131 | 0.208 | 6.466 | 6.178 | 0.515 | 3.03 |
| | N132 | 0.204 | 6.821 | 6.468 | 0.548 | 3.29 |
| | N133 | 0.210 | 7.903 | 7.642 | 0.650 | 3.71 |
| | N134 | 0.192 | 6.590 | 6.086 | 0.493 | 3.17 |
| | N135 | 0.216 | 7.531 | 7.203 | 0.640 | 3.54 |
| | **Average** | **0.206** | **7.062** | **6.715** | **0.569** | **3.35** |
| Curing Time 7 days | N731 | 0.298 | 7.128 | 6.766 | 0.786 | 3.36 |
| | N732 | 0.340 | 8.299 | 7.937 | 0.872 | 3.82 |
| | N733 | 0.222 | 7.558 | 7.225 | 0.636 | 3.94 |
| | N734 | 0.210 | 9.005 | 8.622 | 0.702 | 3.52 |
| | N735 | 0.227 | 9.129 | 8.765 | 0.776 | 3.48 |
| | N736 | 0.241 | 8.692 | 8.093 | 0.736 | 3.63 |
| | N737 | 0.210 | 7.341 | 7.068 | 0.555 | 3.41 |
| | **Average** | **0.250** | **8.165** | **7.782** | **0.723** | **3.59** |
| Curing Time 14 days | N1431 | 0.201 | 6.697 | 6.483 | 0.532 | 3.88 |
| | N1432 | 0.196 | 6.143 | 5.681 | 0.466 | 3.85 |
| | N1433 | 0.242 | 7.562 | 6.910 | 0.712 | 3.72 |
| | N1434 | 0.234 | 9.625 | 8.842 | 0.872 | 4.10 |
| | N1435 | 0.258 | 8.740 | 8.113 | 0.821 | 3.77 |
| | **Average** | **0.226** | **7.753** | **7.206** | **0.680** | **3.89** |
| Curing Time 28 days | N2831 | 0.222 | 7.004 | 6.611 | 0.615 | 3.68 |
| | N2832 | 0.251 | 8.295 | 7.707 | 0.775 | 3.30 |
| | N2833 | 0.290 | 7.868 | 7.569 | 0.769 | 2.97 |
| | N2834 | 0.229 | 8.402 | 8.105 | 0.752 | 2.92 |
| | **Average** | **0.248** | **7.892** | **7.498** | **0.728** | **3.22** |

**Table A.9 Brazilian Indirect Tensile Strength used on 5mm thickness for TSL C**

| TSL C 5mm | Sample No | Def (mm) | Load (kN) | Stress (MPa) | Energy (Joules) | TSL (mm) |
|---|---|---|---|---|---|---|
| Curing Time 1 day | N151 | 0.217 | 7.892 | 7.168 | 0.648 | 5.11 |
| | N152 | 0.208 | 7.286 | 6.965 | 0.596 | 4.92 |
| | N153 | 0.263 | 8.447 | 8.218 | 0.746 | 5.65 |
| | N154 | 0.195 | 6.904 | 6.621 | 0.547 | 5.10 |
| | N155 | 0.188 | 6.511 | 6.167 | 0.501 | 5.28 |
| | **Average** | **0.214** | **7.408** | **7.028** | **0.608** | **5.21** |
| Curing Time 7 days | N751 | 0.247 | 9.005 | 8.488 | 0.864 | 5.39 |
| | N752 | 0.289 | 10.741 | 10.335 | 1.200 | 5.48 |
| | N753 | 0.306 | 8.729 | 8.176 | 1.066 | 5.62 |
| | N754 | 0.231 | 9.508 | 9.245 | 0.819 | 5.78 |
| | N755 | 0.252 | 10.090 | 9.630 | 0.947 | 5.46 |
| | N756 | 0.299 | 9.064 | 8.636 | 0.979 | 5.45 |
| | N757 | 0.247 | 10.242 | 9.849 | 0.944 | 5.31 |
| | N758 | 0.241 | 10.128 | 9.640 | 0.916 | 5.55 |
| | **Average** | **0.264** | **9.688** | **9.250** | **0.967** | **5.51** |
| Curing Time 14 days | N1451 | 0.255 | 10.951 | 10.086 | 1.013 | 5.78 |
| | N1452 | 0.239 | 9.687 | 8.899 | 0.876 | 5.55 |
| | N1453 | 0.260 | 9.170 | 8.459 | 0.859 | 5.82 |
| | N1454 | 0.243 | 8.433 | 7.723 | 0.756 | 5.65 |
| | N1455 | 0.303 | 9.642 | 8.843 | 0.976 | 5.63 |
| | **Average** | **0.260** | **9.577** | **8.802** | **0.896** | **5.69** |
| Curing Time 28 days | N2851 | 0.285 | 8.292 | 7.869 | 0.789 | 5.48 |
| | N2852 | 0.245 | 9.463 | 9.017 | 0.894 | 5.70 |
| | N2853 | 0.245 | 9.659 | 9.094 | 0.940 | 5.78 |
| | N2854 | 0.356 | 8.209 | 7.854 | 0.810 | 5.56 |
| | N2855 | 0.200 | 7.910 | 7.496 | 0.646 | 5.24 |
| | **Average** | **0.267** | **8.707** | **8.266** | **0.816** | **5.63** |

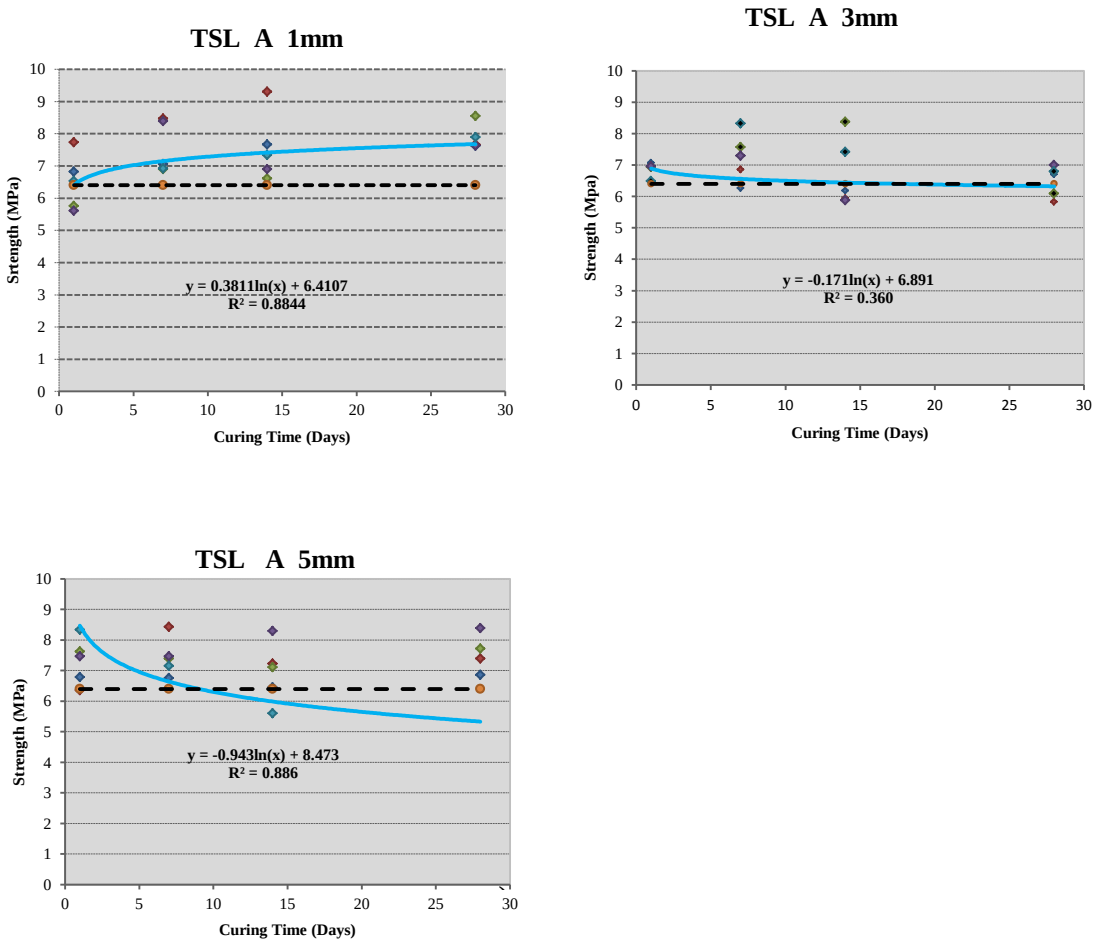


**Figure A.1 TSL A Brazilian Test graphs a), b), c)**

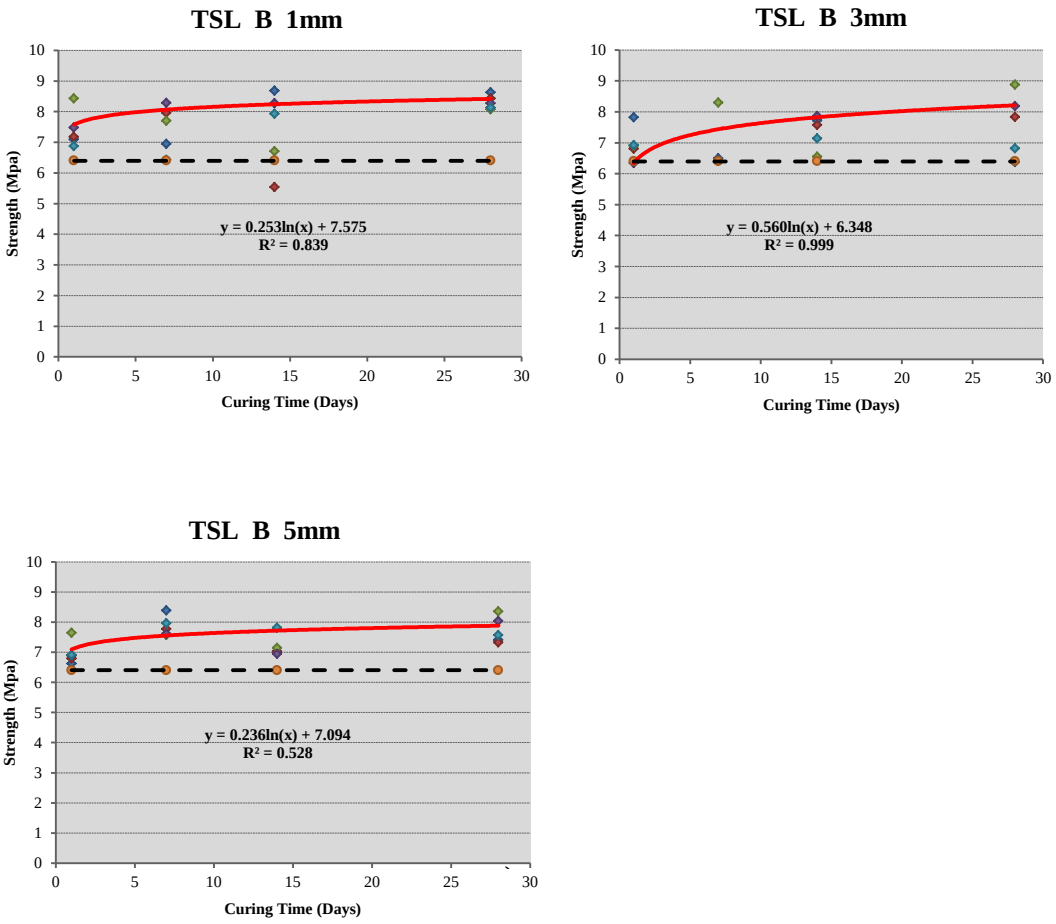


**Figure A.2 Brazilian Test graphs a), b), c)**

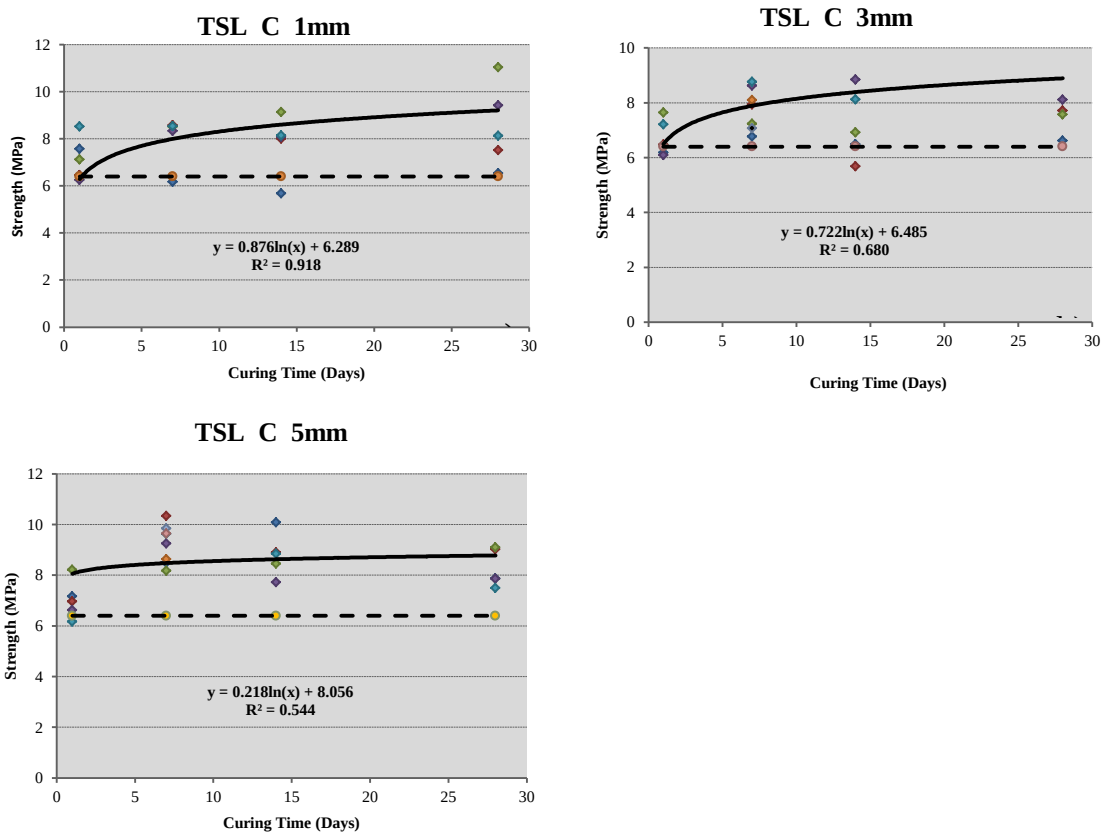


**Figure A.3 Brazilian Test graphs a), b) and c)**

# Appendix B Compression Tests

**Table B.1 Compression Results for TSL A**

| TSL A | | At maximum load | | | | |
|---|---|---|---|---|---|---|
| | **Sample No** | **Def (mm)** | **Load (kN)** | **Strain** | **Stress (MPa)** | **Stiffness (MN/m)** |
| **Curing Time 1 day** | LA11 | 5.808 | 0.098 | 0.082 | 0.086 | 0.016 |
| | LA12 | 5.778 | 0.104 | 0.081 | 0.093 | 0.031 |
| | LA13 | 4.986 | 0.101 | 0.071 | 0.087 | 0.030 |
| | LA14 | 3.477 | 0.101 | 0.049 | 0.084 | 0.090 |
| | **Average** | **5.012** | **0.101** | **0.071** | **0.087** | **0.042** |
| **Curing Time 7 days** | LA71 | 1.013 | 4.875 | 0.014 | 4.271 | 10.740 |
| | LA72 | 0.933 | 4.755 | 0.013 | 4.116 | 11.344 |
| | LA73 | 0.925 | 5.864 | 0.013 | 5.055 | 13.047 |
| | LA74 | 1.122 | 5.884 | 0.016 | 5.030 | 8.332 |
| | LA75 | 1.053 | 5.523 | 0.015 | 4.682 | 9.784 |
| | **Average** | **1.009** | **5.380** | **0.014** | **4.631** | **10.649** |
| **Curing Time 14 days** | LA141 | 1.043 | 7.066 | 0.014 | 6.155 | 15.314 |
| | LA142 | 0.846 | 6.277 | 0.012 | 5.508 | 14.488 |
| | LA143 | 0.796 | 7.421 | 0.011 | 6.459 | 16.418 |
| | LA144 | 0.939 | 9.511 | 0.013 | 8.523 | 17.333 |
| | LA145 | 0.670 | 5.433 | 0.013 | 8.523 | 16.280 |
| | **Average** | **0.859** | **7.142** | **0.013** | **7.034** | **15.967** |
| **Curing Time 28 days** | LA281 | 0.750 | 11.523 | 0.011 | 10.499 | 23.704 |
| | LA282 | 0.709 | 12.394 | 0.010 | 11.288 | 27.365 |
| | LA283 | 0.766 | 10.796 | 0.011 | 9.612 | 18.947 |
| | LA284 | 0.748 | 12.518 | 0.011 | 11.039 | 25.546 |
| | LA285 | 0.765 | 12.081 | 0.011 | 10.756 | 26.700 |
| | LA286 | 0.900 | 7.917 | 0.012 | 6.824 | 14.570 |
| | LA287 | 0.872 | 7.448 | 0.012 | 6.575 | 15.300 |
| | LA288 | 0.863 | 8.116 | 0.012 | 7.150 | 16.627 |
| | LA289 | 0.861 | 7.644 | 0.012 | 6.931 | 16.080 |
| | LA2810 | 0.879 | 10.011 | 0.012 | 8.812 | 20.539 |
| | **Average** | **0.811** | **10.045** | **0.011** | **8.949** | **20.538** |

**Table B.2 Compression Results for TSL B**

| TSL B | | At maximum load | | | | |
|---|---|---|---|---|---|---|
| | **Sample No** | **Def (mm)** | **Load (kN)** | **Strain** | **Stress (MPa)** | **Stiffness (MN/m)** |
| **Curing Time 1 day** | T11 | 0.830 | 0.983 | 0.012 | 0.877 | 2.286 |
| | T12 | 1.001 | 1.014 | 0.014 | 0.878 | 1.813 |
| | T13 | 0.867 | 0.976 | 0.012 | 0.878 | 4.043 |
| | T14 | 0.812 | 0.959 | 0.011 | 0.835 | 2.343 |
| | T15 | 1.106 | 0.959 | 0.015 | 0.833 | 1.243 |
| | T16 | 0.990 | 0.945 | 0.014 | 0.824 | 1.596 |
| | **Average** | **0.934** | **0.972** | **0.013** | **0.854** | **2.221** |
| **Curing Time 7 days** | T71 | 0.529 | 11.991 | 0.0076 | 10.027 | 34.390 |
| | T72 | 0.601 | 11.519 | 0.0085 | 9.815 | 33.492 |
| | T73 | 0.557 | 11.378 | 0.0079 | 9.425 | 36.238 |
| | T74 | 0.482 | 10.713 | 0.0069 | 9.056 | 33.795 |
| | T75 | 0.510 | 9.921 | 0.0073 | 8.716 | 33.337 |
| | T76 | 0.522 | 8.853 | 0.0074 | 7.810 | 28.649 |
| | **Average** | **0.534** | **10.730** | **0.008** | **9.142** | **33.317** |
| **Curing Time 14 days** | T141 | 0.778 | 17.175 | 0.011 | 14.699 | 40.855 |
| | T142 | 0.591 | 17.892 | 0.008 | 15.316 | 52.503 |
| | T143 | 0.811 | 16.845 | 0.012 | 14.372 | 43.842 |
| | T144 | 0.621 | 15.966 | 0.009 | 13.641 | 44.891 |
| | T145 | 0.725 | 15.611 | 0.010 | 13.822 | 39.960 |
| | **Average** | **0.705** | **16.698** | **0.010** | **14.370** | **44.410** |
| **Curing Time 28 days** | T281 | 0.900 | 18.780 | 0.013 | 16.484 | 40.895 |
| | T282 | 0.645 | 19.025 | 0.009 | 16.744 | 48.770 |
| | T283 | 0.672 | 16.355 | 0.010 | 14.500 | 42.134 |
| | T284 | 0.700 | 17.620 | 0.010 | 15.657 | 43.533 |
| | T285 | 0.688 | 19.228 | 0.010 | 16.017 | 53.109 |
| | **Average** | **0.721** | **18.202** | **0.010** | **15.880** | **45.688** |

**Table B.3 Compression Results for TSL C**

| TSL C | | At maximum load | | | | |
|---|---|---|---|---|---|---|
| | **Sample No** | **Def (mm)** | **Load (kN)** | **Strain** | **Stress (MPa)** | **Stiffness (MN/m)** |
| **Curing Time 1 day** | ND11 | 0.678 | 1.372 | 0.010 | 1.135 | 2.733 |
| | ND12 | 0.649 | 1.444 | 0.009 | 1.240 | 3.272 |
| | ND13 | 0.569 | 1.417 | 0.008 | 1.231 | 3.269 |
| | ND14 | 0.674 | 1.558 | 0.009 | 1.302 | 3.652 |
| | **Average** | **0.642** | **1.448** | **0.009** | **1.227** | **3.232** |
| **Curing Time 7 days** | ND71 | 0.994 | 22.242 | 0.014 | 19.122 | 44.602 |
| | ND72 | 0.751 | 24.336 | 0.011 | 21.014 | 52.015 |
| | ND73 | 0.779 | 20.320 | 0.011 | 17.298 | 45.619 |
| | **Average** | **0.841** | **22.299** | **0.012** | **19.145** | **47.412** |
| **Curing Time 14 Days** | ND141 | 0.965 | 25.228 | 0.014 | 21.388 | 49.441 |
| | ND142 | 0.782 | 27.123 | 0.011 | 23.066 | 60.930 |
| | ND143 | 0.748 | 27.826 | 0.011 | 23.901 | 61.384 |
| | **Average** | **0.832** | **26.726** | **0.012** | **22.785** | **57.251** |
| **Curing Time 28 Days** | ND281 | 0.684 | 27.116 | 0.010 | 23.161 | 62.540 |
| | ND282 | 0.567 | 26.679 | 0.008 | 22.661 | 69.832 |
| | ND283 | 0.595 | 27.412 | 0.008 | 23.585 | 73.297 |
| | **Average** | **0.615** | **27.069** | **0.009** | **23.135** | **68.556** |

# Appendix C 3-point Bending Tests

**Table C.1 Bending Test Results TSL A**

| TSL A | | At maximum load | | | | | | |
|---|---|---|---|---|---|---|---|---|
| 10mm Groove | | Sample No | Def (mm) | Load (kN) | Stress (MPa) | Strain | slope m (MN/m) | TSL Thickness (mm) |
| Red Sandstone | Control | C1 | 0.099 | 0.924 | 5.409 | 0.094 | 10.687 | 0.00 |
| | | C2 | 0.097 | 0.886 | 5.218 | 0.092 | 11.141 | 0.00 |
| | | C3 | 0.087 | 0.897 | 5.222 | 0.082 | 11.260 | 0.00 |
| | | **Average** | **0.094** | **0.902** | **5.283** | **0.089** | **11.030** | **0.00** |
| | Curing Time 1 day | C11 | 0.362 | 0.793 | 4.652 | 0.341 | 1.922 | 4.18 |
| | | C12 | 0.393 | 0.890 | 5.106 | 0.374 | 2.154 | 4.10 |
| | | C13 | 0.218 | 0.273 | 1.592 | 0.206 | 1.361 | 3.72 |
| | | C14 | 0.432 | 0.862 | 4.836 | 0.415 | 1.824 | 3.64 |
| | | **Average** | **0.351** | **0.705** | **4.047** | **0.334** | **1.815** | **3.91** |
| | Curing Time 7 days | C71 | 0.307 | 0.910 | 5.350 | 0.289 | 3.876 | 2.72 |
| | | C72 | 0.269 | 0.904 | 5.288 | 0.254 | 3.536 | 3.20 |
| | | C73 | 0.250 | 0.921 | 5.421 | 0.236 | 4.316 | 2.92 |
| | | **Average** | **0.275** | **0.912** | **5.353** | **0.260** | **3.909** | **2.95** |
| | Curing Time 14 days | C141 | 0.391 | 1.048 | 6.187 | 0.365 | 3.780 | 5.06 |
| | | C142 | 0.215 | 0.983 | 5.789 | 0.201 | 5.207 | 4.02 |
| | | C143 | 0.435 | 1.017 | 5.911 | 0.408 | 3.363 | 4.54 |
| | | C144 | 0.282 | 1.065 | 6.034 | 0.268 | 4.882 | 3.42 |
| | | **Average** | **0.331** | **1.028** | **5.980** | **0.310** | **4.308** | **4.26** |
| | Curing Time 28 days | C281 | 0.226 | 0.935 | 5.519 | 0.212 | 3.660 | 3.80 |
| | | C282 | 0.148 | 0.910 | 5.266 | 0.140 | 6.781 | 3.00 |
| | | C283 | 0.232 | 0.928 | 5.462 | 0.218 | 4.562 | 3.22 |
| | | **Average** | **0.202** | **0.924** | **5.416** | **0.190** | **5.001** | **3.34** |

**Table C.2 Bending Test Results TSL B**

| TSL B | | At maximum load | | | | | | |
|---|---|---|---|---|---|---|---|---|
| 10mm Groove | | Sample No | Def (mm) | Load (kN) | Stress (MPa) | Strain | slope m (MN/m) | TSL Thickness (mm) |
| Red Sandstone | Curing Time 1 day | T11 | 0.196 | 0.246 | 1.473 | 0.183 | 1.324 | 3.50 |
| | | T12 | 0.244 | 0.966 | 5.422 | 0.233 | 4.498 | 4.22 |
| | | T13 | 0.220 | 0.869 | 4.977 | 0.209 | 4.180 | 3.96 |
| | | T14 | 0.191 | 0.315 | 1.802 | 0.182 | 1.806 | 4.62 |
| | | **Average** | **0.213** | **0.599** | **3.419** | **0.202** | **2.952** | **4.08** |
| | Curing Time 7 days | T71 | 0.181 | 0.373 | 2.280 | 0.168 | 2.240 | 3.86 |
| | | T72 | 0.219 | 0.552 | 3.248 | 0.206 | 2.483 | 4.94 |
| | | T73 | 0.193 | 0.487 | 2.788 | 0.184 | 2.424 | 4.35 |
| | | **Average** | **0.198** | **0.471** | **2.772** | **0.186** | **2.382** | **4.38** |
| | Curing Time 14 days | T141 | 0.531 | 0.421 | 2.564 | 0.494 | 0.496 | 4.96 |
| | | T142 | 0.236 | 1.134 | 6.452 | 0.224 | 5.470 | 4.48 |
| | | T143 | 0.340 | 0.525 | 3.053 | 0.321 | 1.788 | 3.98 |
| | | T144 | 0.365 | 1.038 | 6.082 | 0.342 | 2.781 | 4.95 |
| | | **Average** | **0.368** | **0.780** | **4.538** | **0.345** | **2.634** | **4.59** |
| | Curing Time 28 days | T281 | 0.529 | 0.976 | 5.851 | 0.491 | 1.898 | 3.74 |
| | | T282 | 0.459 | 0.986 | 5.739 | 0.432 | 2.280 | 5.10 |
| | | T283 | 0.512 | 0.532 | 3.131 | 0.481 | 1.044 | 4.22 |
| | | T284 | 0.298 | 0.504 | 2.998 | 0.279 | 1.626 | 4.52 |
| | | **Average** | **0.449** | **0.749** | **4.430** | **0.421** | **1.712** | **4.40** |

**Table C.3 Bending Test Result for TSL C and D**

| TSL C and D | | At maximum load | | | | | | |
|---|---|---|---|---|---|---|---|---|
| | | Sample No | Def (mm) | Load (kN) | Stress (MPa) | Strain | slope m (MN/m) | TSL Thickness (mm) |
| Red Sandstone 10mm Grooved (TSL C) | Curing Time 1 day | NDB11 | 0.112 | 0.532 | 3.069 | 0.106 | 6.246 | 3.26 |
| | | NDB12 | 0.121 | 0.373 | 2.206 | 0.113 | 3.014 | 3.72 |
| | | NDB13 | 0.133 | 0.569 | 3.182 | 0.128 | 5.748 | 3.68 |
| | | NDB14 | 0.260 | 1.465 | 8.593 | 0.244 | 6.377 | 3.46 |
| | | **Average** | **0.157** | **0.735** | **4.263** | **0.148** | **5.346** | **3.53** |
| | Curing Time 7 days | NDB71 | 0.221 | 1.207 | 7.098 | 0.207 | 5.785 | 2.82 |
| | | NDB72 | 0.151 | 0.659 | 3.885 | 0.142 | 4.419 | 3.40 |
| | | NDB73 | 0.327 | 0.693 | 3.987 | 0.311 | 3.243 | 2.68 |
| | | NDB74 | 0.240 | 0.542 | 3.229 | 0.224 | 2.962 | 3.64 |
| | | **Average** | **0.235** | **0.775** | **4.550** | **0.221** | **4.102** | **3.14** |
| | Curing Time 14 days | NDB141 | 0.244 | 1.196 | 6.932 | 0.231 | 5.070 | 3.02 |
| | | NDB142 | 0.260 | 0.645 | 3.762 | 0.246 | 2.651 | 3.94 |
| | | NDB143 | 0.294 | 0.724 | 4.321 | 0.277 | 3.156 | 3.58 |
| | | NDB144 | 0.172 | 1.262 | 7.133 | 0.163 | 8.250 | 2.42 |
| | | **Average** | **0.242** | **0.957** | **5.537** | **0.229** | **4.782** | **3.24** |
| | Curing Time 28 days | NDB281 | 0.163 | 1.145 | 6.606 | 0.154 | 7.796 | 3.70 |
| | | NDB282 | 0.157 | 1.169 | 6.767 | 0.149 | 9.156 | 3.58 |
| | | NDB283 | 0.136 | 1.193 | 6.949 | 0.128 | 9.507 | 3.69 |
| | | NDB284 | 0.194 | 1.203 | 6.933 | 0.183 | 6.722 | 3.70 |
| | | **Average** | **0.162** | **1.177** | **6.814** | **0.154** | **8.295** | **3.67** |
| Red Sandstones No Groove (TSL C) | Control No Groove | NGBC1 | 0.219 | 2.536 | 14.843 | 0.206 | | 0.00 |
| | | NGBC2 | 0.192 | 2.553 | 15.034 | 0.181 | | 0.00 |
| | | NGBC3 | 0.251 | 2.299 | 13.387 | 0.236 | | 0.00 |
| | | NGBC4 | 0.178 | 2.485 | 14.470 | 0.168 | | 0.00 |
| | | NGBC5 | 0.184 | 2.447 | 14.250 | 0.173 | | 0.00 |
| | | NGBC6 | 0.202 | 2.460 | 14.330 | 0.190 | | 0.00 |
| | | **Average** | **0.204** | **2.463** | **14.386** | **0.192** | | **0.00** |
| | Curing Time 7 days | NGB71 | 0.182 | 2.147 | 12.554 | 0.171 | | 4.22 |
| | | NGB72 | 0.200 | 1.902 | 10.876 | 0.190 | | 2.68 |
| | | NGB73 | 0.239 | 2.040 | 12.479 | 0.220 | | 4.60 |
| | | NGB74 | 0.180 | 2.116 | 11.813 | 0.172 | | 3.92 |
| | | NGB75 | 0.242 | 2.343 | 13.700 | 0.226 | | 4.52 |
| | | **Average** | **0.208** | **2.110** | **12.284** | **0.196** | | **3.99** |
| White Sandstone 10mm Grooved (TSL D) | Control Grooved | WSC1 | 0.112 | 0.277 | 1.527 | 0.107 | | 0.00 |
| | | WSC2 | 0.134 | 0.297 | 1.703 | 0.125 | | 0.00 |
| | | WSC3 | 0.135 | 0.277 | 1.539 | 0.128 | | 0.00 |
| | | WSC4 | 0.141 | 0.277 | 1.555 | 0.133 | | 0.00 |
| | | WSC5 | 0.140 | 0.290 | 1.568 | 0.132 | | 0.00 |
| | | **Average** | **0.132** | **0.284** | **1.579** | **0.125** | | **0.00** |
| | Curing Time 7 days | WSB71 | 0.188 | 1.052 | 5.999 | 0.176 | | 3.65 |
| | | WSB72 | 0.389 | 1.269 | 6.832 | 0.375 | | 3.25 |
| | | WSB73 | 0.375 | 1.234 | 6.706 | 0.353 | | 4.50 |
| | | WSB74 | 0.243 | 1.265 | 7.290 | 0.228 | | 4.30 |
| | | **Average** | **0.299** | **1.205** | **6.707** | **0.283** | | **3.93** |

# Appendix D Physical Model Tests

**Table D.1 Cumulative Deformation Applied to the Side Plates in Millimetres**

| | 0 | 0+1 | 0+1+2 | ...+3 | ...+4 | ...+5 | ...+6 | ...+7 | ...+8 |
|---|---|---|---|---|---|---|---|---|---|
| **TSL A 45$^0$** | 1 | 3 | 7 | | | | | | |
| **Right** | 0 | 2 | 4 | | | | | | |
| **Hand side** | 0 | 2 | 4 | | | | | | |
| **TSL A 45$^0$** | 0 | 1 | 5 | | | | | | |
| **Left** | 1 | 4 | 5 | | | | | | |
| **Hand side** | 1 | 3 | 5 | | | | | | |
| **TSL A 60$^0$** | 0 | 1 | 1 | 3 | 5 | | | | |
| **Right** | 0 | 1 | 1 | 2 | 3 | | | | |
| **Hand side** | 0 | 0 | 0 | 2 | 5 | | | | |
| **TSL A 60$^0$** | 0 | 0 | 2 | 6 | 10 | | | | |
| **Left** | 0 | 0 | 0 | 3 | 5 | | | | |
| **Hand side** | 0 | 0 | 0 | 3 | 3 | | | | |
| **TSL A 80$^0$** | 0 | 1 | 2 | 3 | | | | | |
| **Right** | 0 | 0 | 2 | 5 | 8 | 19 | 23 | | |
| **Hand side** | 0 | 2 | 5 | 9 | 22 | 29 | 37 | | |
| **TSL A 80$^0$** | -1 | 0 | 2 | 3 | | | | | |
| **Left** | 0 | 4 | 6 | 10 | 17 | 27 | 27 | | |
| **Hand side** | 0 | 7 | 9 | 12 | 14 | 16 | 16 | | |
| **TSL B 45$^0$** | 0 | 2 | 6 | 8 | 10 | 13 | 15 | | |
| **Right** | 0 | 1 | 3 | 5 | 7 | 9 | 12 | | |
| **Hand side** | 0 | 1 | 4 | 6 | 8 | 10 | 13 | | |
| **TSL B 45$^0$** | 0 | 2 | 6 | 9 | 13 | 13 | 15 | | |
| **Left** | 0 | 1 | 3 | 5 | 7 | 11 | 15 | | |
| **Hand side** | 0 | 2 | 4 | 6 | 8 | 9 | 12 | | |
| **TSL B 60$^0$** | 0 | 2 | 4 | 5 | | | | | |
| **Right** | 1 | 1 | 3 | 6 | | | | | |
| **Hand side** | 0 | 3 | 6 | 10 | | | | | |
| **TSL B 60$^0$** | 1 | 4 | 5 | 7 | | | | | |
| **Left** | 0 | 2 | 3 | 6 | | | | | |
| **Hand side** | 0 | 1 | 2 | 5 | | | | | |
| **TSL B 80$^0$** | 0 | 2 | 3 | 4 | 4 | | | | |
| **Right** | 0 | 1 | 4 | 6 | 11 | | | | |
| **Hand side** | 0 | 2 | 4 | 6 | 8 | | | | |
| **TSL B 80$^0$** | 0 | 0 | 1 | 2 | 2 | | | | |
| **Left** | -5 | 2 | 6 | 9 | 9 | | | | |
| **Hand side** | 0 | 2 | 2 | 4 | 4 | | | | |

| | 0 | 0+1 | 0+1+2 | ...+3 | ...+4 | ...+5 | ...+6 | ...+7 | ...+8 |
|---|---|---|---|---|---|---|---|---|---|
| **TSL C 45$^0$** | 0 | 1 | 3 | 3 | 4 | 6 | 8 | 9 | 10 |
| **Right** | 0 | 2 | 2 | 2 | 3 | 4 | 6 | 9 | 17 |
| **Hand side** | 0 | 1 | 4 | 4 | 6 | 8 | 10 | 14 | 23 |
| **TSL C 45$^0$** | 0 | 2 | 2 | 3 | 5 | 7 | 8 | 11 | 13 |
| **Left** | 0 | 2 | 2 | 5 | 8 | 10 | 12 | 16 | 25 |
| **Hand side** | 0 | 3 | 3 | 5 | 7 | 9 | 11 | 13 | 15 |
| **TSL C 60$^0$** | 0 | 0 | 2 | 4 | 4 | 7 | | | |
| **Right** | 0 | 1 | 2 | 4 | 4 | 8 | | | |
| **Hand side** | 0 | 1 | 2 | 5 | 5 | 10 | | | |
| **TSL C 60$^0$** | 0 | 3 | 4 | 4 | 6 | 6 | | | |
| **Left** | 0 | 0 | 1 | 1 | 2 | 3 | | | |
| **Hand side** | 0 | 0 | 1 | 1 | 3 | 5 | | | |
| **TSL C 80$^0$** | 0 | 1 | 2 | 3 | 3 | 3 | | | |
| **Right** | 0 | 3 | 6 | 10 | 21 | 29 | | | |
| **Hand side** | 0 | 3 | 6 | 8 | 11 | 12 | | | |
| **TSL C 80$^0$** | 0 | 0 | 0 | 1 | | | | | |
| **Left** | 0 | 2 | 6 | 11 | 16 | 18 | | | |
| **Hand side** | 0 | 2 | 3 | 4 | 5 | 5 | | | |

1. The value (0), in Table D.1, represents the amount of deformation measured when the internal support steel frame was removed.

2. The value (0+1), represent the amount of deformation measured after item 1, above but when first loading deformation was applied and (0 +1+2), (…+3) after the second and third loading deformation respectively et cetera.